UNIVERSITY OF OTTAWA

Towards *in vitro* pharmacokinetic assessment of novel targeted covalent inhibitors for human tissue transglutaminase

by

Karine Bourgeois

A THESIS

SUBMITTED TO THE FACULTY OF GRADUATE STUDIES

IN PARTIAL FULFILMENT OF THE REQUIREMENTS FOR THE

MASTER OF SCIENCE DEGREE IN CHEMISTRY

OTTAWA, ONTARIO

APRIL, 2019

Abstract

Human tissue transglutaminase (TG2) is a calcium-dependent multifunctional enzyme that natively catalyzes the post-translational modification of proteins, namely by the formation of isopeptide bonds between protein- or peptide-bound glutamine and lysine residues. This ubiquitously expressed enzyme plays important roles in cellular differentiation, extracellular matrix stabilization, and apoptosis, to name a few. However, its unregulated activity has been associated with many pathologies such as fibrosis, cancer, neurodegenerative disorders and celiac disease. Most of these disorders are associated with unregulated acyl-transferase activity. As such, the Keillor group has directed its efforts towards the development of TG2 inhibitors.

Over the years, the Keillor group has synthesized large libraries of targeted covalent inhibitors against TG2. These compounds have undergone pharmacodynamic testing in order to examine their kinetic parameters of inhibition. Having gained knowledge of their enzyme kinetics, the logical next step was to consider their pharmacokinetic profiles. In the context of this thesis, we considered two important pharmacokinetic properties: membrane permeability and off-target reactivity.

Firstly, we aimed to evaluate our inhibitors for their ability to permeate the cell membrane. In efforts to do so, we were able to adapt, optimize, and validate a parallel artificial membrane permeability assay (PAMPA) utilizing hexadecane as our artificial membrane. We were able to test a few of our own inhibitors and found that compounds NC9, VA4 and AA9 possess Log P_e values of -5.26 ± 0.01, -4.66 ± 0.04 and -6.5 ± 0.5 respectively.

Secondly, we sought to investigate the susceptibility of our inhibitors to glutathione addition reactions under physiological conditions. We adapted and optimized a colorimetric assay using Ellman's reagent (DTNB) and found that our inhibitors are minimally reactive with glutathione.

The methods developed over the course of this work provide protocols that can be adopted for the characterization of future inhibitors in the Keillor group, along the process of developing TG2 inhibitors into drug candidates.

Keywords: enzyme, transglutaminase, targeted covalent inhibitor, pharmacokinetics, membrane permeability, off-target reactivity

Acknowledgements

First and foremost, I want to thank Jeff for welcoming me into his research group, and for the continuous guidance and support that he so kindly offered me through the challenges that I faced as a graduate student. Jeff, as much as I appreciated your ways of fulfilling your role as a supervisor, I can't forget to acknowledge your awesome sense of humor and dad jokes as well.

I would also like to thank past and present Keillor group members, for acting as both friends and work colleagues. In particular, I would like to thank Nicole McNeil for mentoring me through all my challenges as a graduate student, even when she was so busy with her very many other responsibilities in the lab. I would also like to say a special thank you to Kelvin Tsao (my lobster) for never failing to lend me a helping hand throughout my master's, even though we worked on completely different projects! I will forever be grateful for the important lessons you both have taught me.

I would also like to thank my committee members, Dr. Boddy and Dr. Shuhendler, and the Centre for Chemical and Synthetic Biology, for offering such a collaborative and supportive atmosphere to work in.

Lastly, I would like to thank my friends and family back home, who offered unconditional love, encouragement and support, even though they had no idea what I was talking about with respect to science half of the time.

This thesis is dedicated to everyone in my support system, who genuinely believed in me even when I didn't believe in myself.

Table of Contents

List of Tables

List of Figures and Illustrations

List of Symbols, Abbreviations and Nomenclature

Symbol	Definition
ADME	Absorption, distribution, metabolism, excretion
°C	degrees Celsius
% v/v	percent by volume
Arg	arginine
Asp	aspartic acid
COSY	homonuclear correlation spectroscopy
Cys	cysteine
DMSO	dimethylsulfoxide
DTNB	5,5'-dithio-bis-(2-nitrobenzoic acid)
EDTA	ethylenediaminetetraacetic acid
GSH	glutathione, reduced
GSSG	glutathione, oxidized
GTP	guanosine 5'-trisphosphate
h	hour
His	histidine
HPLC	high-performance liquid chromatography
hTG2	human tissue transglutaminase
LC-MS	liquid chromatography tandem mass spectrometry
MOPS	3-(N-morpholino)propanesulfonic acid
NMM	N-methylmaleimide
NMR	nuclear magnetic resonance
PK/PD	pharmacokinetics/pharmacodynamics
RT	room temperature
Thr	threonine
TNB	2-thio-5-nitrobenzoic acid
Trp	tryptophan

Chapter One: **Introduction**

1.1 Medicinal Chemistry and Drug Development

There is a long history of plants being used to treat various diseases. In fact, the knowledge of toxic or therapeutic properties of plants predates the knowledge of precise targets or mechanisms. Natural selection has provided a slow and steady stream of bioactive small molecules that exist in plants, roots, vines and fungi.

Synthetic organic chemistry was born in 1828 when Friedrich Wöhler synthesized urea from inorganic substances, thereby disproving vital force theory. The birth date of medicinal chemistry, however, is not as clear-cut. During the early stages of medicinal chemistry development in the 19th century, chemists were primarily concerned with the isolation of medicinal agents found in plants. Popular examples of pharmaceutically active substances derived from plants include morphine from opium poppy, nicotine from the tobacco plant, cannabinoids from cannabis leaves, caffeine from tea and coffee, quinine from the cinchona tree, and salicylates from the bark of the white willow tree. The isolation of these active compounds in medicinal plants presented a major challenge for analytical chemists at the time.

Morphine was the first alkaloid to be isolated in a pure state. This was done by a 23-year old apothecary, Friedrich Willhelm Sertürner (1873–1841). [1] While working as an apprentice in a pharmacy, Sertürner isolated meconic acid from raw opium. The following year he obtained a substance with the properties of a weak base, which he administered to a dog who then fell into a deep sleep. This led Sertürner to believe he had discovered the specific narcotic element of opium, which was named morphine after *Morpheus*, the Greek god of dreams. Sertürner tested the effects on himself and some young friends and took unusually large doses of 100 mg — they all

experienced symptoms of severe opium poisoning for several days. Shortly after, other alkaloids were isolated from opium, including codeine and papaverine. Many of these alkaloids were later demonstrated to be considerably toxic in their pure forms.

While nature has provided a myriad of bioactive compounds to be put to use, each of these molecules must necessarily present a reproductive advantage in order for nature to "invest" in its synthesis. Until the 19th century, nature's therapeutic compounds were all that were available to us humans, but that changed in 1869 with the discovery and preparation of chloral hydrate (Noctec®) by none other than Justus von Liebig, a well-known Professor of Chemistry in Munich. [2] The first known analgesics and antipyretics were phenacetin and acetanilide, both of which were indirect byproducts from coal-tar. A white willow tree bark extract was used to treat various fevers and inflammation for centuries — the observed therapeutic effects were attributable to salicylic acid, a compound that also irritated the gastric mucosa. This issue was fixed by introducing a simple chemical modification to yield acetylsalicylic acid, better known as Aspirin®, the first blockbuster drug. [3]

In the modern era, medicinal chemists and chemical biologists aim to identify novel small molecules that potently and selectively modulate the function of target proteins. As such, they are concerned with the design and creation of new synthetic pharmaceutical agents or bioactive compounds. Practically speaking, this calls for identification and systematic synthetic modification of new compounds to evaluate their structure-activity relationships (SAR) and make them suitable for therapeutic use. Consequently, large libraries of compounds are synthesized and screened for their long-term potential for development. These libraries are narrowed down to a so-called "hit" series, from which compounds display suitable SAR and chemical characteristics. These compounds can then be further improved with respect to the desired primary activity [4], secondary

activities [5], and physicochemical properties to ensure that the agent will be useful when studied under *in vivo* conditions. For example, chemical modifications of "hit" compounds can be useful to improve the recognition of binding geometries, resulting in greater affinities for their intended targets (primary activity) as compared to other possible related or unrelated targets (secondary activity). Furthermore, physicochemical properties can be manipulated such that the desired pharmacokinetic/pharmacodynamic (PK/PD) and toxicologic profiles are achieved, rendering compounds suitable for introduction into animal and human studies.

The final synthetic chemistry stages of this long process involve the production of a lead compound in a reasonable quantity and quality to allow large scale animal testing, and then human clinical trials. Synthetic routes must be optimized such that bulk industrial production is possible, and optimal drug formulation can be discovered. In Canada, the average time of the full drug development and approval process from initial research, preclinical studies, through the 3 phases of clinical trials to drug approval is 12 years (between 8 and 15 years).

1.2 Pharmacology

It is important to distinguish between what a drug does and how it acts. Amoxicillin cures a strep throat, and omeprazole promotes the healing of duodenal ulcers. Pharmacology asks "how?". Amoxicillin inhibits the synthesis of cell wall mucopeptide by the bacteria responsible for infection [6], and omeprazole inhibits gastric acid secretion by acting as a specific irreversible inhibitor of the H^+/K^+-ATPase system found at the secretory surface of gastric parietal cells. [7] From this, we can infer that pharmacology is simply the science of drugs. More specifically, it is a branch of biology concerned with the study of drug actions, where a drug can be defined as any man-made, natural,

or endogenous compound that affects the normal or abnormal biochemical or physiological function of the cell, tissue, organ, or organism.

Pharmacology as a scientific discipline only started to bloom during the mid-19th century, in the midst of the important biomedical advances of that period. Before the second half of the nineteenth century, the potency and specificity of available drugs were only vaguely explained with respect to chemical powers and affinities to certain organs or tissues. In light of the need to understand exactly how drugs produce their effects, the first pharmacology department was set up in Estonia by Rudolf Buchheim in 1847.

Today, the science of pharmacology is divided into two main areas, namely pharmacodynamics (PD) and pharmacokinetics (PK). Simply put, pharmacodynamics studies the effects of a drug on biological systems, whereas pharmacokinetics studies the effects of biological systems on a drug. Together, they allow us to have a comprehensive understanding with respect to drugs' effects through dose-response relationships. [8]

1.2.1 Pharmacodynamics

Pharmacodynamics is a branch of pharmacology that pertains to the effects of drugs and their mechanism of action. It aims to answer the question "how does the drug affect the body and its target?". As part of this thesis, this topic will only briefly be discussed.

Generally speaking, drugs deliver their effect by binding to target proteins or receptors in a structurally specific way within the organism. Pharmacodynamic responses are greatly influenced by receptor binding and sensitivity, as well as chemical interactions. The concentration of the drug at the receptor site influences the drug's effects — we call this the dose-response relationship. [8]

Important pharmacodynamic considerations include, but are not limited to, receptor mechanisms, dose-response curves, and therapeutic indexes. Receptor mechanisms describe how drugs bind at the cellular level and in turn initiate their pharmacodynamic effects. Dose-response curves provide a plot of the drug concentrations against the effects of the drugs, thus allowing comparison of their efficacy and potency. Lastly, therapeutic indexes provide measures of the toxicity and safety of drugs and are calculated by dividing the median toxic doses by the median effective doses. The pharmacodynamic profile of a given drug can be affected by physiological changes due to disease states, genetic mutations, or interactions with other drugs. [8]

1.2.2 Pharmacokinetics

Pharmacokinetics is a branch of pharmacology that pertains to the movement of drugs within the body. As such, it studies the effects of drugs on biological systems to answer the question "how does the body affect the drug?".

In broad terms, pharmacokinetics discusses the absorption, distribution, metabolism and elimination (ADME) of chemicals from the biological systems. Sometimes, liberation and/or toxicity are also considered. Together, these properties affect the drug levels and kinetics of drug exposure to the tissues. As a result, they influence the performance and pharmacological activity of the compound as a drug. [9]

1.2.2.1 Absorption

For a compound to reach a tissue after administration, it usually has to enter bloodstream before making its way into the target cells; this often happens following contact with mucous surfaces like those found in the gastrointestinal tract. In pharmacokinetics, this process is termed

absorption. This parameter is of utmost importance in drug development and medicinal chemistry, mainly because a drug must be absorbed before any therapeutic effect can occur. Drugs that absorb very poorly when taken orally must usually be administered in other less desirable, more invasive ways such as intravenously or by inhalation. Generally speaking, we consider that absorption is a nonfactor in the case of intravascular administration, as there is virtually no loss of drug and bioavailability – that is the fraction of an administered dose of unchanged drug that enters systemic circulation – borders 100%. [10]

Factors influencing product bioavailability include drug solubility, permeability, the rate of *in vivo* dissolution, bioactivity, resonance, inductive effects, isosterism and bio-isosterism. [11] Other contributing factors include individual traits, like the integrity of the GI tract, physiological status, site of drug absorption, membrane transporters, and extrinsic variables such as the effect of food or concomitant medication. [10] Overall, the pharmacokinetic profile of a drug can be manipulated with relative ease by adjusting factors that affect absorption.

By having a comprehensive understanding of a drug's physicochemical properties and the physiological processes affecting drug absorption, pharmaceutical scientists are able to develop formulations that will maximize product availability. Additionally, it is important to recognize the potential impact of patients' physiological status, age, gender, and lifestyle in order to tailor dosing regimens to better meet the needs of each individual.

Two important factors that seem to highly impact drug absorption are the rate of dissolution and the ionization state of a compound. Most often, drugs come in the form of tablets that are ingested and pass through the esophagus into the stomach. The rate of dissolution of a drug is a key factor for controlling the duration of its effect. As such, an active ingredient may be available in several dosage forms, all of which differ only in the rate of dissolution. [12] If a drug is supplied in a form

that is not easily dissolved, the active ingredient is released gradually, thus lengthening the duration of action. Slow-release dosage forms can be helpful for maintaining concentrations within an acceptable therapeutic range over a long period of time, as opposed to quick-release dosage forms which often display sharper and shorter peaks in serum concentrations. The rate of dissolution may be adjusted by altering the surface area of the solid (i.e. particle size). For many drugs, reducing the particle size leads to an increase in the specific surface area and in the rate of dissolution. As a result, the dose to achieve the same therapeutic effect is lessened while the solubility remains unaffected. Choosing a suitable polymorph of a compound may also help optimize the rate of dissolution, as different polymorphs exhibit different solubility and dissolution rate characteristics. Lastly, tablets can be coated to reduce the rate of dissolution and control where dissolution takes place. For example, enteric coatings may be applied to a drug, so that the coating only dissolves in the basic environment of the intestines, thus releasing the drug in that specific location. [12]

Further, the gastrointestinal tract is lined with epithelial cells through which drugs must permeate in order to be absorbed and enter systemic circulation. One particular barrier that may prevent absorption of a given drug is the cell membrane, which is made up of lipid bilayers. Pure lipid bilayers are generally permeable only to small, uncharged solutes. As such, the ionization state of a compound will affect its capacity to be absorbed. While permeability favours neutral species, solubility favours charged species. To facilitate movement from the lumen into the circulation, some compounds can employ special exchange proteins and channels.

The proportion of a compound that is ionized at a certain pH can be determined through use of the Henderson-Hasselbalch equation, and from this we can predict whether it will be readily absorbed in a given chemical environment. For instance, in the highly acidic stomach, drugs that are weak

acids like aspirin will be present in their non-ionic form (contrary to weak bases), meaning that they will be easily absorbed in that location. The reverse is also true in the basic environment of the intestines, so weak bases such as caffeine will be more readily absorbed there. [13]

To some extent, medicinal chemists are able to control this aspect of absorption. For instance, an appropriate analog may be chosen so that the drug is more likely to be unionized. Prodrugs of a compound may also be developed by medicinal chemists such that they are more readily taken up by cells, and subsequently metabolized to yield the active compound upon absorption. However, one mustn't forget that altering the chemical structure of a molecule is less predictable than altering its dissolution properties, because changes in chemical structure could lead to changes in the pharmacodynamic properties of said molecule.

1.2.2.2 Distribution

In pharmacokinetics, distribution is defined as the reversible transfer of a drug from one compartment to another within the body. Upon a drug's entry into systemic circulation, whether it be by absorption or direct administration, it is distributed into interstitial and intracellular fluids such that tissues and organs receive different doses. The drug can remain in these different locations for varying amounts of time, depending on the organism's physical volume, vascular permeability, regional blood flow, cardiac output and perfusion rate of the tissues. Other noteworthy factors to consider include the drug's molecular size, polarity, ability to bind tissue and plasma proteins, lipid solubility and pH partition. [14] Drugs are easily distributed to highly perfused organs such as the liver, heart and kidneys. However, distribution to less perfused tissues like muscle, fat and peripheral organs is lower.

1.2.2.3 Metabolism

As soon as chemical compounds enter the body, they begin to undergo chemical alteration and break down through metabolic processes. Metabolism is a critical aspect and determinant of the pharmacokinetic profile of a drug, mainly because the rate of metabolism determines the duration and intensity of a drug's pharmacologic or toxicologic action. Compounds that are highly susceptible to metabolic degradation often show poor bioavailability and high clearance. As metabolism occurs, the parent compound is converted to metabolites that may or may not be pharmacologically inert. In many cases, metabolism deactivates the administered dose of parent drug and metabolites are inert, and this typically reduces the effects on the body. In a different scenario, metabolites can be active and either solely or partially responsible for the pharmacological response. One popular example used to illustrate this is prodrugs, where the parent compound starts out as inert and is metabolized into an active form that delivers the therapeutic effect. [15] Lastly, in some cases, metabolites may be reactive or toxic and responsible for the appearance of adverse effects. As such, a good understanding of the metabolism of a new chemical entity is needed early in the drug discovery process.

The majority of small molecule drug metabolism is carried out by liver redox enzymes, namely the cytochrome P450 enzymes. Generally speaking, drug metabolism is divided into two broad phases being modification (Phase I) and conjugation (Phase II). [16] Phase I reactions typically involve functionalization, where a polar functional group is added to the molecule. Examples of Phase I reactions include hydrolysis of ester or amide groups to their corresponding acid and alcohol/amines, hydroxylation of aromatic and aliphatic carbons, heteroatom dealkylation (secondary/tertiary amines, ethers, thioethers), and heteroatom oxidation (N-, S- oxidation). From there, metabolites are excreted as is, or undergo Phase II metabolism. During this phase,

metabolites are subjected to derivatization reactions in which a polar functionality is introduced onto either the parent molecule or its Phase I metabolite. [16] The resulting Phase II metabolites, also known as conjugates, are typically more polar than the parent compound in the sense that they are more likely to be eliminated from the host. The most common Phase II metabolic pathways include glucuronidation, sulphation, and glutathione conjugation. [16] Parent compounds that bear a polar functionality may pass directly to Phase II metabolism, as exemplified by ibuprofen. Upon conjugation, the drug may be further processed before being recognized by efflux transporters and pumped out of cells.

Because the treatment of several diseases involves the administration of multiple combinations of drugs, it is crucial that metabolic liability and drug-drug interaction potential be optimized for new chemical entities in drug discovery. Co-administered drugs can affect each other's metabolism if they share metabolic pathways catalyzed by the same CYP isoforms. This influences their respective pharmacokinetic profiles and can potentially lead to unwarranted adverse interactions and/or therapeutic failure. Historically, attempts to optimize metabolic liability and drug-drug interaction potential have been done by trial and error through structural modifications of chemical structures based on empirical methods, past experience and intuition. However, recent knowledge of the expression and regulation of cytochrome P450 and other enzyme systems has allowed for greater understanding of the role of drug metabolism in early drug development. [16]

Lastly, various physiological and pathological factors can affect drug metabolism. Of these, we count age, individual variation (e.g. inherited genetic differences in drug metabolic pathways), enterohepatic circulation, nutrition, intestinal flora, and sex differences. Because metabolic enzyme systems are only partially developed at birth, newborns have difficulty metabolizing certain drugs and the process is much slower than in adults. On the other hand, with aging,

enzymatic activity decreases such that the elderly cannot metabolize drugs as easily. Consequently, newborns and the elderly often need much smaller doses per pound of bodyweight than young or middle-aged adults. [16]

1.2.2.4 Elimination

In pharmacokinetics, elimination refers to the irreversible removal of a drug or its metabolite(s) from the body. Typically, compounds and their metabolites are removed from the body via excretion through the kidneys (renal excretion) or in the feces (biliary excretion). [17] Nonvolatile and water-soluble substances are eliminated primarily by renal excretion, in which case the drug passes through the kidneys into the bladder and ultimately into the urine. Alternatively, excretion may happen through the lungs, as is the case with volatile anesthetic gases. To a lesser extent, excretion is also possible through sweat, saliva, or other bodily fluids. If elimination cannot be completed, compounds may bioaccumulate and adversely affect normal metabolism.

1.3 Transglutaminases as Biological Targets

The term "transglutaminase" was first introduced by Clarke *et al*. in 1959 following the discovery of transamidation activity occurring in guinea-pig liver extracts. [18] Since then, additional proteins sharing this same activity have been identified in unicellular organisms, invertebrates, fish, mammals, and plants.

Transglutaminases undertake the role of catalyzing the Ca^{2+}-dependent post-translational modifications of proteins, more specifically by the formation of isopeptide bonds. This most often occurs through protein cross-linking via ε-(γ-glutamyl)lysine bonds, i.e. between a free amine group (such as protein- or peptide-bound lysine) and the acyl group at the end of the side chain of

protein- or peptide-bound glutamine, as depicted in scheme 1.1 below. [19] Alternatively, there can be incorporation of many primary amines at the level peptide-bound glutamine residues. The resulting cross-linked protein products are highly resistant to mechanical challenge and proteolytic degradation, and they accumulate in a number of tissues including but not limited to skin, hair, and blood.

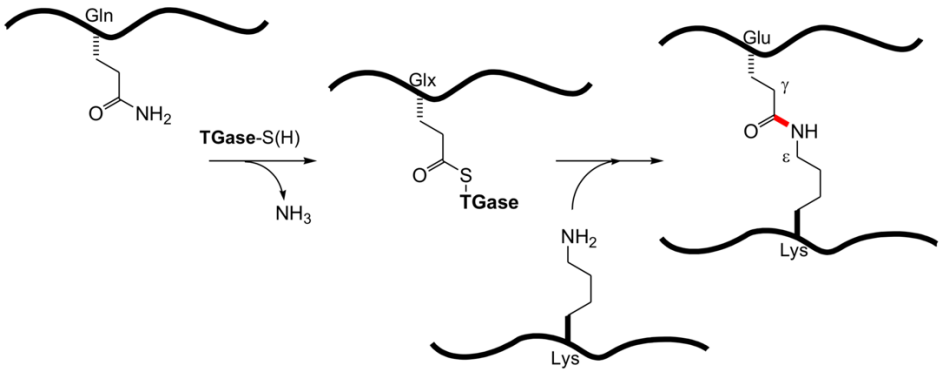

Scheme 1.1. Transamidation reaction catalyzed by TGases.

The structural components of TGases are conserved across all members of the superfamily. In particular, they are made up of four domains being the N-terminal β-sandwich domain, the catalytic core domain, and two C-terminal β-barrel 1 and β-barrel 2 domains as depicted in figure 1.1 below. Within the catalytic core domain exists a catalytic triad of Cys-His-Asp, which is also conserved throughout transamidation-active members of the family. [20]

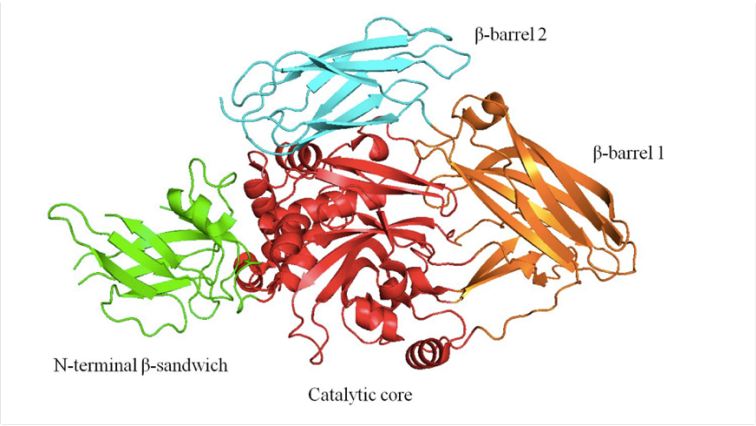

Figure 1.1. Structural components of TGases (TG2, PDB 1KV3).

To this day, nine transglutaminase genes have been identified in humans, eight of which are the catalytically active TGases 1 through 7 and factor XIII (FXIII). The remaining member is the catalytically inactive erythrocyte membrane protein band 4.2.

1.3.1 TG1 (Keratinocyte TGase)

Keratinocyte TGase in humans can be found in the stratified squamous epithelia of the skin and upper digestive tract, as well as in the lower female genital tract. More specifically, it is found anchored to the keratinocyte plasma membrane via fatty acyl linkages at its N-terminus. [21] Its catalytic activity has been known to be activated by means of proteolytic cleavage, increased Ca^{2+} levels, and interaction with tazarotene-induced gene 3 (TIG3). Research has shown that TG1 plays an important role in the covalent cross-linkage of cornified cell envelopes, which is required for

epidermal tissue homeostasis. Where TG1 lacks, lamellar ichthyosis, a severe congenital skin disorder characterized by large scales and variable redness, manifests. [21]

1.3.2 TG2 (Tissue TGase)

Unlike other members of the transglutaminase family, Tissue TGase is a 78-kDa enzyme that in humans is expressed ubiquitously, and localized both intracellularly (cytosol, nuclear membrane) and extracellularly. [20] The structure of TG2 is made up of four domains being the N-terminal β-sandwich domain, the catalytic core domain, and two C-terminal β-barrel 1 and β-barrel 2 domains. The catalytic core domain holds a catalytic triad made up of Cys277, His335 and Asp358, which are located at the end of a tunnel bordered by residues Trp241, Trp332 and Thr360, all of which were identified by solving the crystal structure of the active form. [22] This catalytic triad as well as the 3D structure are conserved across other TGase family members. [20] Similarly to all TGases, TG2's activity has been known to be activated by Ca^{2+}, where it adopts an open conformation. However, it is also deactivated by GTP, an allosteric regulator that leads to a closed conformation of the enzyme. [22]

In addition to the transamidation reaction, TG2 exhibits GTPase, ATPase, protein kinase, and protein disulfide isomerase (PDI) activity. [23] While TG2 is particularly notable for being the autoantigen in celiac disease, its unregulated activity has been associated with a variety of other pathologies such as fibrosis, Alzheimer's disease, Huntington's disease, and cancer. This enzyme will be discussed in greater detail in section 1.4.

1.3.3 TG3 (Epidermal TGase)

Epidermal TGase [24] is present in hair follicles, epidermis, and brain. Similarly to TG2, TG3 binds to and hydrolyzes GTP. It catalyzes the cross-linking of trichohyalin and keratin intermediate filaments to harden the inner root sheath of hair follicles, which is critical for hair fiber morphogenesis. It also requires proteolysis to become active. While gluten sensitivity often presents as celiac disease, in certain cases it may manifest itself as dermatitis herperiformis, a blistering skin disease characterized by granular IgA deposits in the papillary dermis; the dominant autoantigen of this disease is epidermal transglutaminase. [25]

1.3.4 TG4 (Prostate TGase)

As its name suggests, TG4 [26] expression is restricted to the prostate gland. The biological and pathological roles of prostate TGase are unclear; very few biological functions have been assigned to this isozyme. In prostate cancer, TG4 expression is controversial, with reports showing a possible differential expression in normal epithelial cells and prostate cancer cells. [26] Nonetheless, a few studies have provided evidence that TG4 is able to regulate the invasiveness and migratory property of prostate cancer cells. In 2017 it was demonstrated that TG4 is important to the epithelial-mesenchymal transition, a process by which epithelial cells lose their cell polarity and cell-cell adhesion, thus acquiring migratory and invasive properties, in prostate cancer cells. [27]

1.3.5 TG5

TG5 has yet to be fully characterized at the functional level, however we know that like TG1 and TG3 it is mainly expressed in stratified squamous epithelia, such as the upper layers of the epidermis and in human hair follicles. [20] GTP and ATP are known to inhibit the protein

crosslinking of TG5, whereas Ca^{2+} reverses this inhibition. The protein crosslinking function performed by TG5 is vital for maintaining cell-cell adhesion between the outermost layers of the epidermis. As such, TG5 inactivating mutations result in peeling skin syndrome, an autosomal recessive skin disorder. [28]

1.3.6 TG6

TG6 expression is localized in the human testes and lungs, and in the brain of mice. [20] TG6 is similar to TG2 in that in can be detected in the cell cytosol as well as the cell surface, suggesting that it may have independent intra- and extracellular functions that may employ the enzyme's ability to bind GTP or act as a Ca^{2+}-dependent crosslinking enzyme, respectively. TG6 is thought to play a critical role in cortical and cerebellar neurons, [29] and mutations in the TGM6 gene have been associated to spinocerebellar type 35 ataxia, [30] as well as acute myeloid leukemia. [31]

1.3.7 TG7

TG7 was discovered transcriptionally by taking advantage of DNA sequence homologies among TG family members, but little is known about its' gene regulation or function. [32] Like TG6, expression is seemingly restricted to testes, lungs, and brain. In 2011, pepZ3S was identified as a peptidic substrate and is being studied as a probe for TG7 activity. [33] Although one report suggests that TG7 transcript levels are increased in breast cancer cells of patients with poor prognoses, no other claims have been made to directly associate TG7 with any known disease. [33] Its mRNA has been found to be highly expressed in kidneys, testis and thymus.

1.3.8 Factor XIII (plasma TGase)

The circulating zymogen factor XIII is an important component of the blood coagulation cascade that crosslinks fibrin. This pro-TGase circulates in plasma as a tetramer made up of two 83.2 kDa A subunits and two 79.7 kDa B subunits (FXIII-A_2B_2), all of which are held together noncovalently. [34] The A subunit is catalytically active and is synthesized by hepatocytes, monocytes and megakaryocytes. The B subunit rather acts as a carrier for the catalytic A subunit in plasma; it is synthesized by the liver and is secreted as a monomer that binds free A in plasma. The primary structure of both subunits was determined by cDNA cloning and amino acid sequence analysis.

FXIII is converted into the active TGase factor XIIIa via thrombin-dependent proteolysis in the presence of Ca^{2+} as a cofactor. The final activation steps lead to the dissociation of the B subunit and a 37-amino acid peptide from the N-terminal end of the A subunit, thus yielding FXIIIa, in which the active site is accessible. Among known substrates of FXIIIa, we find proteins of the coagulation and fibrinolytic systems, adhesive proteins, and cytoskeletal proteins. These classes of substrates correlate with the major functional roles of FXIIIa, being its involvement in blood coagulation and fibrinolysis, wound healing, and other lesser defined cellular functions. [34]

1.3.9 Erythrocyte Protein Band 4.2 (Band 4.2)

Erythrocyte membrane protein band 4.2 (EBP42) is an ATP-binding protein that may regulate the association of protein 3 and ankyrin. It probably plays a role in erythrocyte shape and mechanical property regulation. [35] Mutations in the EPB42 gene have been associated with recessive spherolytic elliptocytosis and recessively transmitted hereditary hemolytic anemia. [35]

The EPB42 amino acid sequence displays homology with both guinea pig liver transglutaminase (32% identity for a 446-amino acid overlap) and the catalytic A subunit of factor XIII (27% identity for a 639-amino acid overlap), as determined by sequencing using full-length cDNA. [35] More importantly, the region of greatest correspondence includes a 49-amino acid sequence of band 4.2, which is 69% and 51% identical to guinea pig liver transglutaminase and the catalytic A subunit of factor XIII, respectively. [35] These regions contain the active sites of the aforementioned enzymes, which are made up of the five residues Gly-Gln-Cys-Trp-Val. However, in EPB42, the cysteine residue is replaced with an alanine, which explains its lack of transamidation activity. [35]

1.4 Human Tissue Transglutaminase

Of all the isozymes discussed previously, the Keillor group focuses primarily on TG2. Similarly to TG3, TG5 and TG6, this TGase doubles as a guanine nucleotide-binding protein. A key feature of TG2 is the large conformational change that it undergoes in going from a compact catalytically-inactive "closed" form to an active "open" form.

1.4.1 Biological Function

TG2 is primarily a cytosolic protein, where its transamidation activity is generally turned off due to low Ca^{2+} concentrations in the environment. Consequently, it adopts the function of a classical GTP-binding protein. [36] In contrast, when Ca^{2+} concentrations are higher like in the extracellular environment, its main function is transamidation. This activity is also regulated by the isomerization of disulfide bonds within its tertiary structure. [36]

A number of physiological roles have been assigned to TG2. In the intracellular environment, TG2 is thought to play a pro-apoptotic as well as an anti-apoptotic role, depending on the cellular

context and biological cues. [37] Extracellular TG2 is believed to be involved in cell adhesion, matrix assembly, wound healing, receptor signaling, and a variety of cellular behaviours including proliferation, invasion, motility and survival. [38]

1.4.2 Mechanism of Action

The Cys277 residue situated in the active site of TG2 is imperative to the enzyme's crosslinking activity. It attacks γ-glutamyl residues on acyl donor substrates, on proteins and peptides, to drive formation of a thioester intermediate. The resulting acylated enzyme can then either react with an amine donor, typically an ε-lysyl side chain of another protein/peptide, which associates with TG2 at a second substrate binding site. This results in isopeptide bond (crosslink) formation. Alternatively, in the absence of a suitable amine donor, the thioester is hydrolyzed to form glutamic acid, resulting in a net deamidation. [19]

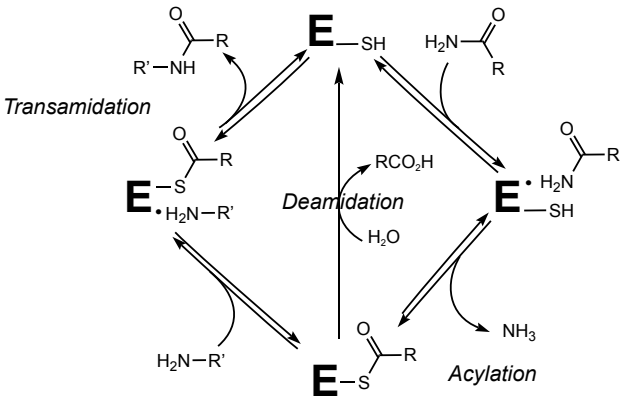

Scheme 1.2. Mechanism of action of tranglutaminases

1.4.3 Allosteric Regulation and Conformational Changes

TG2 can function as a G protein or as a transamidation enzyme, and because of this it can be regarded as a bifunctional enzyme. It catalyzes the Ca^{2+}-dependent post-translational modification of proteins, and binds and hydrolyzes GTP in a Ca^{2+}-independent manner. The structure of TG2 is made up of four domains: an *N*-terminal β-sandwich that contains integrin and fibronectin binding sites, a catalytic core domain that contains a catalytic triad (Cys277, His335, Asp358) for acyl transfer reaction, and two *C*-terminal β-barrels. The spatial arrangement of these domains changes based on the presence of cofactors in the environment. [39]

TGases are present in both intracellular and extracellular contexts, and their activity is tightly regulated under physiological conditions, based on the chemical environment. Ca^{2+}, guanine nucleotides and redox potential are known to modulate TG2 crosslinking activity, as depicted in figure 1.2. The transamidation activity of TG2 is allosterically activated by Ca^{2+} and inhibited by certain guanine nucleotides, notably GTP, GDP and GMP. [39] The presence of the guanine nucleotides is attributed to a significant interaction between domains 3 and 4 and the catalytic core domain, leading to closed, catalytically inactive conformation of the enzyme. On the other hand, Ca^{2+} binding alters the conformation such that domains 3 and 4 are further apart, thus leading to an open conformation in which the active site is accessible, and the acyl transfer crosslinking reaction can occur. [39] One molecule of TG2 binds up to six Ca^{2+} with an apparent overall dissociation constant of 90 μM. In contrast, GTP and GDP bind TG2 with a dissociation constant of 1.6 μM. GTP-bound TG2 is unable to crosslink proteins, whereas crosslinking activity is only observed in presence of high concentrations of Ca^{2+}. [39]

Inside living cells, TG2 is most often found bound to GTP and GDP, and calcium concentrations are relatively low. As such, TG2 would exist predominantly in a closed conformation, and

transamidation activity would be turned off. This could explain why overexpression of TG2 is not always associated with increased intracellular crosslinking activity. In a recent study, using TG2 that is covalently conjugated to enhanced Yellow Fluorescent Protein (YFP) and cyan fluorescent proteins (CFP) at the *N*- and *C*- terminus, respectively, Pavlyukov *et al*.[40] observed closed/inactive TG2 at perinuclear location. In contrast, crosslinking-active TG2 was present at the cell membrane. Using the fluorescence resonance energy transfer (FRET)-based approach, they observed that TG2 changed from closed to open conformation in response to ionophore-induced calcium influx. In addition, Caron *et al*.[41] reported that an acrylamide-based TG2 inhibitor from the Keillor group induces the open conformation, whereas a cinnamoyl triazole inhibitor stabilizes the closed conformation. These pieces of evidence suggest that intracellular TG2 in predominantly in a closed, catalytically inactive conformation. Nonetheless, despite low intracellular calcium concentrations, multiple transamidation and crosslinking substrates of intracellular TG2 have been identified. This suggests that locally increased calcium and/or as yet uncharacterized interacting proteins may facilitate the formation of open TG2. Certain authors have suggested that relatively low calcium concentrations may be sufficient to activate the TG2-binding proteins inside the cell (e.g. using yeast-2-hybrid or proteomics approach).[20]

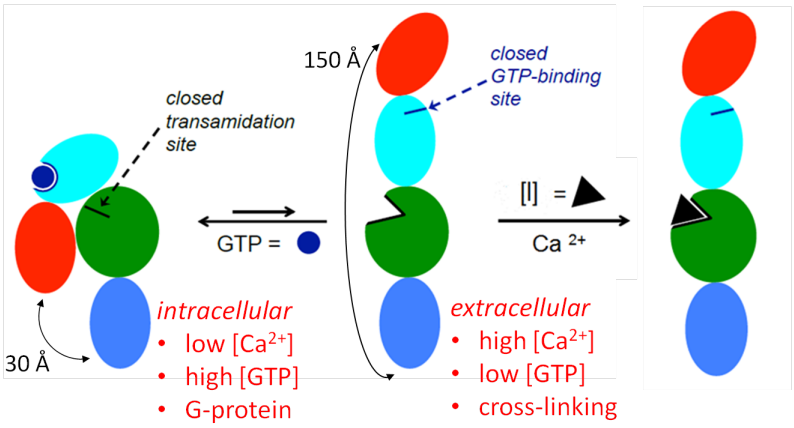

Figure 1.2. Closed (left) and open (right) conformations of TG2.

1.4.4 Pathological Implications

TG2 has implications in the pathogenesis of a plethora of diseases, such as celiac disease [42], neurodegenerative disorders [43], diabetes [44], pulmonary fibrosis [45], renal scarring [46], and certain types of cancer [47]. The pathology or etiology of diseased states involving TG2 are mainly associated with its unregulated protein cross-linking and deamidation roles, rather than its function as a G-protein. As such, inhibition of the TG2 active site offers a potential strategy with respect to therapeutic treatment of these diseases. To date, the greatest potential for doing so revolves around fibrosis, cancer and celiac disease. This is because we know both the specific nature of the enzyme's role within said pathologies, and its physiological location.

1.4.4.1 Celiac Disease

Celiac disease is a chronic autoimmune disease affecting the small intestine. Genetically predisposed individuals are subjected to near total atrophy of villi in the jejunum following exposure to dietary gluten peptides like those found in wheat, rye and barley. Consequently, their

capacity to absorb nutrients is greatly hindered. TG2 is implicated in the development of celiac disease as it is responsible for deamidating gluten peptides, thereby converting them into immunogenic T-cell antigens. [42] This triggers the activation of inflammatory gluten-reactive T-cells. Additionally, B-cell activation gives rise to the production of TG2-targeting autoantibodies which, coupled with antibodies against deamidated gluten, are highly specific to celiac disease. [42]

1.4.4.2 Neurodegenerative diseases

An important feature of neurodegenerative diseases like Alzheimer's disease, Parkinson's disease, Huntington's disease, and other polyglutamine diseases, is the accumulation and deposition of cross-linked proteins in the affected brain. Research has shown that such accumulating proteins, namely amyloid-beta, tau, α-synuclein and huntingtin to name a few, are all substrates of TG2. Proteomic analyses of protein aggregates in diseased brains has suggested that TG2 could be involved in their formation. [43]

1.4.4.3 Fibrosis

Fibrosis is characterized by the formation of excess fibrous connective tissue in an organ or tissue in a reparative or reactive process. On the microscopic scale, it is caused by the accumulation of fibroblasts and extracellular matrix proteins that destroy normal tissue structure and function. This pathologic process can occur in a multitude of organs including the lungs, liver, heart, skin and kidneys. There are a handful of mechanisms through which TG2 may promote tissue fibrosis. First and foremost, TG2 is able to cross-link extracellular collagen and fibronectin among other extracellular matrix (ECM) proteins, making them more resistant to degradation [45]. Additionally, the cytosolic G-protein function of TG2 has implications in cell survival and cell cycle progression.

Cell adhesion and mobility are enhanced in a transamidation independent fashion as a result of TG2 binding to integrins on the cell surface and fibronectin in the ECM. Lastly, TG2 has also been demonstrated to enhance the production and maturation of fibrillar fibronectin in an enzymatically independent manner. [45]

1.4.4.4 Cancer

Studies show that cancer cells express elevated levels of TG2. In fact, elevated TG2 levels are associated with an aggressive cancer phenotype and drug resistance in most of these tumours. TG2 levels are especially enhanced in cancer stem cells - it appears TG2 is required for their survival, migration, and invasion. [48] A correlation between elevated TG2 levels and cancer aggressiveness was reported in the case of colorectal, breast, pancreatic, ovarian, esophageal squamous cell cancer, glioblastomas, malignant melanomas, renal, and cervical squamous cell carcinomas and hepatocellular carcinomas. [49] TG2 was found to be a biomarker of cervical intraepithelial neoplasia. Several mechanisms have been proposed as to how TG2 promotes cancer survival, tumour progression and invasion, but many of these effects are attributed to TG2 in the extracellular matrix; TG2 can alter the structure and stability of the ECM in a way that it supports the integrin-dependent ECM-binding and migration of cancer cells. [48]

1.5 Known Irreversible Inhibitors for Human Tissue Transglutaminase

The Keillor group among other scientists have devoted many years of research geared towards the discovery of both reversible and irreversible inhibitors for TG2. In the context of this thesis, we will focus on irreversible inhibitors.

Past members of the Keillor group have reviewed the field of TG2 inhibitors in depth. [50] Here, we will focus on the work of two active groups in the field, namely the Khosla and Keillor groups. Firstly, the Khosla group has developed compound **KCC009** (k_{inact}/K_I = 2.00 x 10^3 $M^{-1}min^{-1}$, k_{inact} = 1.3 min^{-1}, K_I = 0.74 mM), which possesses a 3-halo-4,5-dihydroisoxazole group as a reactive electrophilic moiety. [51] This irreversible inhibitor displays high selectivity for TG2 and has proven effective *in vivo* using a mouse model. Compound **ERW1041E** (k_{inact}/K_I = 16.9 x 10^3 $M^{-1}min^{-1}$, k_{inact} = 0.110 min^{-1}), a more efficient inhibitor, was then developed following optimization of the aforementioned scaffold. [52] This newer compound has also been tested *in vivo* and showed inhibition of the activity of TG2 in the small intestine of a mouse. [53]

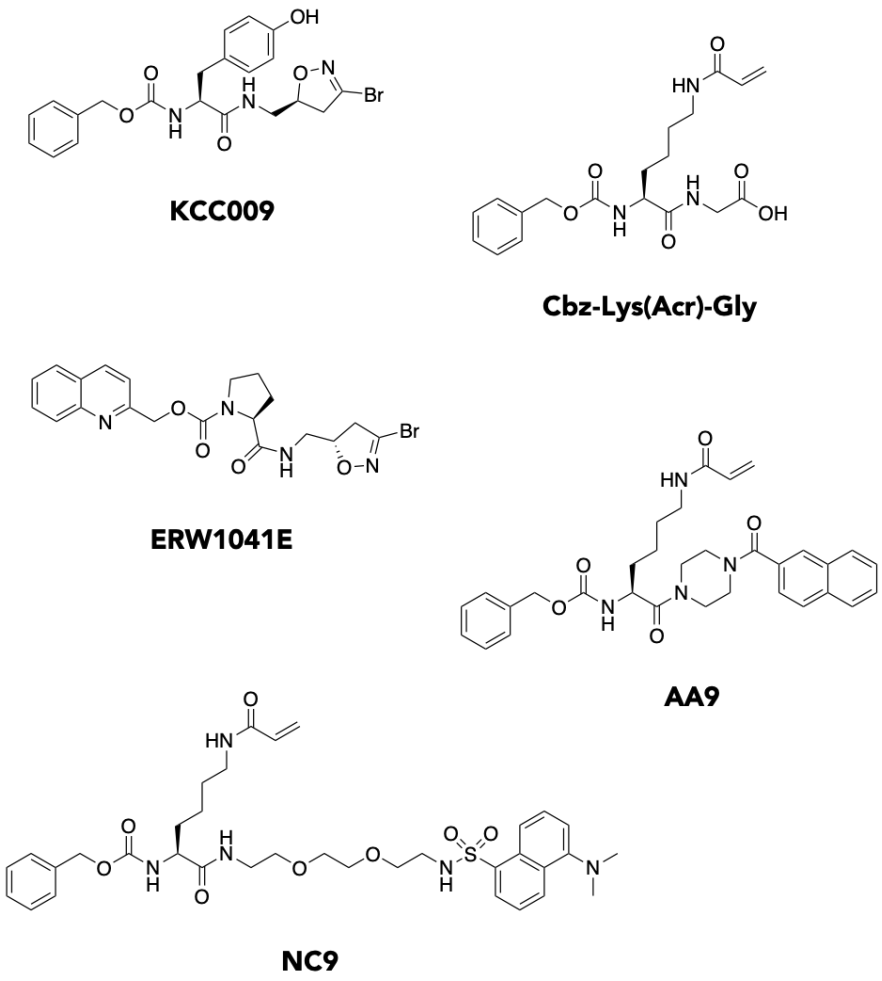

Scheme 1.3. Chemical structures of some targeted covalent inhibitors for TG2.

Further, the Keillor group has developed an inhibitor based on a well-known substrate, Cbz-Gln-Gly. They accomplished this by replacing the glutamine side-chain of said substrate with an acrylol group, yielding Cbz-Lys(Acr)-Gly, their most efficient irreversible inhibitor (k_{inact}/K_I = 3.0 x 10^6 $M^{-1}min^{-1}$, K_I = 150 nM against guinea pig liver TGase (gplTG) as a model for TG2). [54] They further derivatized this inhibitor to obtain **NC9**, which has a lower efficiency (k_{inact}/K_I = 1.4 x 10^4 $M^{-1}min^{-1}$, K_I = 29 μM against gplTG) but could be used as a probe in cellular studies for TG2 localization

because of its fluorescent dansyl group. [54] NC9 was shown to show some promising biological activity, so it was considered to be a 'hit' compound, and was further optimized into **AA9** (k_{inact}/K_I = 101 x 10^3 $M^{-1}min^{-1}$, K_I = 8.9 μM against TG2). [55] At this point, the Keillor group possesses a library of compounds that have been tested with respect to pharmacodynamics (reactivity with TG2). Considering the promising pharmacodynamic profiles with respect to enzyme kinetics of these compounds, it became evident to us that we needed to assess their pharmacokinetic properties as well. A list of names and structures for the compounds evaluated in this thesis are presented in appendix A.

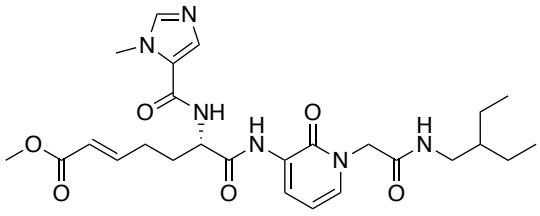

Scheme 1.4. Compound ZED1227, the first TG2 inhibitor to reach phase I clinical trials for the treatment of celiac disease.

Lastly, in recent years, Zedira GmbH have passed one of their irreversible inhibitors, ZED1227, into phase 2a clinical trials for the treatment of celiac disease. [56] This is the first direct-acting transglutaminase blocker to reach clinical trials.

1.6 Goal of the Research Presented Herein

The primary goal of the research presented herein was to develop methods for assessing the pharmacokinetic profiles of targeted covalent inhibitors (TCIs) for human tissue transglutaminase. A clear understanding of the pharmacokinetic properties of compounds is beneficial as it allows for optimization of compounds where need be, to make them suitable for *in vivo* applications and clinical contexts. Overall, the research presented may be divided into two categories as described below.

1.6.1 Cell permeability

In order for a drug to reach its target inside living cells, it has to be able to first cross the cell membrane. Over the course of this work, we adapted a parallel artificial membrane permeability (PAMPA) assay procedure as a means to measure passive diffusion of our inhibitors through a simulated cell membrane.

1.6.2 Off-target reactivity

Our TCIs possess an electrophilic warhead that may be susceptible to reactions with other abundant nucleophiles in cells, such as glutathione. Over the course of this work, we adapted and optimized a procedure to estimate the susceptibility of inhibitors to glutathione addition.

Chapter Two: **Cell Permeability**

2.1 Drugs and the Cell Membrane

As we know, a universal feature of cell membranes is a 10-nm thick phospholipid bilayer. Spanning this bilayer or attached to the outer or inner leaflets are glycoproteins that may act as ion channels, receptors, intermediate messengers (G-proteins) or enzymes. [57] Cells take up molecules and ions from the extracellular matrix, creating a constant flow in and out. Paradoxically, the relative concentrations and phospholipid bilayers prevent essential ions from penetrating the cell. To overcome these challenges, molecules move across the cell membrane by utilizing various different modes of transport. Generally speaking, said modes of transports are divided into two main categories, namely, active transport and passive transport. The latter is more relevant to drugs.

2.1.1 Modes of Transport Across the Cell Membrane

2.1.1.1 Active Transport

Active transport refers to the movement of molecules or ions across the cell membrane in an energy-dependent manner. Generally speaking, this applies to molecules that move against their concentration gradient, thus requiring energy. Two types of active transport have been characterized: primary active transport that utilizes ATP, and secondary active transport that utilizes an electrochemical gradient. [57]

2.1.1.2 Passive Transport

Passive transport refers to the movement of molecules or ions across the cell membrane in a manner through which no energy input is necessary. Contrary to active transport, there is no need for energy because it is driven by the tendency of the system to increase in entropy. Rates of passive transport are dependent on the permeability of the cell membrane, which, in turn, depends on the characteristics of the membrane lipids and proteins. Four kinds of passive transport have been identified: filtration, osmosis, simple diffusion, and facilitated diffusion. [57] Often, drugs permeate cells via facilitated diffusion, where molecules or ions are brought across the membrane through specific transmembrane integral proteins.

2.1.2 Drug Transfer Across the Cell Membrane

In pharmacokinetics (ADME), the cell permeability of compounds pertains to absorption and bioavailability, both of which were discussed in chapter I. Many drugs need to permeate one or more cell membranes in order to reach their site of action. Often, these compounds are weak acids or bases that may exist in either their ionized or electronically neutral states, depending on the pH. It is widely known that unionized forms of drugs are generally lipid-soluble, and readily diffuse through the cell membrane by dissolution in the lipid bilayer. The rate at which this transfer occurs, however, is dependent on the pKa of the drug in question. [58]

Only the unbound fraction of a drug in plasma is free to cross the cell membrane; drugs vary greatly in the degree of plasma protein binding. Practically speaking, the extent of this binding is of importance only if the drug is highly protein-bound (more than 90%). Albumin and globulins, both of which possess many binding sites, are known to bind drugs. The number and characteristics of their respective binding sites are determined by the pH of plasma. Overall, albumin has a tendency

to bind neutral or acidic drugs such as barbiturates, whereas globulins (particularly α−1 acid glycoprotein) are known to bind basic drugs like morphine. [59]

The ability of drug molecules to cross lipid bilayers by passive diffusion is tightly related to their ability to partition into and out of the hydrophobic membrane interior. A fairly but not excessively hydrophobic character is optimal for transport. More often than not, highly polar molecules will fail to penetrate the membrane, whereas extremely hydrophobic molecules will enter readily but fail to exit it, as illustrated in figure 2.1. [58]

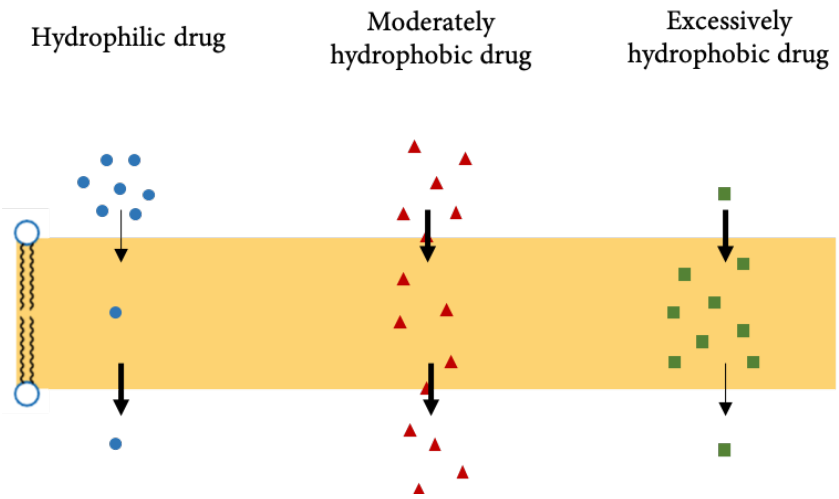

Figure 2.1. Passive diffusion of drugs across the cell membrane. Bold arrows indicate favourable transfers.

One may improve the ability of a drug to cross lipid bilayers by removing charged or polar functional groups. However, structural changes may cause a shift in the observed pharmacological effects, as discussed in chapter I. Alternatively, one may improve the membrane penetration of a drug by turning it into a prodrug, in which polar or ionizable groups are masked with hydrophobic

residues such as esters. After uptake, these hydrophobic groups are enzymatically cleaved in order to release the active drug. [58]

While passive diffusion is the most common mode of drug transport across cell membranes, many drugs, and in particular drug metabolites, are also subject to protein-mediated active or passive transport. An important class of membrane proteins involved in drug transport are the so-called ABC (ATP-binding cassette) transporters. ABC transporters are prominently found within the small intestine, the liver, the kidneys, and the blood brain barrier. Typically, they oppose the intracellular accumulation of drug molecules by extruding them back out of the cell, for example into the gut lumen or into the blood stream. They often have rather broad substrate specificities, allowing them to transport/extrude a rather large number of drugs. However, they are also known to play a crucial role in the development of multidrug resistance because of increased expulsion of the drug from the cell. [60]

Lastly, organic cation transporters and organic anion transporters are other major types of membrane proteins involved in drug transport, particularly in the kidneys and the liver. Although they are not driven by ATP, some are powered by ion co-transport or antiport; that is, they perform secondary active transport. Like ABC transporters, organic anion and cation transporters tend to have broad substrate specificities. [61]

2.1.2.1 Lipinski's Rule of Five

Lipinski's rule of five (RO5) is a rule of thumb used to estimate the druglikeness of a compound. In simple terms, it allows us to estimate whether a chemical compound with a certain pharmacological or biological activity has the chemical and physical properties necessary to make

it orally active as a drug in humans. The rule was formulated by Christopher A. Lipinski in 1997, based the observation that most orally administered drugs are relatively small and moderately lipophilic molecules. [62] While it gives no indication on the pharmacological activity of compounds, it describes molecular properties important for a drug's pharmacokinetic properties (ADME) in the human body. The rule is important to keep in mind throughout the drug discovery process when a pharmacologically active lead structure is optimized step-wise to increase the activity and selectivity of the compound as well as to ensure drug-like physicochemical properties are maintained as described by Lipinski's rule. Candidate drugs that conform to the RO5 tend to have more success in clinical trials, therefore they have an increased chance at reaching the market.

Lipinski's rule states that an orally active drug should have no more than one violation of the following four criteria: 1) no more than five hydrogen bond donors, that is the total number of N-H and O-H bonds, 2) no more than ten hydrogen bond acceptors, that is all nitrogen or oxygen atoms, 3) a molecular mass inferior to five hundred Daltons, and 4) an octanol-water partition coefficient, Log P, not greater than five. All numbers are multiples of five, hence the name of the rule. As with many other rules of thumb, there are several exceptions to Lipinski's rule. [63]

2.1.2.2 Expanding on Lipinski's Rule

While Lipinski's rule has served as the main guide for the correlation of physical properties with successful drug development, all while relating to oral bioavailability, certain limitations exist. First and foremost, there is a lack of quantitative assessment of oral bioavailability in the data analyzed. Further, they assume that all orally administered drugs are intended to be absorbed, and that oral bioavailability is generally high for orally administered drugs. Finally, the rules disregard the fact that many properties other than bioavailability, such as crystallinity, ease of formulation,

chemical stability, and practical availability by synthesis or isolation, all have some degree of importance in the choice of a compound for drug development. [64]

To expand on Lipinski's rules, other properties have been discussed with respect to oral bioavailability. Navia has suggested that molecular flexibility is beneficial to membrane permeation, and by extension, to bioavailability. [65] Hirschmann has suggested that water complexation by amide bonds is a negative contributor to oral bioavailability. [64] Lastly, a high polar surface area was recognized to have a negative impact on intestinal absorption. [66]

2.1.2.3 Veber's Rule

In 2002, Veber *et al*. looked at bioavailability measurements in rats for over 1 100 drug candidates in order to examine the importance of molecular properties that were thought to influence druglikeness. [64] Their examination put into question the 500 g/mol molecular weight cut-off proposed by Lipinski, as it did not significantly separate compounds with poor oral bioavailability from those with acceptable values. They found that reduced molecular flexibility, as measured by the number of rotatable bonds, and low polar surface area or total hydrogen bond count (sum of donors and acceptors) are important predictors of good oral bioavailability, in a way that is independent of molecular weight. Overall, their observations suggested that compounds that meet only the two following criteria: 1) ten or fewer rotatable bonds, and 2) polar surface area equal to or less than 140 $Å^2$ (or 12 or fewer H-bond donors and acceptors), will have a high probability of good oral bioavailability in rats. [64]

2.2 *In vitro* Methods for Examining Cell Permeability (Absorption)

As a constant, membrane permeation is recognized as a common requirement for oral bioavailability in the absence of active transport, and failure to achieve this usually results in poor oral bioavailability. In the early stages of drug discovery, it is important that compounds be evaluated for cell permeability as an indication of absorption. Compounds that are not able to be absorbed are virtually useless in clinical contexts.

2.2.1 Cell Layer Based Methods

The first practical method to be developed for assessing *in vitro* permeability in the drug discovery process was the cell layer method. This type of assay aims to model the epithelial cell layer permeability barrier that compounds encounter in the small intestine. Caco-2, an immortal human carcinoma cell line, is the best known and most widely used cell line for this assay. [67] Desirable aspects of this cell line are its morphology and multiple permeability mechanisms. Caco-2 develops microvilli on its apical surface that resemble the morphology of GI epithelial cells that line the intestinal villi. These cells also express cell membrane transporters on the apical surface, such as P-glycoprotein (Pgp), breast cancer resistant protein (BCRP), and multidrug resistance protein 2 (MRP2). This provides the opportunity to investigate various permeability mechanisms. [68]

Typically, in these assays, cells are plated in the insert of a device called the cell culture insert. The cells settle into a porous filter support and grow to confluence over the course of 21 days, covering the surface of the support. Ideally, cells will form a monolayer, but a mix of monolayers and multilayers might form. Most importantly, there should be no gaps, otherwise test compound will be free to pass through the porous filter. [69]

A variety of permeability experiments can be performed using this arrangement, the simplest of which consists of placing the test compound in buffer on the apical (A) side of the membrane and having buffer without test compound on the basolateral (B) side. The test compound can then diffuse from the apical compartment through the cells and into the basolateral compartment. Aliquots from the two compartments can be removed at specific time points and their concentrations can be measured by HPLC or LC/MS techniques, allowing for calculation of the rate of permeation ($P_{A>B}$). These experiments may also be done under different conditions with respect to pH, so as to mimic different parts of the GI tract. [69]

The experiment described above (apical to basolateral) provides a value for permeability in the absorptive direction, which models absorption in the GI tract. As such it can assist in the prediction of *in vivo* absorption of compounds. The reverse experiment can also be done (basolateral to apical), and allows us to study the permeability of test compounds by cell membrane transporters ($P_{B>A}$). When $P_{A>B}$ and $P_{B>A}$ are identical, it typically indicates that permeation happens via passive diffusion. [69]

The main drawback of cell layer based permeability assays have to do with reproducibility. Caco-2 data are not likely to completely agree between experiments, because there can be divergences in the characteristics of the cell lines, culturing conditions (e.g. serum source, frequency of media changes), and practice (e.g. experimental apparatus, percent DMSO, media components). As such, while trends are usually similar, the actual permeability values themselves may differ. [69]

2.2.2 Artificial Membrane Based Methods

The parallel artificial membrane permeability assay (PAMPA), as invented by Kansy *et al.* [70], is advantageous because although it is slightly less relevant, it reduces the cost and increases the

throughput of permeability assays. Instead of using living cells as barriers, the PAMPA barrier is often made up of phospholipids (e.g. phosphatidyl choline) solubilized in a long-chain hydrocarbon (e.g. dodecane). In the context of the research presented herein, this was the technique of choice.

2.3 Parallel Artificial Membrane Permeability Assay (PAMPA)

PAMPA is a screening technique used to estimate passive diffusion permeability (transcellular permeation) with no consideration of active transport. [70] Typically, the apparatus used to conduct these experiments consists of a donor compartment and an acceptor compartment, which are separated by a porous filter onto which the artificial membrane is placed, as illustrated in figure 2.2. Multi-well plate "sandwiches" have been designed for high-throughput operation.

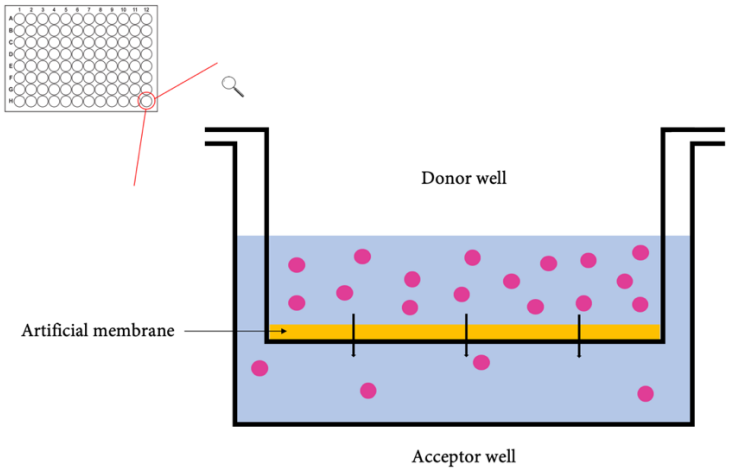

Figure 2.2. Schematic of the PAMPA setup. Artificial membrane mixture in placed at the bottom of the donor wells (filter plate). Blank aqueous buffer in placed in the acceptor wells, and compound dissolved in buffer is placed in the donor wells. Molecules diffuse from the donor wells through the artificial membrane and into the acceptor wells.

The acceptor compartment is typically filled with blank aqueous buffer, and the donor compartment contains the donor solutions, which are prepared by diluting test compounds in aqueous buffer. A few microlitres of an artificial membrane solution are placed onto the porous filter and soak down into the holes of said filter to form the artificial barrier, at the bottom of the donor compartment. The "sandwich" is kept at a constant temperature and humidity for a duration of 1 to 18 hours, depending on the protocol followed and the permeability of the compounds. Samples may be taken from both the acceptor wells and the donor wells, and the concentration of compound in the wells may be measured using an LC/MS, LC/ultraviolet (UV), or a UV plate reader instrument. The unused "donor solution" that was not placed in the donor wells can be used as a standard for measuring the concentration of compounds in the donor and acceptor wells, to calculate the permeability. The permeability often is termed effective permeability (P_e). [69]

Like Caco-2, there are several different ways in which PAMPA may be used. Variations are similar between the two different assays. Sometimes, the assay is run with the same pH on each side of the barrier. Other times, the pH is neutral on the acceptor side and lower on the donor side, to simulate the GI tract. Further, various different artificial membrane mixtures have be used, such as 2% phosphatidylcholine in dodecane, 20% egg lecithin in dodecane, and hexadecane alone. Various thicknesses of barriers have also been used with different filter supports. All of these conditions affect the data but allow modification of the experiment to model a specific set of conditions of interest. [69]

One of the biggest advantages of PAMPA is that no cell culture maintenance is required. The artificial barrier is created rather quickly at the time of the experiment. Further, plate readers may be used as detection methods, rendering the assay high throughput. While PAMPA can only serve

as a measure of passive diffusion, it still provides a way to evaluate this important property independent of other permeability mechanisms. Lastly, it has been shown to correlate to human jejunal permeability with approximately the same reliability as Caco-2. As such, it allows for some degree of long-distance projection to *in vivo* absorption. [69]

2.4 Methodology

In order to study the cell permeability of our compounds, we were inspired by a protocol routinely used by Millipore, based on work published in the *Journal of Medicinal Chemistry* and the *European Journal of Pharmaceutical Sciences*. In their efforts to predict drug passive, transcellular permeability in early drug discovery, Wohnsland and Faller [71] and Bujard *et al*. [72], developed a new hexadecane membrane (HDM)-PAMPA technique protocol using high-throughput screening. Because their primary goal was centred around assay development, they used a variety of well-known, characterized, marketed drugs as controls. In essence, their artificial membrane solutions were made up of 5% hexadecane in hexanes, which they placed in the donor wells of their microtitre polycarbonate (PC)-filter plate. To allow for evaporation of the hexanes, the plate was placed in a fume hood with constant shaking for one hour. They placed blank buffer in the lower acceptor compartment, and test compounds diluted in buffer went in the upper donor compartment. The resulting sandwich was incubated at room temperature, with constant shaking at 75 rpm, over the course of four hours. After incubation, the sandwich was disassembled, and the acceptor and donor wells were transferred to a 96-well black plate and analyzed by UHPLC-UV. Log P_e values were calculated as reported by Wohnsland and Faller. [71]. The calculation is described in section 2.4.2.

2.4.1 Assay Materials and Setup

The cell permeability of our inhibitors was tested by incubating our inhibitors in the PAMPA set up described above, using Millipore MultiScreen filter plates (MPC4NTR10, 0.4 μM PCTE filter). Physiologically relevant conditions were modelled by using 14 mM KH_2PO_4 and 54 mM Na_2HPO_4 buffer at pH 7.4. A solution of 5% v/v hexadecane in hexanes was prepared, and 15 μL was placed at the bottom of the upper porous donor compartment. The 96-well filter plate was left in the fume hood for one hour with constant shaking such that the hexanes would evaporate, leaving a uniform layer of hexadecane at the bottom of the wells. Blank buffer (200 μL) was placed inside the lower acceptor compartment in the presence of DMSO (5% v/v), and the dried filter plate (donor compartment) was placed on top. Test compound solutions in buffer were placed into the donor compartment in the presence of DMSO (5% v/v), making up a total volume of 150 μL. A lid was placed on top of the donor compartment and the sandwich was placed in a closed container at the bottom of which a wet paper towel was carefully placed, in order to maintain humidity and limit evaporation. This entire assembly was incubated over the course of 5 hours at 37 °C, with constant shaking at 75 rpm. After incubation, the contents of the acceptor compartment were transferred into a different 96-well plate and absorbances were read using a BioTek Synergy H4 hybrid microplate reader. In a separate 96-well plate, solutions at theoretical equilibrium, that is the resulting concentration if the donor and acceptor compartments were simply combined, were prepared and analyzed similarly.

2.4.2 Log P_e Calculation

The rate of permeation is reported as Log P_e, (not to be mistaken with Log P, the octanol-water partition coefficient). Log P_e values can be calculated from the following equation as reported by Wohnsland and Faller. [71]

$$\log P_e = \log\left[C * -\ln\left(1 - \frac{A_{acceptor}}{A_{equilibrium}}\right)\right]$$

$$\text{where } C = \frac{V_D V_A}{(V_D + V_A) * Area * Time}$$

In this equation, V_D is the volume of the donor compartment (0.200 cm^3), V_A is the volume of the acceptor compartment (0.150 cm^3), Area is the active surface area of the membrane which is defined as the product of the membrane area and the porosity (24 cm^2 × 20% = 0.048 cm^2, value provided by the manufacturer), Time is the incubation time for the assay (18 000 s), $A_{acceptor}$ is the measured absorbance of the compound in the acceptor compartment, and $A_{equilibrium}$ is the measured absorbance of the compound at theoretical equilibrium. As such, the rate of permeation relates to the concentrations used as well as the area of membrane. As a general rule, there are benchmark Log P_e values that are associated to low, moderate and high permeability of compounds (figure 2.3). These benchmarks can be useful for comparison purposes. [69]

Figure 2.3. Benchmark Log P_e values.

2.5 Results and Discussion

2.5.1 Control Experiments

Controls for PAMPA were chosen such that a broad range of Log P_e values would be covered. The chosen marketed drugs [72] as illustrated in figure 2.3 were ketoprofen, ibuprofen, carbamazepine, lidocaine, and imipramine, whose absorbance maxima ranged from 260 to 285 nm (λ_{max} values were measured using a Cary UV-VIS spectrophotometer). Because these wavelengths were well within the range at which polystyrene 96-well plates absorb, we opted to use UV-transparent 96-well plates, which were suitable for analyses at the wavelengths required.

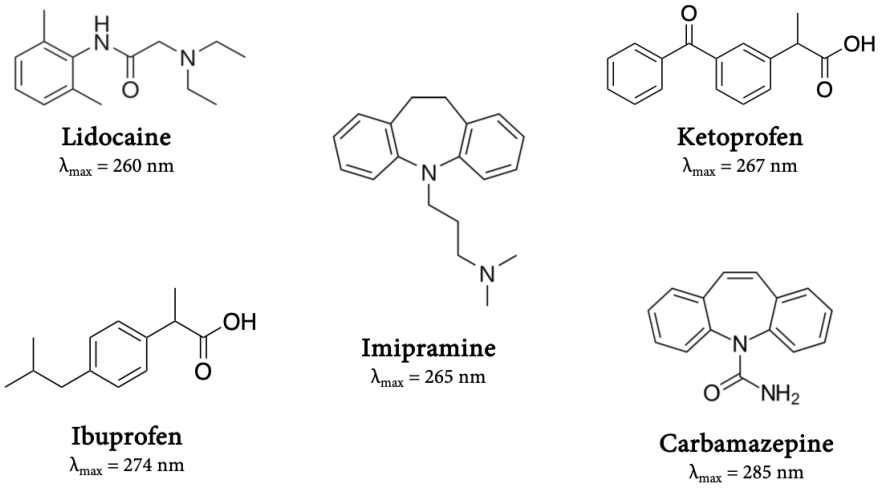

Figure 2.4. Chemical structures and absorbance maxima wavelengths for the chosen PAMPA controls

Additionally, the assay concentrations for certain controls needed to be increased for detection purposes. Certain compounds intrinsically do not absorb as intensely as others, and low permeability profiles evidently result in low acceptor solution concentrations. These factors can

result in the inability to detect a given compound. 265 nm was the wavelength of choice for the validation of our PAMPA protocol, because each control absorbs sufficiently at that wavelength.

Table 2.1. PAMPA control experiment results. The experimental Log P_e values of five marketed drugs were measured and compared to literature reported values.

Control	[Control] (μM)	Reported Log P_e [72]	Experimental Log P_e
Ketoprofen	400	-5.50	-5.6 ± 0.1
Ibuprofen	400	-4.65	-4.3 ± 0.1
Carbamazepine	100	-3.92	-3.91 ± 0.05
Lidocaine	400	-3.75	-3.64 ± 0.01
Imipramine	200	-3.70	-3.79 ± 0.03

The experimental Log P_e values of five marketed drugs were measured in triplicates, in the presence of 5% DMSO, using the PAMPA protocol described in section 2.4.1. As seen in table 2.1, the experimental results are not significantly different than the Log P_e values that have been previously reported in the literature (statistical analysis was done using a one-value Student's t-test; example shown in appendix B). [72] Given that all of our relative errors are below 5%, we can comment with confidence that the method is precise. Overall, we succeeded at optimizing and validating a PAMPA protocol using hexadecane as our artificial membrane and a microplate reader as our detection method.

2.5.2 Investigating the Effect of DMSO on Membrane Permeability

DMSO is considered a small amphiphile, making it susceptible to rapid incorporation at the lipid-water interface of membranes. It is known that DMSO causes a hydrophobic membrane to become floppier, which could enhance permeability. In fact, its powerful ability to increase skin permeability has been exploited for applications in topical or transdermal drug delivery. [73] Knowing that one of our inhibitors, VA4, displays very low aqueous solubility (20 % v/v DMSO required to dissolve it), we sought to investigate whether DMSO concentrations have an effect on the membrane permeability of compounds in PAMPA. For this purpose, we tested our least permeable control, ketoprofen, in the presence of increasing concentrations of DMSO ranging from 5 to 20 % v/v. Log P_e values were calculated and compared with each other (data presented in table 2.3).

Table 2.2. Investigating the effect of DMSO concentration on Log P_e values. Ketoprofen was run in triplicates through PAMPA assays at a concentration of 400 μM in the presence of 5, 10, 15 and 20% DMSO respectively. Absorbances of theoretical equilibrium (172 μM) and acceptor solutions were measured at 265 nm using a microplate reader, and Log P_e values were subsequently calculated and compared.

% DMSO	Log P_e
5	-5.9 ± 0.2
10	-6.2 ± 0.2
15	-6.7 ± 0.7
20	-5.9 ± 0.3

Overall, this experiment showed no significant difference in between calculated Log P_e values for increasing DMSO concentrations ranging from 5 to 20 % v/v, as determined by statistical analysis with a Student's t-test (example shown in appendix B) to compare two experimental means. As such, we can justify comparing permeability profiles of different inhibitors that would require testing in the presence of larger concentrations of DMSO for solubility purposes, in particular VA4.

2.5.3 Switching Detection Methods – HPLC-UV

When the time came to test our inhibitors, we quickly realized that a microplate reader would not serve as a suitable instrument for the detection of our inhibitors, because the vast majority of our compounds absorbed so weakly at wavelengths below 260 nm. As such, we reverted to using reversed-phase HPLC with UV detection (method described in appendix B). To ensure reproducibility between detection methods, we sought to test one of our controls and compare results obtained with the microplate reader and the HPLC-UV. We initially chose to test our least permeable control, ketoprofen, through PAMPA using HPLC-UV detection and saw that that the compound may have been degrading over time, as seen in figure 2.5.

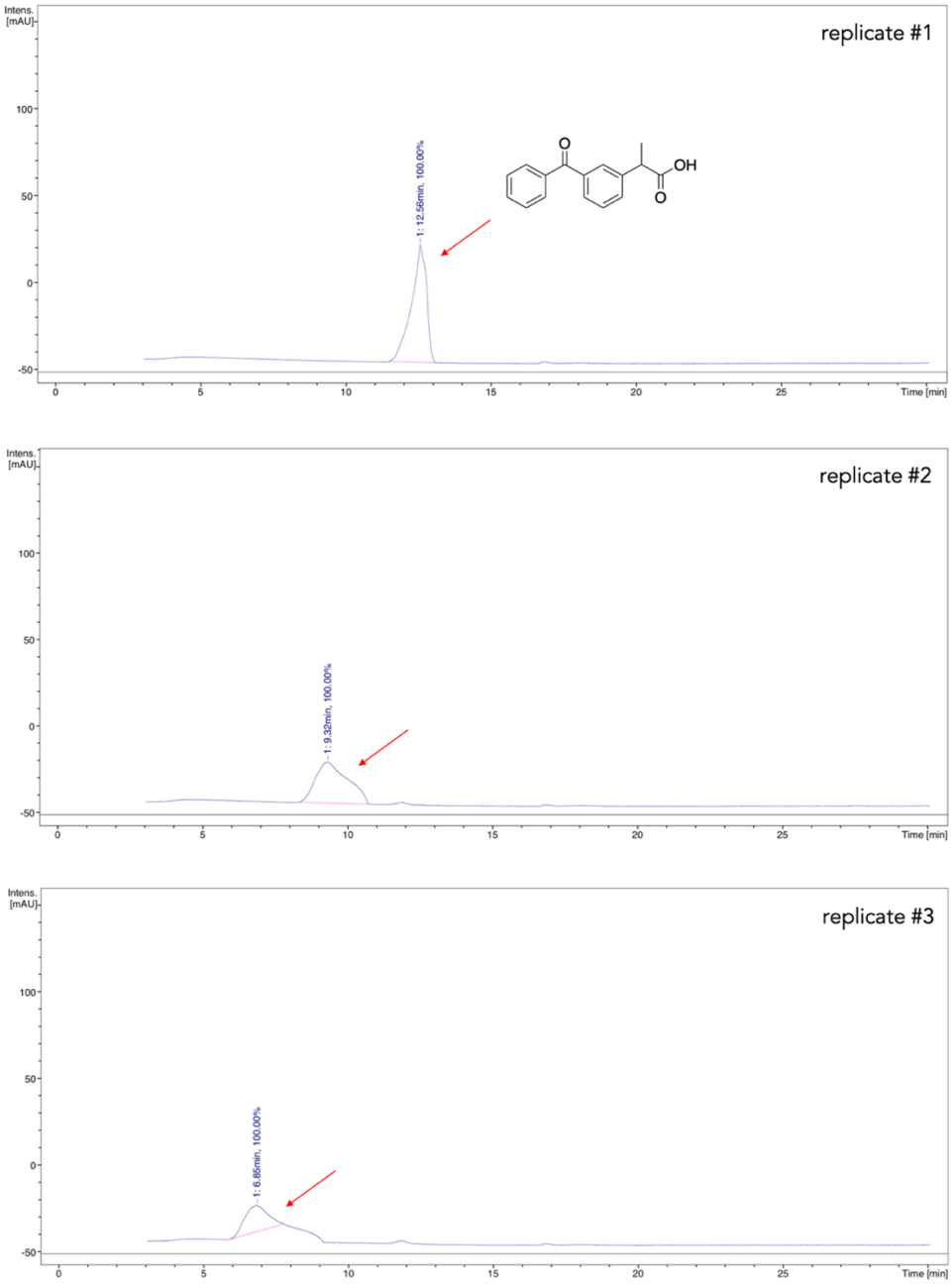

Figure 2.5. Ketoprofen is unstable over time. Theoretical equilibrium solutions of ketoprofen (214 µM) in aqueous buffer (14 mM KH_2PO_4 and 54 mM Na_2HPO_4, pH 7.4) were prepared in triplicate and then analyzed by HPLC-UV at 260 nm. Replicates were run approximately 30 minutes apart (the time of one run).

We hypothesized that ketoprofen, possessing a benzophenone group, could be susceptible to photoreduction over time in buffered solution. Upon researching the literature, we found that on exposure to light in aqueous buffer, ketoprofen has been reported to undergo a decarboxylation process, producing radical derivatives and photoproducts. [74] More specifically, spectroscopic studies have found that the main product yielded under aerobic conditions is 3-benzoylphenylethane. [75] In fact, photodecarboxylation of ketoprofen proceeds by two pathways being the formation of a benzylic radical, and the formation of a benzylic carbanion. [76] This could explain the broadening and shifting of its corresponding peak by HPLC-UV analysis. As such, ketoprofen was not a reliable control for the validation HPLC-UV as an appropriate detection method for PAMPA.

We then evaluated lidocaine, imipramine, ibuprofen and carbamazepine by HPLC-PAMPA. We found that lidocaine, imipramine, and ibuprofen all showed no significant peaks on their respective chromatograms (data not shown). This likely had to do with their ionization states at physiological pH, because lidocaine and imipramine possess tertiary amines (pKa ~10.75 for the protonated species) and ibuprofen possesses a carboxylic acid (pKa ~4.5). While modifications to the HPLC method could have been useful to remedy this, we found that the electronically neutral carbamazepine showed a nicely defined peak on its chromatogram at a retention time of 13.04 minutes, using a wavelength of 285 nm, as seen in figure 2.5.

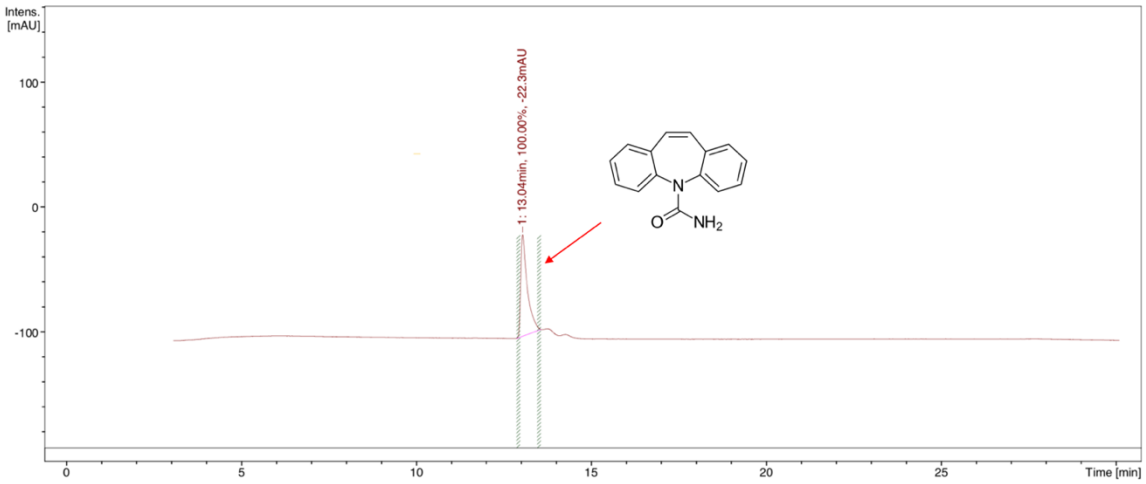

Figure 2.6. HPLC trace of carbamazepine. A solution of carbamazepine at theoretical equilibrium (214 µM) was prepared in aqueous buffer (14 mM KH_2PO_4 and 54 mM Na_2HPO_4, pH 7.4) and analyzed by HPLC-UV at 285 nm.

We concluded that carbamazepine would be a reliable control for the validation of HPLC-UV as suitable detection method for PAMPA. As such, we ran the assay, and utilized the peak areas in the calculation of a Log P_e value equal to -4.07 ± 0.03 for carbamazepine. This value is similar to our previous experimental value of -3.91 ± 0.05, determined using the microplate reader. Even further, our experimental results match well with the literature reported value of -3.92 [72], once again validating the assay as well as HPLC-UV as an appropriate detection method for PAMPA.

2.5.4 Testing Our Compounds – Preliminary Results

Having validated HPLC-UV as a reliable detection method for PAMPA, we could now move on to testing our inhibitors in our optimized assay conditions. All inhibitors were tested in the presence of 5% v/v DMSO unless stated otherwise. Compounds NC9, VA4 and AA9 were evaluated for

cell permeability with success. Their log P_e values were calculated to be -5.26 ± 0.01, -4.66 ± 0.04, and -6.5 ± 0.5 respectively, as seen in table 2.3.

Table 2.3. PAMPA results for some of our inhibitors. Entry 1 was tested using the microplate reader prior to switching detection methods, because it possesses a dansyl group that absorbs strongly at 330 nm. Entry 2 was tested in the presence of a higher concentration of DMSO (20% v/v) due to its low aqueous solubility.

Entry number	Compound	Assay concentration (μM)	Experimental Log P_e
1	NC9	500	-5.26 ± 0.01
2*	VA4	100	-4.66 ± 0.04
3	AA9	400	-6.5 ± 0.5
4	NM-III-46	150	n.d.
5	NM-III-72	150	n.d.
6	NM-V-12	500	n.d.
7	NM-V-14	500	n.d.
8	NM-V-36	500	n.d.

* 20% DMSO

While clear detection was possible for entries 4 to 8 at their theoretical equilibrium concentrations (data shown in appendix B), nothing could be detected in their respective acceptor solutions (data not shown). This was an indication that their membrane permeability was lower than that of AA9, meaning that their Log P_e values were even lower than -6.5. If we wanted to measure an accurate Log P_e value, we could increase the assay concentration such that the acceptor solution would be more concentrated.

To re-iterate, we were able to adapt, optimize and validate a PAMPA protocol using a hexadecane artificial membrane with two different detection methods – a multiplate reader and an HPLC-UV. Experimental conditions were optimized, and the method was validated using five well characterized and marketed drugs being ketoprofen, imipramine, lidocaine, ibuprofen and carbamazepine. Further, we have tested some of our inhibitors and confirmed that the Log P_e values for NC9, VA4 and AA9 are just above or surrounding -6.0, which is borderline for moderate permeability. As we know, moderate permeability profiles are associated to Log P_e values ranging from -5.70 and -4.70. Compounds displaying Log P_e values below -5.70 are considered to have low permeability.

Having taken a literature method, adapted it for use in the Keillor group, and defined a procedure that can be used routinely for future inhibitors to be developed in the group, we can conclude that the primary goal of this project was successfully attained. This method will not only allow for the assessment of future compounds; it will also act as a tool to guide the optimization of chemical structures for the amelioration of their pharmacokinetic profiles, and by extension, their potential for more advanced drug development.

Chapter Three: **Off-target Reactivity**

3.1 Off-target Effects of Drugs

In pharmacology, an off-target is commonly defined as a receptor, enzyme, or other biological target that, when affected by a drug, causes undesirable side-effects. If a drug is capable of binding to unexpected targets that alter pathways different from the one intended, severe downstream effects may occur. An example of this is the drug doxorubicin, a very effective anti-cancer drug that causes congestive heart failure while treating tumours. [77] Doxorubicin is an uncoupling reagent that inhibits the proper function of complex I of the electron transport chain in mitochondria, thus leading to the production of reactive oxygen species and the inhibition of ATP production. The toxicity observed is seemingly restricted to cardiac tissue, although some toxicity has been reported in other tissues as well. [77]

In the process of drug design and development, it is crucial that pharmaceutical companies ensure that drug candidates do not show significant activity at any of a range of off-targets, most of which are discovered by chance. However, even if off-target reactivity receives a negative connotation because of its occasional contribution to undesirable side effects and/or toxicity, in some cases it can be taken advantage of for therapeutic purposes. Historically, pharmaceutical companies have found great success by repurposing (or repositioning [78]) drugs as a result of there being side effects. One popular example of this is Pfizer's Viagra [78], originally created to treat angina but later repurposed for treating erectile dysfunction. Another widely known example is Celgene's thalidomide [78], first used as a sedative and hypnotic, then used to alleviate morning sickness, and later repurposed for the treatment of leprosy and multiple myeloma.

3.2 Thiols as Biological Off-targets

Cysteine is one of the least abundant amino acids, yet it is routinely found to be a highly conserved residue within functional (regulatory, catalytic or binding) sites in proteins, as conveniently exemplified by TGases. Among the side chains of the 20 natural amino acids, the thiol group of cysteine has the highest nucleophilicity, making it susceptible to modification by compounds with electrophilic functional groups such as Michael acceptors, as depicted in scheme 3.1. [79] This unique reactivity of cysteine gives functional sites their specialized properties with respect to nucleophilicity, high affinity metal binding, and/or ability to form disulphide bonds.

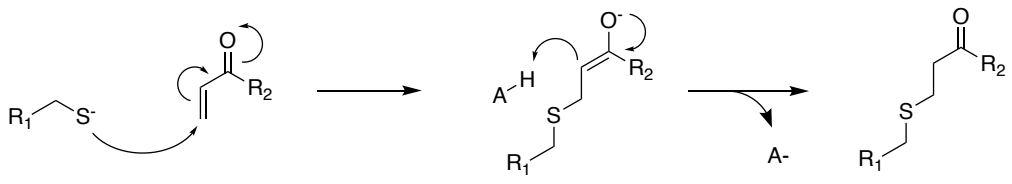

Scheme 3.1. Reaction mechanism for a thiolate reacting with an acrylamide at physiological pH.

3.3 Protein Thiols

Mammalian tissues are rich in protein thiols, with concentrations ranging from 20 to 40 mM. Many intracellular proteins are known to undergo thiol group modification. Protein cysteines may be oxidized to free thiols, intra or interprotein disulphides, nitrosothiols and sulphenic, sulphinic or sulphonic acids. In the highly reduced environment of the cytosol, because of high intracellular concentrations of GSH and the GSH/GSSG ratio of 30-100, cysteines of cytosolic proteins are predominantly in the form of free thiols. [80] On the other hand, extracellular proteins are mainly found as disulphides due to the oxidative environment. Though proteins on plasma membrane are at the interface between an oxidising and reducing environment, many studies have shown the

presence of exofacial protein thiols, which are kept in their reduced state by protein disulphide isomerases. [81]

Albumin is by far the most abundant protein found in plasma, making up more than 50% of the total plasma protein. The thiols in the body, especially those present on proteins, are considered major plasma antioxidants – most of them are present over albumin. The Cys-34 residue of albumin accounts for the majority of free thiol in plasma. [82] Given its pKa value of 5, at physiological pH, albumin-Cys34 exists for the most part as a thiolate anion that is highly reactive with metals, thiols, and disulphides. Being a carrier protein, albumin is also known to carry other thiols (e.g. glutathione and cysteinylglycine) along with other metabolites. Albumin is a relevant thiol for off-target reactivity studies; however, it is outside the specific focus of this thesis.

3.3.1 Glutathione

Glutathione (GSH) is arguably among the most important antioxidants found in plants, animals, fungi and bacteria. This ubiquitous tripeptide (L-γ-glutamyl-L-cysteinylglycine, scheme 3.2) is usually the most abundant intracellular thiol, found at millimolar concentrations (0.5 – 10 mM). It is known to be multifunctional within many important biological phenomena including the synthesis of proteins and DNA, transport, enzyme activity, and metabolism. Furthermore, it is capable of preventing damage to cellular components under conditions of oxidative stress, where reactive oxygen species like peroxides, free radicals and heavy metals are present.

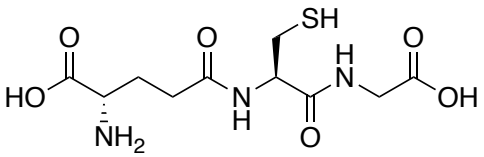

Scheme 3.2. Chemical structure of glutathione.

Eukaryotic cells have three major reservoirs of GSH being the cytosol (90%), mitochondria (10%) and small percentage in the endoplasmic reticulum. [83] The γ-glutamyl linkage allows for intracellular stability and the thiol group is required for GSH's functions. The peptide bond linking the *N*-terminal glutamate and the cysteine residue of GSH is through the γ-carboxyl group of glutamate rather than the conventional α-carboxyl group. This unusual arrangement resists degradation by intracellular peptidases and is subject to hydrolysis by only one known enzyme γ-glutamyltranspeptidase (GGT), which is on the external surfaces of certain cell types. Additionally, the *C*-terminal glycine moiety of GSH protects it from cleavage by intracellular γ-glutamylcyclotransferase. As such, GSH resists intracellular degradation and is only metabolized extracellularly. [80]

Within live cells, glutathione reduces disulphide bonds formed within cytoplasmic proteins to cysteines by serving as an electron donor. As a result, it is converted to its oxidized form, glutathione disulphide (GSSG). Upon oxidation, it can be reduced back by glutathione reductase, using NADPH as an electron donor. The ratio of GSH to GSSG within cells is often used as a measure of cellular oxidative stress. [80]

Because of its high abundance in cells, glutathione is an important off-target to consider in the drug development process. As mentioned in chapter 1, our targeted covalent inhibitors (TCIs) are equipped with an electrophilic acrylamide warhead. This warhead, which is meant to target the activated Cys277 residue located in TG2's active site, could potentially react with other free thiols in cells, like glutathione, in a Michael addition. If that were the case, the resulting adduct would likely be pumped out of cells and excreted, as glutathione conjugation is one of the possible Phase II reactions carried out in drug metabolism. That being said, if our compounds were to react quickly

with glutathione before being able to reach their intended target, no therapeutic effect would be observed, rendering them virtually useless in clinical contexts.

3.4 *In vitro* Methods for Examining Thiol Reactivity

3.4.1 Mass Spectrometry and Nuclear Magnetic Resonance Based Thiol Detection

The reactions of test compounds and GSH can be directly monitored using either mass spectrometry (MS) or nuclear magnetic resonance (NMR). These methods often employ quite laborious and time-consuming procedures. Additionally, since the number of primary hits usually surpasses the capacity of these methods, thiol reactivity assessment that can be applied to a high-throughput screening format is required.

3.4.2 Chromophore Based Thiol Detection

3.4.2.1 Fluorescent Probes for Thiol Detection

Among widely used methods for thiol reactivity assessments are fluorescence-based assays. One of them is a competitive binding assay using GSH and fluorescein-5'-maleimide; while this assay is very simple and easy to use, it requires kinetic measurements, giving it the disadvantage of not being high-throughput. [84] Another fluorescence method that can be made high-throughput was reported and implicates the fluorescence change of a thiol-containing probe caused by covalent modification with test compounds. [85] In recent years, another assay was developed and is based on the competitive reaction of a free thiol (e.g. glutathione) between test compounds and a fluorescent probe, *o*-maleimide BODIPY. [86] Lastly, several coumarin derivatives [87] as well as a chromene derivatives [88] have been reported as colorimetric probes to detect biological thiols.

3.4.2.2 Colorimetric Thiol Detection

Thiol reactivity assessments may also be achieved via colorimetric assays. As of late, the most popular chromogenic reagent used to do so is 5,5'-dithio-bis-(2-nitrobenzoic acid), also known as Ellman's reagent or DTNB. DTNB reacts with free thiols to release the chromophore 5-thio-2-nitrobenzoic acid (TNB), which can be analyzed spectrophotometrically. [89] Other reagents have also been reported useful in lieu of Ellman's reagent, one of them being 4,4'-dithiodipyridine (4-DPS). 4-DPS reacts with free thiols to release the chromophore 4-thiopyridone tautomer, also detectable via spectrophotometry. [89]

3.5 Colorimetric Glutathione Reactivity Assay Using Ellman's Reagent

As mentioned prior, the most widely used chromogenic reagent for thiol detection is DTNB. This compound possesses a highly oxidizing disulphide bond, which is stoichiometrically reduced by free thiols in an exchange reaction, yielding a mixed disulphide as well as one molecule of 5-thio-2-nitrobenzoic acid (TNB) as depicted in scheme 3.3 below.

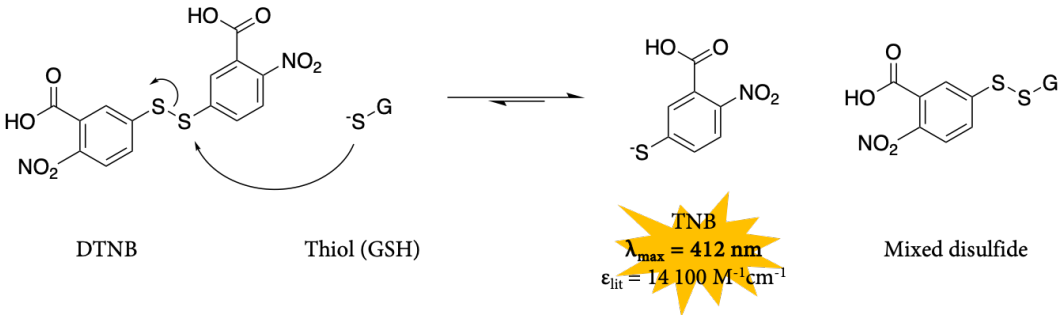

Scheme 3.3. Reaction of glutathione with Ellman's reagent.

TNB is an excellent leaving group with a thiol pKa of 4.5, effectively making it a thiolate at physiological pH. [89] While DTNB has weak absorption at 412 nm, the extinction coefficient for TNB is reported to be 14 100 $M^{-1}cm^{-1}$ at pH 7. The extinction coefficient value drops substantially at a lower pH, reflecting the protonation of the orange thiolate species. [89] Ellman's reagent has been found useful for measuring low-molecular mass thiols such as glutathione in both pure solutions and biological samples, such as blood. It may also be used to measure the number of thiol groups on proteins. [89]

In recent years, an emerging alternative to Ellman's reagent has been 4,4'-dithiodipyridine (4-DPS, scheme 3.4). The reduction of 4-DPS leads to the formation of the strongly absorbing resonance stabilized 4-thiopyridone tautomer, whose absorbance is pH independent (extinction coefficient 21 000 $M^{-1}cm^{-1}$ at 324 nm).[89]

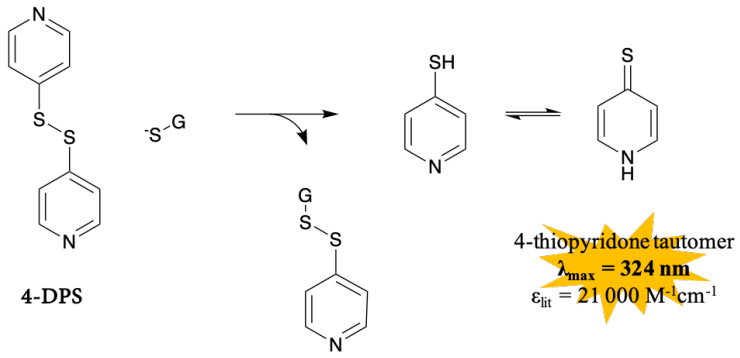

Scheme 3.4. Reaction of glutathione with 4-DPS.

While this is a clear advantage in favour of 4-DPS, the longer wavelength maximum for TNB over the pyridone product of 4-DPS, makes DTNB more suitable for the quantification of thiols in solutions that strongly absorb in the near UV. In addition, the electroneutral 4-DPS displays lower

solubility (~ 3 mM in water) compared to the dianion form of DTNB at pH 7. In this work, we used DTNB.

3.6 Methodology

With the aim to study the reactivity of our compounds with glutathione, we were inspired by work published in the *Journal of Toxicology Research* based on the assay routinely used by Pfizer. In their drug discovery efforts, Russel T. Naven *et al*. employed a high-throughput, plate-based assay using Ellman's reagent to determine the reactivity of cysteine-reactive compounds with glutathione. [90] In essence, they incubated test compounds with glutathione at room temperature and physiological pH. DTNB was used to determine the remaining thiol concentration after 60, 80 and 180 minutes. Thiols react with DTNB to form a mixed disulphide and TNB, whose concentration can be measured spectrophotometrically using a multi-well plate reader. This procedure was adapted for the assay described below.

3.6.1 Assay Materials and Setup

The reactivity of our inhibitors with glutathione was tested by incubating our inhibitors (100 μM) under physiologically relevant conditions, namely using 100 mM MOPS buffer at pH 7.4, with glutathione (100 μM). The mixture was incubated at 37 °C, and the remaining glutathione concentrations were measured hourly, over a period of 5 hours, by quenching the reaction with excess DTNB (1 000 μM). Absorbance was measured at 412 nm on a BioTek Synergy H4 hybrid

microplate reader, and back titration calculations were initially performed using an extinction coefficient of 14 100 $M^{-1}cm^{-1}$, as suggested by literature findings. [89]

3.6.2 Control Experiments

To validate DTNB as an appropriate reagent for the measurement of glutathione concentrations, we utilized *N*-methylmaleimide (NMM) as a positive control and DMSO as a negative control. *N*-methylmaleimide being a Michael acceptor is known to react quickly with free thiols such as glutathione in a Michael thiol addition reaction to yield a succinimide adduct, in a virtually irreversible manner (scheme 3.5). On the other hand, DMSO is not expected to participate in any reaction with glutathione.

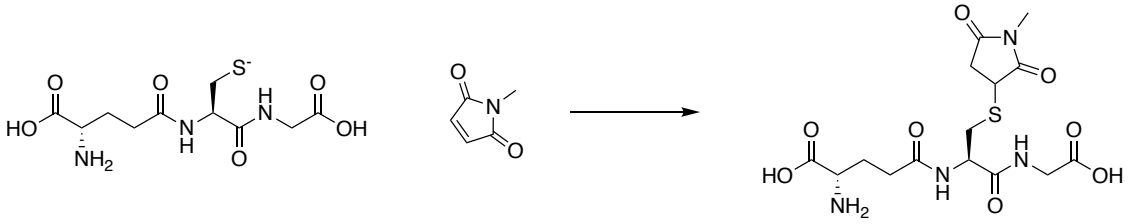

Scheme 3.5. Michael addition reaction of glutathione with N-methylmaleimide to yield succinimide adduct.

In our negative control experiment, 100 μM of GSH was incubated at 37 °C in the presence of DMSO (5% v/v) under physiologically relevant conditions, namely using 100 mM MOPS buffer at pH 7.4. The same conditions were maintained in the case of the positive control, with NMM and GSH incubated at equimolar concentrations (100 μM). Reactions were quenched with DTNB hourly over a 5-hour time period, and absorbances were measured at 412 nm. The negative control was expected to generate an absorbance signal corresponding to the totality of the glutathione

originally placed in solution (100 μM). On the other hand, the positive control was expected give us a corrected absorbance signal of zero at 412 nm, corresponding to a null concentration or glutathione. However, preliminary results from these controls did not corroborate our expectations. More specifically, we observed a steady decline in thiol concentration (data not shown), in the absence of inhibitor, which warranted further investigation.

3.6.2.1 Reaction Reaches an Equilibrium End-point

As our first step to investigate our confusing preliminary results, we opted to assess the stability of DTNB and glutathione at room temperature over the course of 24 hours. In an NMR experiment, both compounds were incubated (10 mM) at room temperature in deuterated methanol (MeOD) and deuterium oxide (D_2O) respectively. ^{1}H-NMR spectra collected at times zero and 24 hours revealed that the compounds were seemingly stable at room temperature, in their respective deuterated solvents (^{1}H-NMR spectra included in appendix C).

To clarify our peak assignments, we obtained COSY NMR spectra for GSH. The peaks situated at 2.0 ppm and 2.5 ppm were assigned to the glutamine methylene units, of which the methylene unit at 2.0 ppm is shown in the COSY spectrum to be coupled to the alpha-proton of the glutamine residue that appears at 3.7 ppm. The peak at 2.9 ppm was assigned to the methylene group of the cysteine side chain. These protons are diastereotopic, resulting in the splitting of the peak observed in the one-dimensional spectrum, shown in the COSY spectrum to be coupled to the alpha-proton of the cysteine residue that appears at 4.5 ppm.

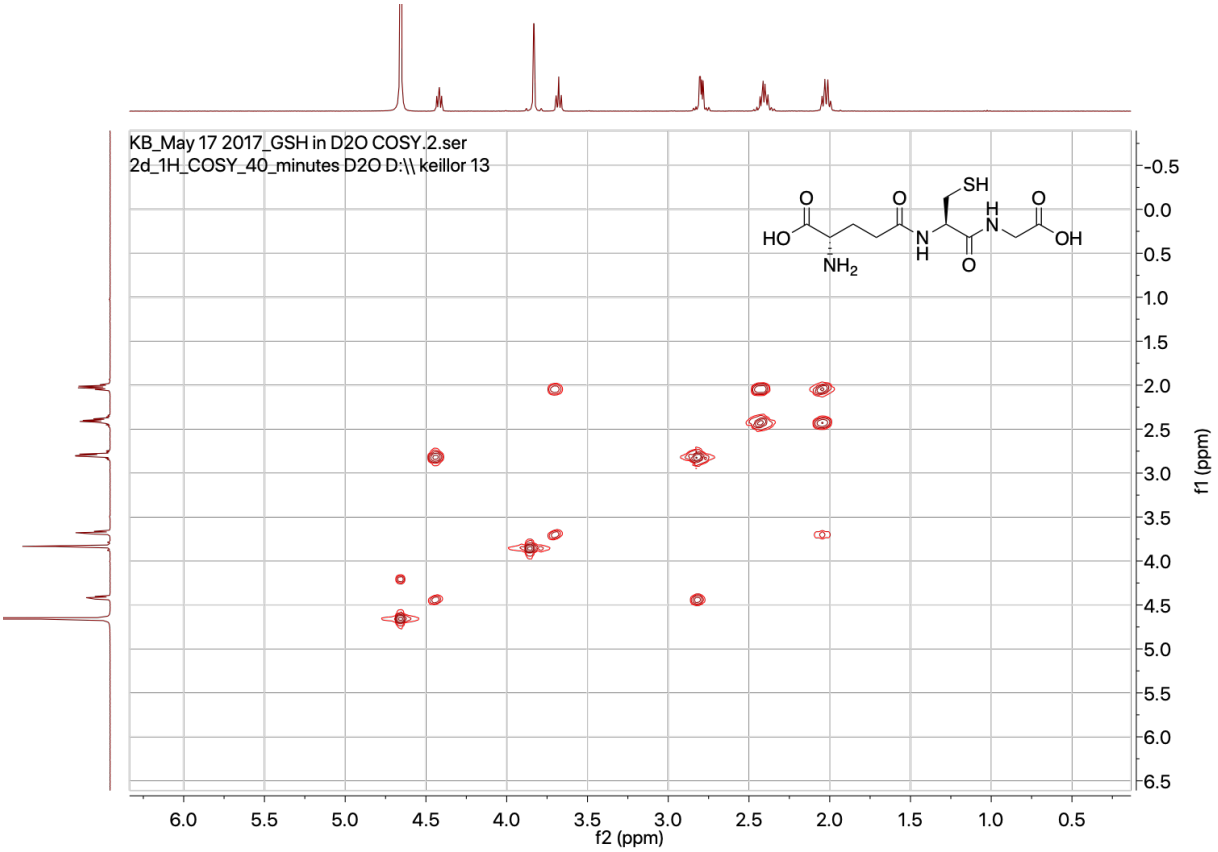

Figure 3.1. COSY NMR spectrum for glutathione (GSH) in D_2O.

We also recorded one-dimensional NMR spectra for both glutathione (GSH) and oxidized glutathione (GSSG), both of which are stacked and shown in figure 3.2. Glutathione disulphide displays an extra peak (doublet of doublets) around 3.3 ppm.

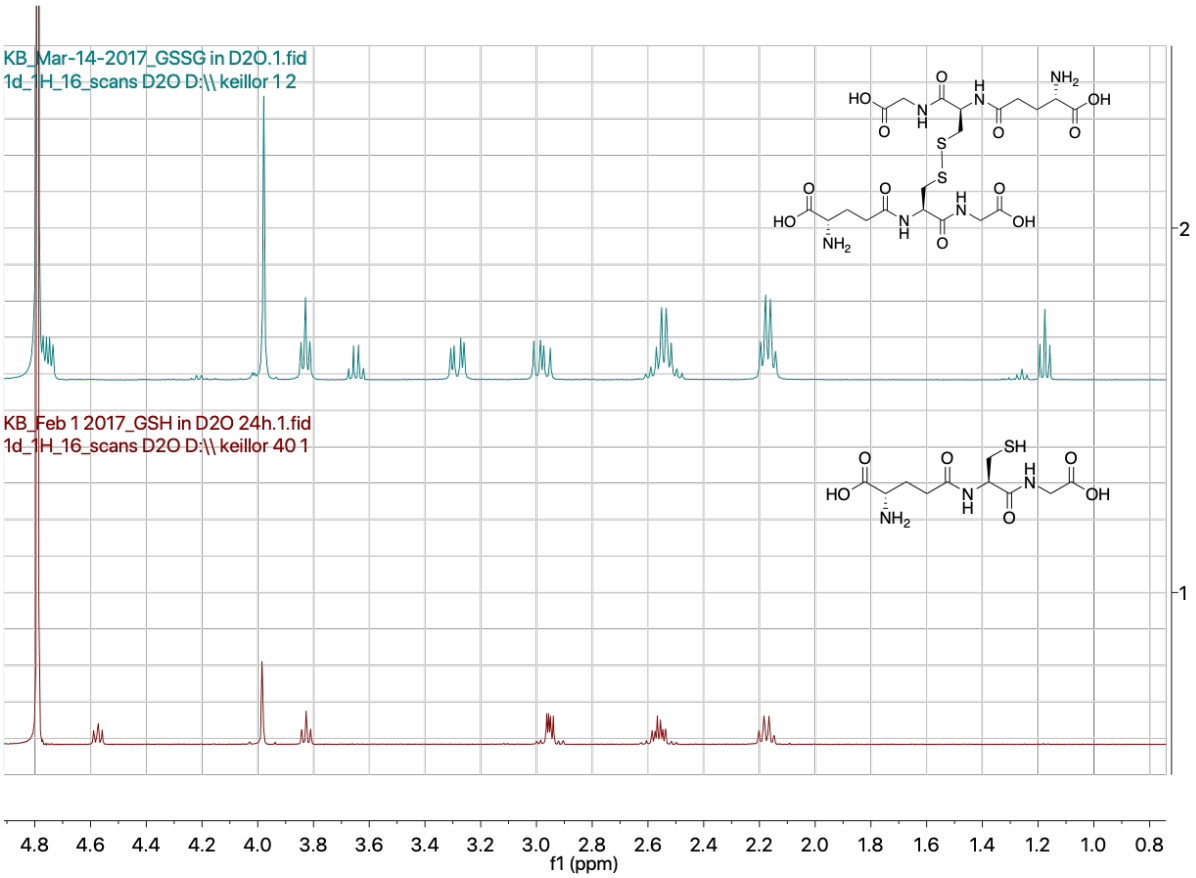

Figure 3.2. Stack of ^{1}H-NMR spectra for glutathione (GSH, bottom spectrum) and glutathione disuphide (GSSG, top spectrum). Peaks for glutathione are assigned in table 3.1.

Table 3.1. Assigned ^{1}H-NMR peaks for glutathione.

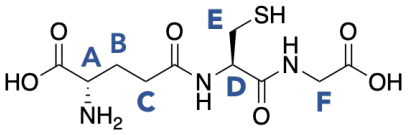

Chemical shift δ (ppm)	Assigned protons
2.2	B
2.6	C
3.0	E
3.8	A
4.0	F
4.6	D

We then analyzed the reaction of glutathione with DTNB, also by ^{1}H-NMR, keeping in mind that a few different products could be present in the reaction tube after reaction. These different products are shown in scheme 3.6 below.

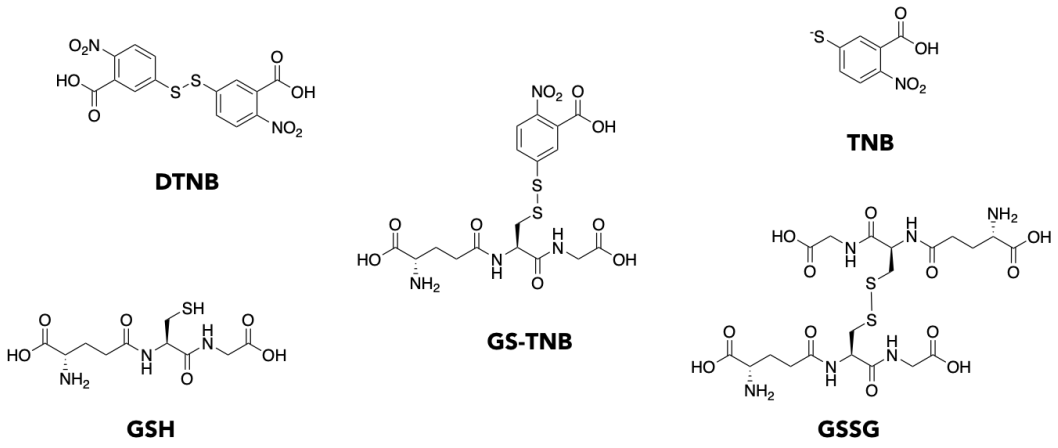

Scheme 3.6. Hypothetical products that could be present in the reaction between glutathione and DTNB. Possible products are unreacted DTNB, unreacted glutathione (GSH), 5-thio-2-nitrobenzoic acid (TNB), oxidized glutathione (GSSG), and the adduct of glutathione with DTNB (GS-TNB).

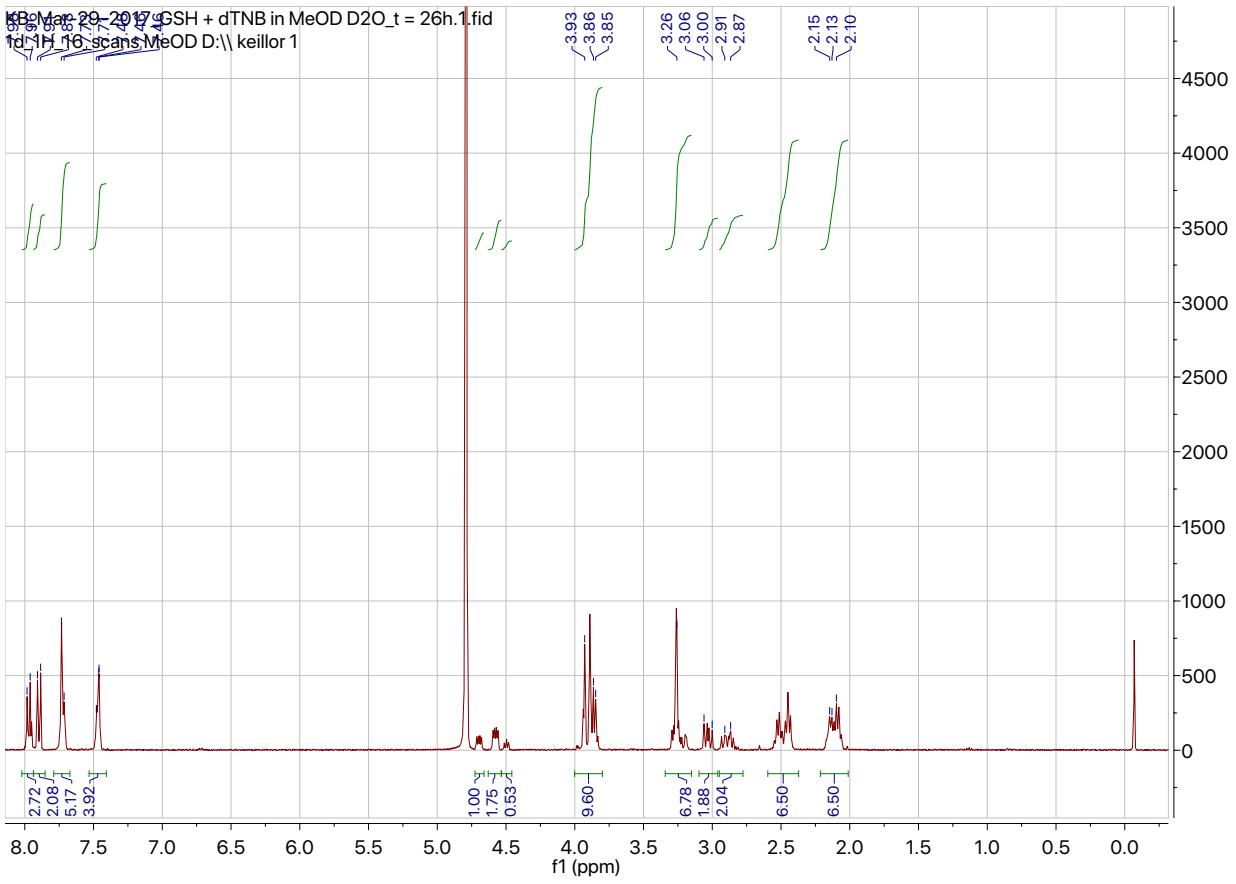

Figure 3.3. 1H-NMR spectrum for the reaction of GSH with DTNB at t = 26 hours. Spectrum was referenced to D_2O. Please note that MeOD displays a peak at around 3.3 ppm, which could drown out other surrounding signals.

The resolution for the 1D ^{1}H-NMR spectrum shown in figure 3.3 is not ideal, but from the COSY spectra presented in figures 3.4 and 3.5, we can infer that the peaks shown appear to be broadening due to the new peaks growing in, as shown by the duplication of the cross-peaks. As such, these NMR experiments have helped us confirm that poorly resolved peaks observed on the 1D spectrum are in fact due to two adjacent signals as shown by COSY.

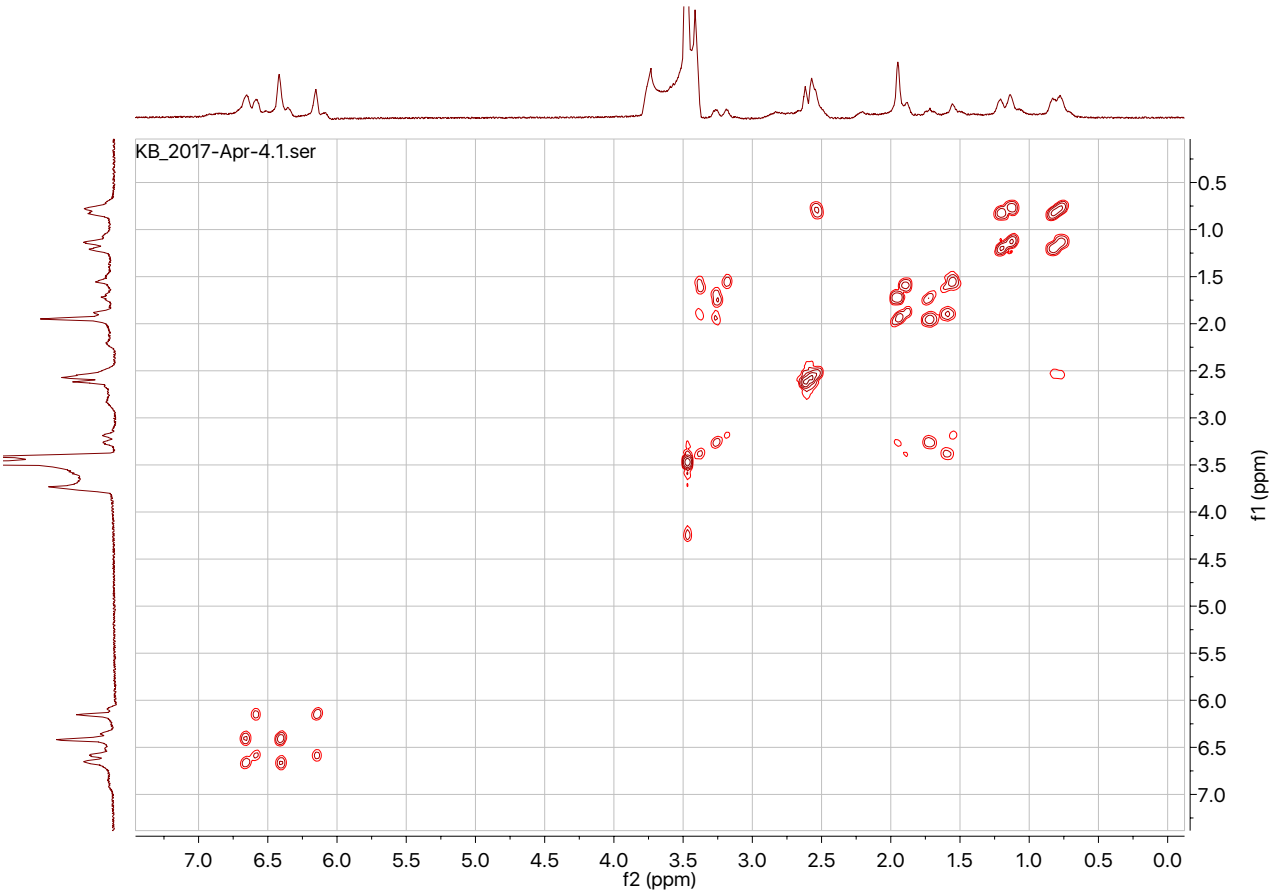

Figure 3.4 COSY NMR for the reaction of DTNB with GSH in a MeOD/D_2O cosolvent (full spectrum).

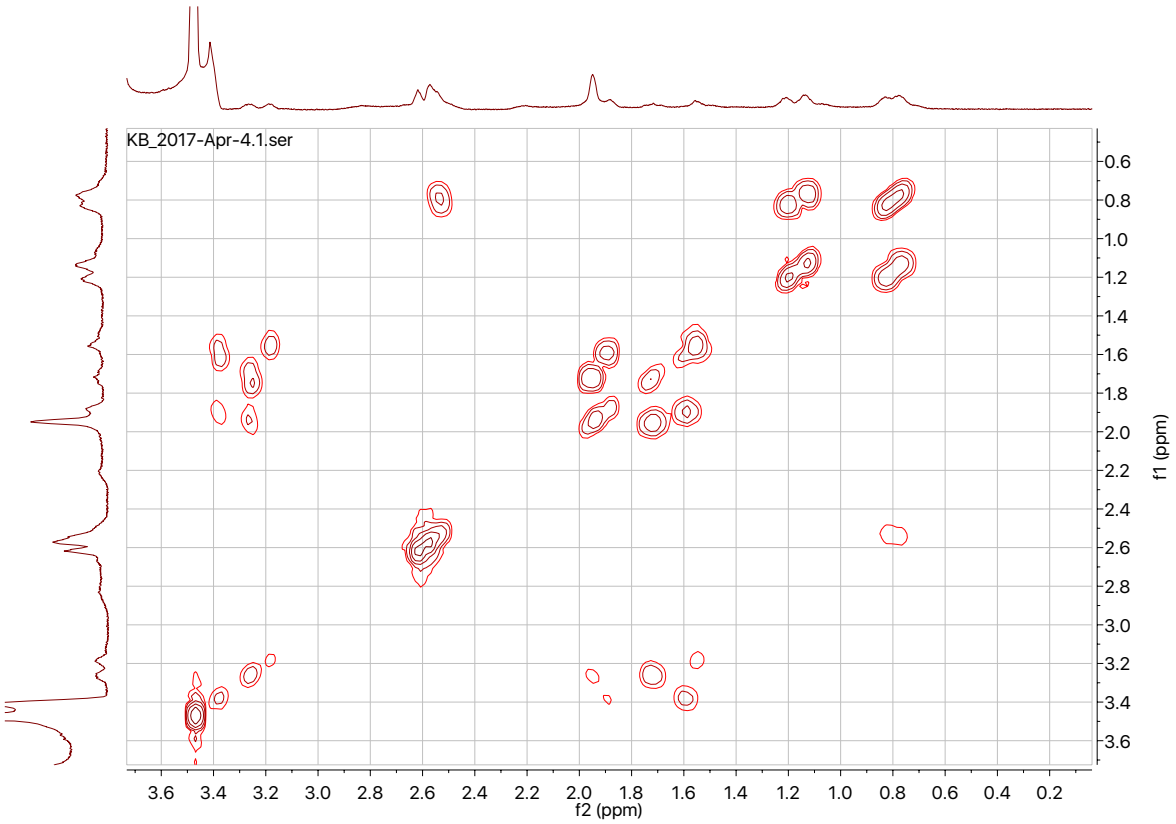

Figure 3.5. COSY NMR for the reaction of DTNB with GSH in a MeOD/D_2O cosolvent (aliphatic region).

To interpret all of our results, it was useful to present spectra as stacks for comparison purposes. In figure 3.5, we show a stack of ^{1}H-NMR spectra for the reaction of glutathione with DTNB at different time points being 0 hours, 2 hours and 5 hours. In reality, time "zero" is the time it takes to load the reaction sample into the spectrometer and acquire a spectrum. We estimate that the time may have been around thirty minutes. When DTNB is added to GSH, the solution is instantaneously yellow, indicating that the reaction has already advanced significantly.

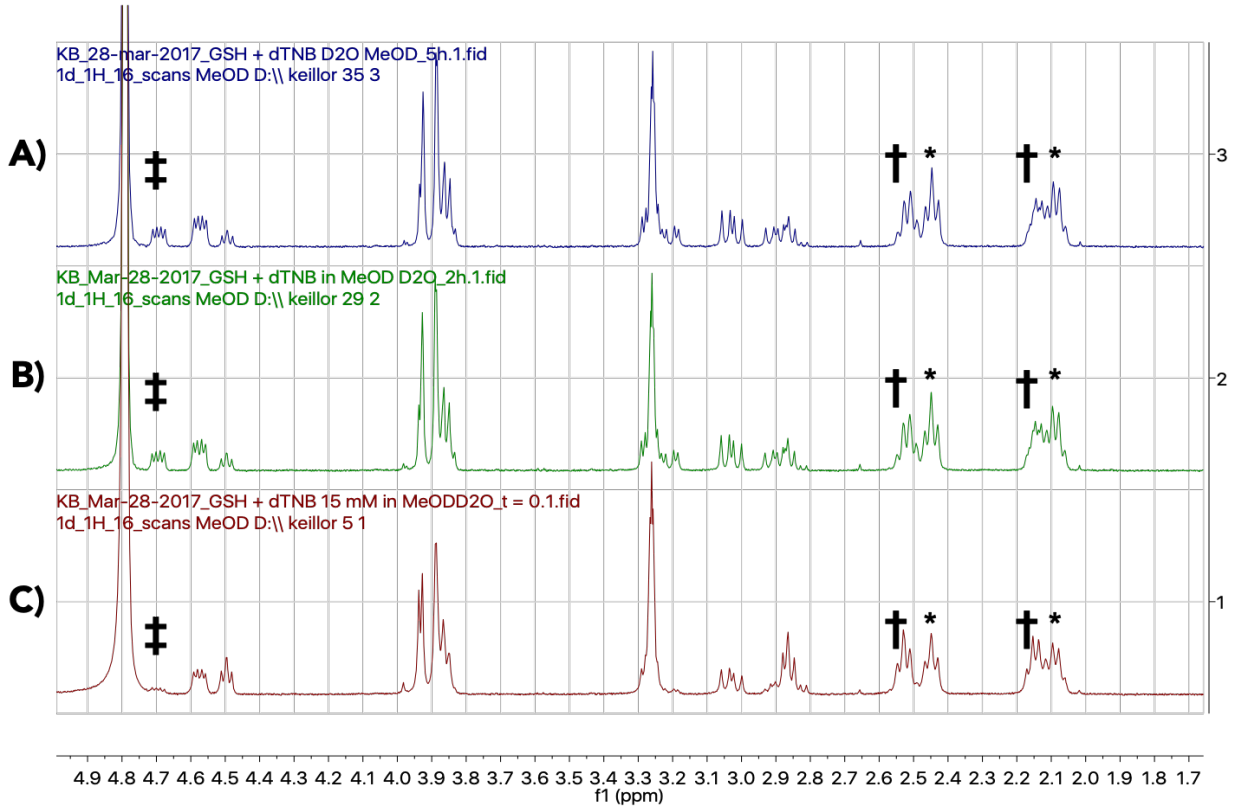

Figure 3.6. ^{1}H-NMR spectra for the reaction of GSH and dTNB in a cosolvent of D_2O and MeOD (aliphatic region), at (A) t = 5 hours, (B) t = 2 hours, and (C) t = 0 hours. There are noticeable differences between t = 0 and t = 2 hours, namely around 3.2 ppm and at 4.7 ppm.

As seen in figure 3.6, for the reaction at t = "zero" hours, we observe peak doubling at around 2.1 ppm and 2.5 ppm. At 4.7 ppm, a new peak is progressively growing in. The peaks marked with an asterisk (*) we have assigned to glutathione, whereas the peaks denoted by a dagger (†) are assigned to the GS-TNB adduct. Further, a new peak is progressively growing at 4.7 ppm, as denoted by a double dagger (‡). This new peak is suggestive of glutathione oxidation into glutathione disulphide. For visualization purposes, the spectra of GSH, the reaction at t = 0 hours and the reaction at t = 2 hours have been stacked in figure 3.7 below.

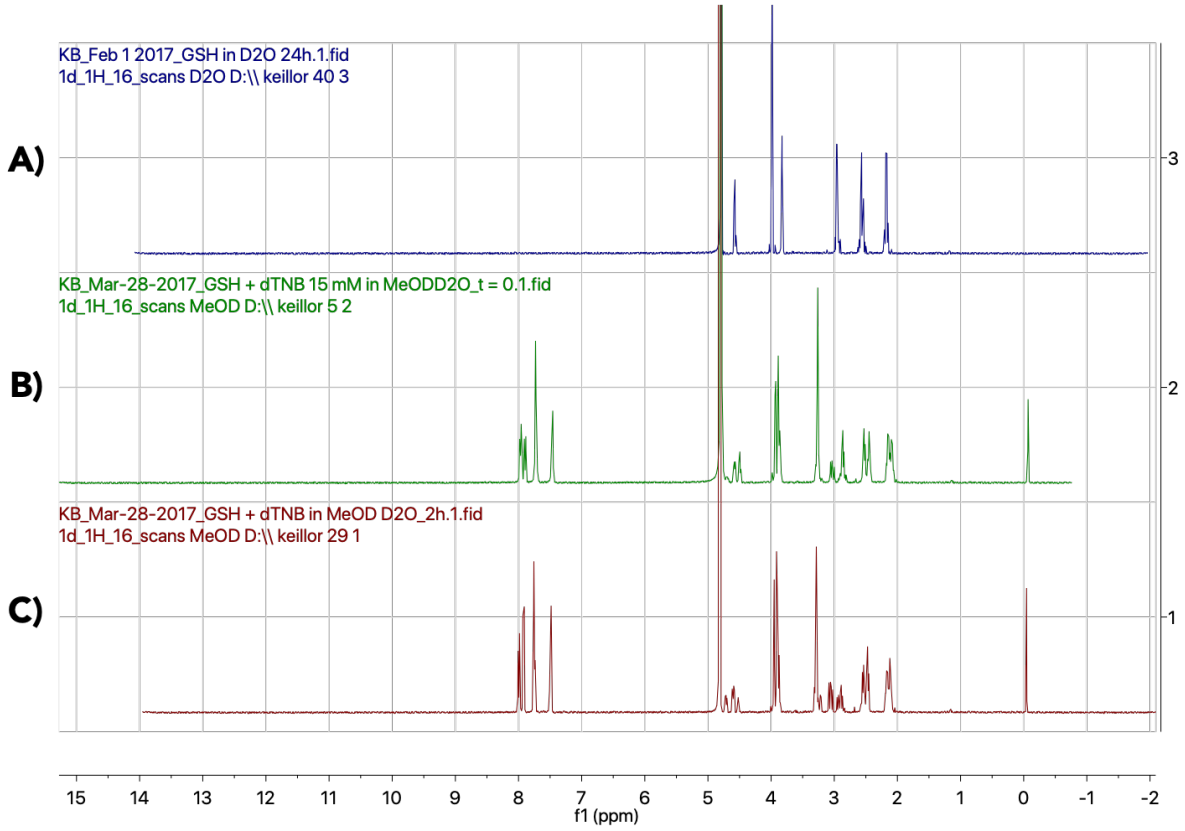

Figure 3.7. ^{1}H-NMR stack of (A) glutathione, (B) reaction of glutathione with DTNB at t = 0, and (C) reaction of glutathione with DTNB at t = 2 hours. The solvent used for (A) was D_2O and the solvent system used for (B) and (C) was a mixture of D_2O and MeOD. Spectra were referenced to D_2O.

Overall, our findings suggest that the reaction between GSH and DTNB may not go to completion, but perhaps reaches an end-point equilibrium, as seen by the presence of glutathione still in solution after reaction. Further, we suspect that glutathione may be susceptible to slow oxidation into glutathione disulphide in the reaction medium.

While NMR analysis provided satisfactory qualitative evidence that an end-point equilibrium is reached in the reaction, other methods could have also been useful to complement our findings. We could have investigated the issue further by HPLC analysis, where the reaction mixture would have been injected onto a reverse phase column (C18). The different peaks could have then been analyzed further by mass spectrometry to identify each species present based on their masses. Alternatively, LC-MS methods could have been useful.

3.6.2.2 Determination of an Apparent Extinction Coefficient for TNB

To account for the observed reaction end-point equilibrium under our experimental conditions, we established a standard curve for the reaction of GSH with DTNB. As such, 1 000 μM of DTNB was incubated with increasing concentrations of GSH ranging from 0 to 200 μM. An apparent extinction coefficient (ε*) for TNB was extracted from the slope of the standard curve (see appendix C) and its numerical value was calculated to be 13 800 ± 153 $M^{-1}cm^{-1}$ as compared to the literature reported value of 14 100 $M^{-1}cm^{-1}$. [89] This value was used in all further calculations. Having determined ε* for TNB, we repeated our control experiments to find that the results corroborated our expectations. We obtained the expected results for both the positive control and the negative control, thus validating our experimental conditions and procedure.

3.7 Assay Results and Discussion

Our glutathione reactivity assay results are presented in two different graphs for visualization purposes. As seen in figures 3.6 and 3.7, our inhibitors displayed minimal reactivity with glutathione, and their reactions were very slow, thereby confirming what we suspected. The inhibitor displaying the highest reactivity with glutathione was compound EP-I-10, with just under

50% of unreacted inhibitor remaining at the end of the incubation period. On the opposite end, the inhibitor displaying the least amount of reactivity with glutathione was compound CHDI, with virtually 100% of unreacted inhibitor remaining after incubation.

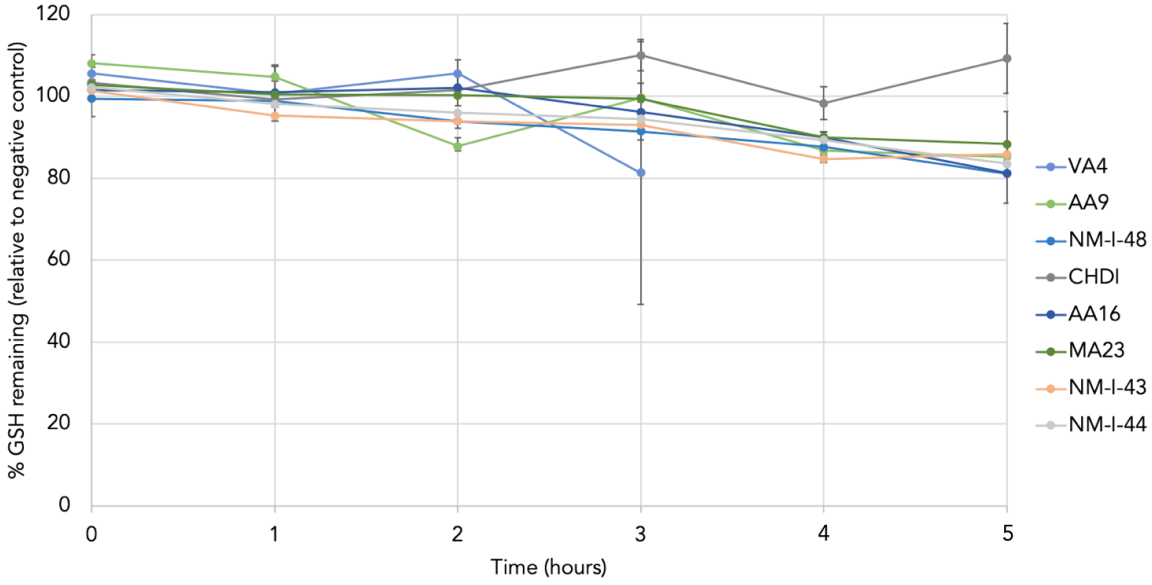

Figure 3.8. GSH reactivity assay results for compounds VA4, AA9, NM-I-48, CHDI, AA16, MA23, NM-I-43 and NM-I-44. Each compound was tested following the protocol described in section 3.5.1, and the extinction coefficient used in calculations is 13 800 ± 153 $M^{-1}cm^{-1}$, as determined in section 3.5.2.3. Note that VA4 was tested in the presence of 20% DMSO, because it has very low aqueous solubility. All other compounds were tested in the presence of 5% DMSO.

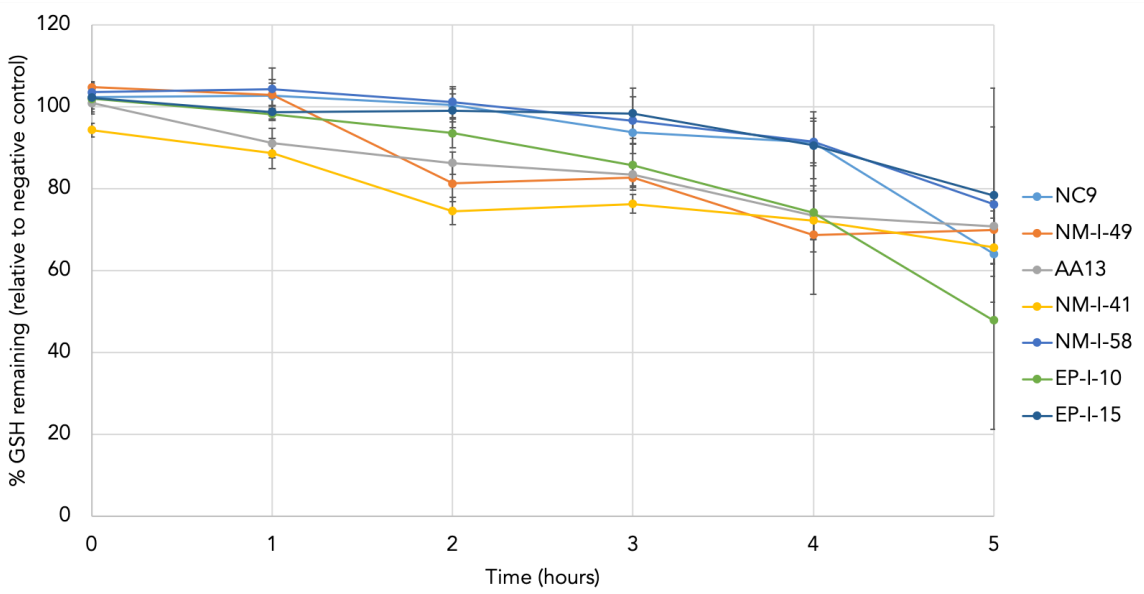

Figure 3.9. GSH reactivity assay results for compounds NC9, NM-I-49, AA13, NM-I-41, NM-I-58, EP-I-10 and EP-I-15. Each compound was tested following the protocol described in section 3.5.1, and the extinction coefficient used in calculations is 13 800 ± 153 $M^{-1}cm^{-1}$, as determined in section 3.5.2.3. All compounds presented here were tested in the presence of 5% DMSO.

While the results presented in figures 3.4 and 3.5 are satisfactory for the most part, the error bars corresponding to the data points situated at 5 hours are significantly bigger than the rest of the assay period. We suspect that this may be due to evaporation of solutions inside the microplate reader during incubation, and the lack of stirring. Certain modifications could be made to the protocol to remedy this. In particular, the incubation could take place inside an incubator shaker at 75 rpm, where the plate would be carefully sealed and placed in a closed container at the bottom of which a wet paper towel lies, so as to keep the humidity constant and avoid evaporation.

It is important to note that glutathione addition is not something that we seek to eliminate entirely. As mentioned in chapter I, glutathione conjugation is one of the phase II metabolic reactions that

allows for clearance of compounds from the body. As such, a balance simply needs to exist to allow for unreacted drug to be excreted from the body. Ideally, the reaction of our inhibitors with TG2 needs to occur much faster than with GSH. Our data suggests that appears to be the case, albeit we did not examine the reaction in enough detail to determine rate constants.

Although we did not look at reactions in enough detail to extract rate constants, research has been done concerning the reactivity of acrylamides with glutathione. As we know, the success in the design of targeted covalent inhibitors depends in part on a knowledge of the factors influencing electrophile reactivity. In an effort to further develop an understanding of structure-reactivity relationships between N-arylacrylamides, Cee *et al*. [91] determined glutathione reaction rates for a family of N-arylacrylamides independently substituted ortho- meta- and para-positions with 11 different groups of common inhibitor design. They incubated their respective inhibitors in the presence of physiologically relevant concentrations of glutathione (5 mM) at pH 7.4 using potassium phosphate buffer and extracted reaction rate constants. Their results suggested that substituent effects on reaction rates showed a linear Hammett correlation for ortho-, meta, and para-substitution. The measured pseudo-first order rate constants were situated between 2.03 and 115×10^{-3} min^{-1} across all compounds, which would translate to second order rate constants of 0.406 and 23 $M^{-1}min^{-1}$. [91] In comparison to our compounds, these values could probably serve as an upper limit for rate constants, because of structural differences. In fact, their compounds are N-arylacrylamides whereas ours are N-alkylacrylamides.

Chapter Four: **Conclusions and Perspectives**

4.1 Cell Permeability

4.1.1 Goal of the Project

The goal of the first project was to evaluate our inhibitors for their ability to permeate the cell membrane. Membrane permeability is an important parameter to consider because it relates directly to absorption (ADME) in pharmacokinetics. As such, we adapted, optimized, and validated a parallel artificial membrane permeability assay (PAMPA) utilizing hexadecane as our artificial membrane.

4.1.2 Results

Over the course of this work, we were able to validate an HDM-PAMPA protocol using two different detection methods: a microplate reader and HPLC-UV. To do this, we chose five well known marketed drugs as controls, such that a wide range of Log P_e values would be covered. Those drugs were ibuprofen, ketoprofen, carbamazepine, imipramine and lidocaine. We were able to reproduce their reported Log P_e values with precision and accuracy (table 2.1). We also examined whether DMSO concentrations would have an effect on the determine membrane permeability and found no significant differences in Log P_e values for ketoprofen, our least permeable control, with DMSO concentrations ranging from 5 to 20 %. Having validated the method, we were able to test a few of our own inhibitors. Among these, we found that NC9, VA4 and AA9 exhibit Log P_e values of -5.26 ± 0.01, -4.66 ± 0.04 and -6.5 ± 0.5 respectively. Other compounds have also been tested using this method (table 2.2), but Log P_e values could not calculated because these were unable to be detected in the acceptor compartments of the PAMPA

setup. This leads us to believe that their Log P_e values are less than -6.5, making them highly impermeable.

4.1.3 Perspectives

First and foremost, we propose to test the rest of our inhibitor libraries for their ability to permeate membranes. In the case where compounds are not permeable enough to yield sufficient concentrations in the acceptor compartment, assay concentrations can be increased such that acceptor solutions are concentrated enough for detection. When we obtain Log P_e values for every one of our inhibitors, we can rank them based on how membrane permeable they are. Those showing the best permeability could then be taken and tested in a Caco-2 assay, which would allow us to estimate how well they could permeate the intestinal wall.

4.2 Off-target Reactivity

4.2.1 Goal of the Project

The goal of the second project was to investigate the susceptibility of our inhibitors to glutathione addition reactions under physiological conditions. As such, we aimed to adapt and optimize a colorimetric assay using Ellman's reagent (DTNB).

4.2.2 Results

First and foremost, we found that the reaction of DTNB with glutathione does not go to completion, but instead reaches an equilibrium end-point. Furthermore, our findings suggest that glutathione oxidizes over time. To take this into account, we established a standard curve of the reaction of glutathione with DTNB to extract an apparent extinction coefficient of 13 800 ± 153 $M^{-1}cm^{-1}$ for

TNB. We were then able to test our inhibitors for susceptibility to glutathione addition and found that they react minimally and slowly (figures 3.6 and 3.7). In most cases, after 5 hours of incubation, over 70% of the initial unreacted inhibitor concentration remained.

4.2.3 Perspectives

While this assay allowed us to examine glutathione reactivity of our inhibitors, we did not examine the reaction in enough detail to determine rate constants. Further, the concentrations used do not perfectly reflect physiological conditions. The glutathione concentration used in our assay was 100 μM, whereas in cellular contexts glutathione concentrations are more realistically situated around 3 to 5 mM. As such, we could run future assays using GSH concentrations that are more physiologically relevant. This would make it so that glutathione would be in large excess, and the reaction would be pseudo-first order. We could extract rate constants for those reactions and compare them to the rate constants of the inhibitors' reactions with TG2. Lastly, the same assay could be adapted further and be put to use with other possible thiol off-targets, such as human serum albumin.

4.3 Projecting Forward – Expanding on PK Assessment of our Compounds

Although we now have a better understanding of the PK of our compounds with respect to membrane permeability and glutathione reactivity, there are many other parameters that need to be investigated in order to obtain a complete picture. Among these we count, for instance, solubility, plasma stability, and microsomal stability.

4.3.1 Solubility

Solubility is a physicochemical property of utmost importance in drug discovery. Adequate solubility is necessary for biochemical and cellular screening assays such as microsomal and plasma stability assays, and physical property assays of lipophilicity and permeability. It also affects the oral bioavailability, as discussed prior.

In drug discovery, we often hear about two types of solubility: thermodynamic solubility and kinetic solubility. In a practical context, the difference between the two lies in the fact that the solid compound is introduced into aqueous medium for determination of thermodynamic solubility whereas the pre-dissolved (usually in DMSO) compound is taken as the starting material for assessing kinetic solubility. As such, assays to determine thermodynamic solubility answer the question: "To what extent does to compound dissolve?" whereas kinetic solubility answers the question: "To what extent does the compound precipitate?". [92]

Logically, thermodynamic stability *should* be the gold standard for optimizing compounds for solubility targeting, for example as solid oral formulations to be used during clinical development and for marketing. However, methods for determining thermodynamic solubility are generally much more labor-intensive than methods for assessing kinetic solubility. This is mainly due to difficulties in automating the handling of solid state compounds in the lower milligram range, which is a prerequisite for assessing thermodynamic solubility. Assays aimed at determining kinetic solubility can be automated much more easily as, instead of involving the handling of solid material that might also be sticky, oily or electrostatic, they simply rely on pipetting the compound in pre-dissolved form – typically as a 10 mM DMSO stock solution. Because stock solutions of our inhibitors have already been made in DMSO, we could easily test their kinetic solubility.

Kinetic solubility assays can be made high-throughput using 96-well plates. Small volumes of concentrated DMSO stock solutions are pipetted into wells containing buffer at pH 7.4. Following shaking of the suspension on an orbital shaker, it can be separated by centrifugation. Immediately after a filtration step, the filtrate may be transferred into a more concentrated mixture of DMSO with buffer pH 7.4, to avoid precipitation from the saturated solution. The concentration of the research compound can then be determined by HPLC with UV detection using an external standard from the same batch of research compound. [92]

4.3.2 Plasma Stability

Plasma stability plays an important role in drug discovery and development. The stability of drug candidates in plasma is essential for maintaining acceptable drug concentration and half-life in order to achieve desired pharmacological effects. Unstable compounds tend to have rapid clearance and short half-lives, ultimately leading to poor *in vivo* performance. Furthermore, they cause difficulties for *in vivo* pharmacokinetic (PK) studies, because the compounds will continue to degrade even after blood samples are taken from the animal in question. Pharmaceutical companies tend to not advance compounds that rapidly degrade in plasma, with the exception of prodrugs, antedrugs and special cases. Screening of plasma stability provides useful information to prioritize compounds for *in vivo* studies and to alert researchers to the possible liabilities of key pharmacophores, so that structural modifications can be applied to improve stability. Furthermore, plasma stability is very useful for screening of prodrugs and antedrugs, where rapid conversion in the plasma is desirable. [93,94]

In general, test compounds in organic solvent are added to buffered plasma (or plasma adjusted to pH 7.4) such that the compound concentration is in the low μM range (1 – 20 μM). This plasma

solution containing test compound is incubated at 37 °C. A volume of the plasma incubate is taken at each time point of interest and immediately placed in organic solvent so as to deactivate plasma enzymes by denaturation (quenching subsequent reaction). Solutions are then centrifuged to remove denatured proteins and a volume of the supernatant is analyzed. The quantification of the compound remaining at each time point allows us to determine its half-life. Typically, detection and quantitation after plasma stability incubation are performed using LC/MS/MS techniques. Plasma contains many components that may interfere with quantitation, thus, a detection instrument with good selectivity is important. [93]

4.3.3 Microsomal Stability

The liver is the most important site of drug metabolism in the body. Approximately 60 % of marketed compounds are cleared by hepatic CYP-mediated metabolism. Liver microsomes are subcellular fractions that contain membrane bound drug metabolising enzymes, and they can be used to determine the *in vitro* intrinsic metabolism of a compound. [16]

Typically, in assays like these, microsomes are incubated with the test compound at 37°C in the presence of a co-factor, NADPH, which initiates the reaction. The reaction is quenched by addition of a methanol containing an internal standard. Following centrifugation, the supernatant can be analyzed via LC-MS/MS. The disappearance of test compound is monitored over a certain time period (e.g. 45 minutes). [95]

The microsomal stability assay is primarily useful for the investigation of Phase I metabolism using NADPH as the enzyme cofactor. However, they can also be used to study Phase II metabolism if the correct incubation conditions are used. Companies like Cytoprex have validated

conditions using the pore forming agent alamethicin in conjunction with appropriate Phase II cofactors like UDPGA. It is also possible to study Phase I and Phase II metabolism in parallel by using all the relevant cofactors in the incubation.

Because microsomes are adaptable to high-throughput screening and allow for the screening of libraries of compounds inexpensively, researchers may use this assay as an initial screen to rank compounds of interest based on their metabolic stability, and then perform a secondary screen on a select number of compounds using hepatocytes.

4.4 Final Remarks and Conclusion

To re-iterate, we were able to set up two new pharmacokinetic assays in the Keillor lab: a glutathione reactivity assay to study off-target reactivity of our compounds, and a parallel artificial membrane permeability assay (PAMPA) to examine their membrane permeability potential. These two tests can be used in a high-throughput manner to better guide our drug discovery and lead optimization process. As for further pharmacokinetic testing, while other methods could be adapted and optimized in the Keillor lab, we are aware that the recent trend is to outsource these analyses at increasingly reasonable price to contract research organizations that specialize in using them. Ultimately, the pharmacokinetic characterization of our most effective inhibitors will be critical in their further development, prior to selecting the most promising candidates for further testing and clinical trials.

mic drop

APPENDIX A

Table A.1. Inhibitor chemical structures

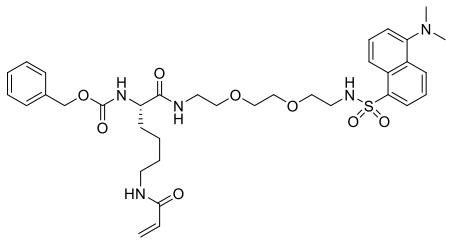

NC9

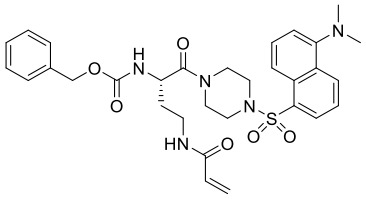

AA15

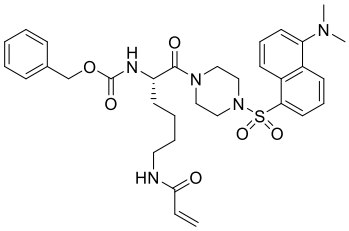

VA4

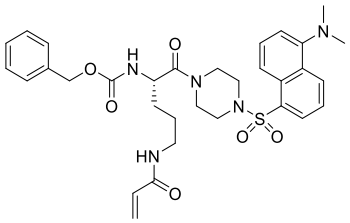

AA16

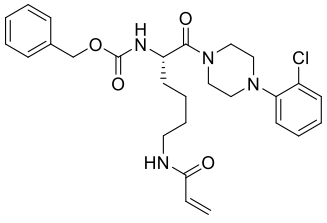

CHDI

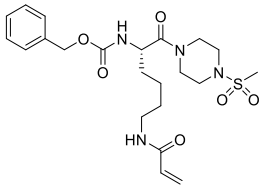

MA23

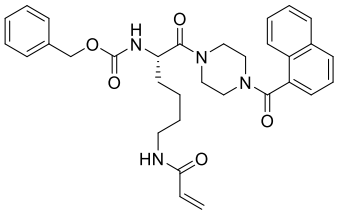

AA9

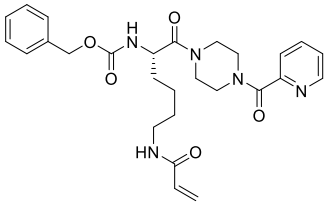

NM-I-41

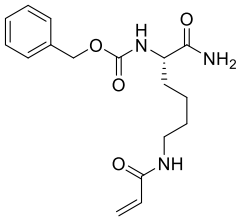

AA13

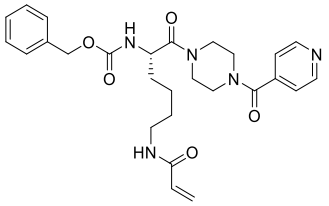

NM-I-43

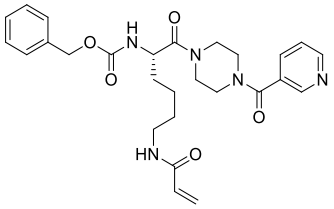

NM-I-44

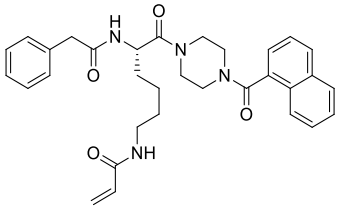

NM-III-46

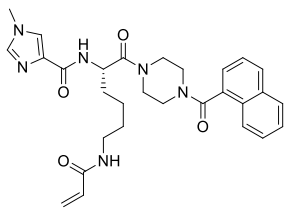

NM-III-72

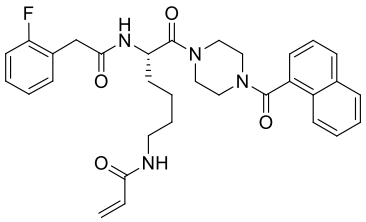

NM-V-12

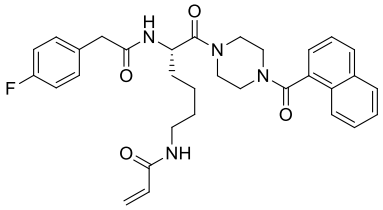

NM-V-14

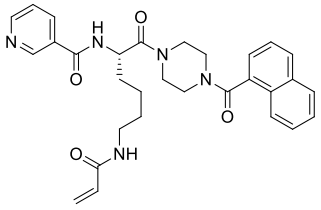

NM-V-36

APPENDIX B

Table B.2. HPLC gradient method (time table) used for sample analysis in the context of PAMPA assays. Theoretical equilibrium and acceptor compartment solutions prepared and obtained during the course of PAMPA assays were analyzed by means of HPLC-UV with a C18 column. A gradient method employing a water/acetonitrile co-solvent was used. The flow rate for the method was set to 0.1 mL/min, and the oven temperature was kept at 25 °C. The total run time is 30 minutes (start delay 3 minutes, runtime 27 minutes).

Time	%Water : %Acetonitrile
0	95 : 5
10	60 : 40
15	50 : 50
20	40 : 60
25	40 : 60
30	95 : 5

Table B.3. Critical t values (t_{crit}) for varying degrees of freedom (Student's t-test)

Degree of freedom (N)	80%	90%	95%	99%	99.9%
1	3.08	6.31	12.7	63.7	637
2	1.89	2.92	4.30	9.92	31.6
3	1.64	2.35	3.18	5.84	12.9
4	1.53	2.13	2.78	4.60	8.61
5	1.48	2.02	2.57	4.03	6.87
6	1.44	1.94	2.45	3.71	5.96
7	1.42	1.90	2.36	3.50	5.41

T-test to compare two experimental means:

$$t_{exp} = \frac{|\overline{X_A} - \overline{X_B}|}{s_{AB}\sqrt{\frac{1}{n_A} + \frac{1}{n_B}}}$$

$$s_{AB} = \sqrt{\frac{(n_A - 1)s_A^2 + (n_B - 1)s_B^2}{n_A + n_B - 2}}$$

$$degree\ of\ freedom\ N = n_A + n_B - 2 = 4$$

n_A is the sample number of dataset A, s_A is the standard deviation of dataset A, and s_{AB} is the grouped standard deviation for datasets A and B.

Example for ketoprofen, comparing the experimental Log P_e values obtained using varying concentrations of DMSO. Here, we compare the results obtained at 15% DMSO (-6.7 ± 0.7) and 5% DMSO (-5.9 ± 0.2), at 95% certainty:

$$s_{AB} = \sqrt{\frac{(3\ -1)(0.7)^2 + (3\ -1)(0.2)^2}{3 + \ 3\ -2}} = \sqrt{\frac{0.98 + 0.08}{4}} = \ 0.51$$

$$t_{exp} = \frac{|-6.7 - (-5.9)|}{0.51\sqrt{\frac{1}{3} + \ \frac{1}{3}}} = \frac{0.8}{0.42} = 1.9$$

$$degree\ of\ freedom\ N = 3 + 3 - 2 = 4$$

$$t_{crit}(95\%) = 2.78$$

$t_{exp} < t_{crit}$, meaning that there is no significant difference between the two experimental means compared here.

T test to compare an experimental mean to a hypothesized (theoretical) value:

$$t_{exp} = \frac{|\overline{X_A} - m_0|}{s_A \sqrt{n_A}}$$

$$degree\ of\ freedom\ N = n_A - 1 = 2$$

Example for ibuprofen, comparing the experimental Log P_e value of -4.3 ± 0.1 to the literature reported value of -4.65, at 95% certainty

$$t_{exp} = \frac{|-4.3 - (-4.65)|}{0.1\sqrt{3}} = \frac{0.35}{0.173} = 2.02$$

$$t_{crit}(95\%) = 4.30$$

$t_{exp} < t_{crit}$, meaning that there is no significant difference between our experimental result and the literature reported value for ibuprofen.

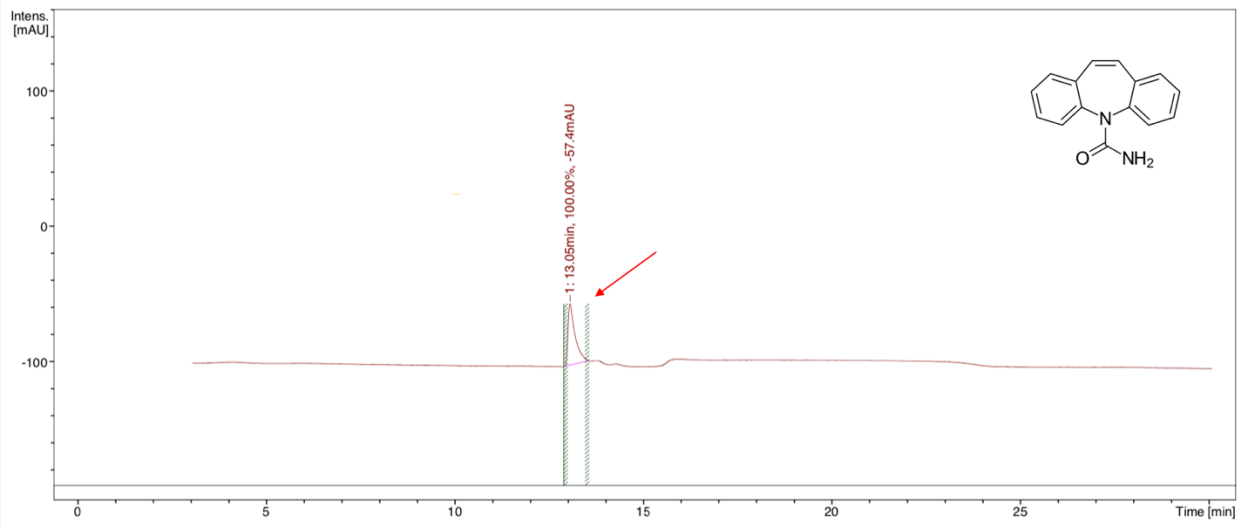

Figure B.1 Chromatogram for the acceptor solution of carbamazepine. Carbamazepine was run through PAMPA at a concentration of 400 μM. The resulting acceptor solution was analyzed by HPLC-UV and the area of its corresponding peak was calculated to be 2 960.0 mAU*s. All samples were run in triplicate, but only one replicate was shown here.

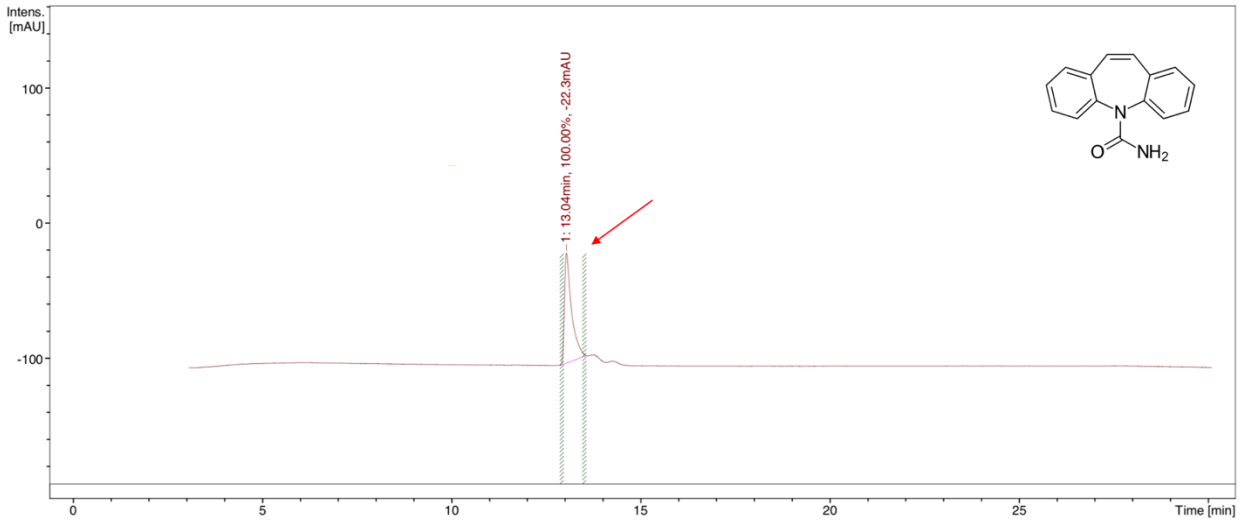

Figure B.2. Chromatogram for the theoretical equilibrium solution of carbamazepine. Carbamazepine was run through PAMPA at a concentration of 400 µM. The theoretical equilibrium solution (172 µM) was analyzed by HPLC-UV and the area of the corresponding peak was calculated to be 5 326.4 mAU*s. All samples were run in triplicate, but only one replicate was shown here.

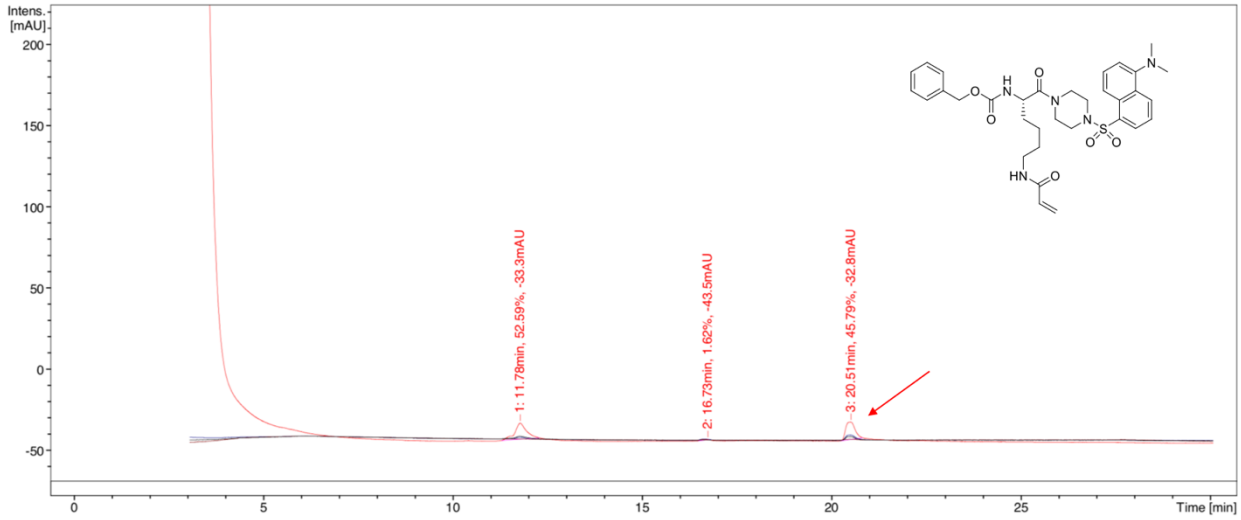

Figure B.3 Chromatogram for the acceptor solution of VA4. Compound VA4 was run through PAMPA at a concentration of 100 µM. The resulting acceptor solution was analyzed by HPLC-UV and the area of the corresponding peak was calculated to be 925.5 mAU*s. All samples were run in triplicate, but only one replicate was shown here.

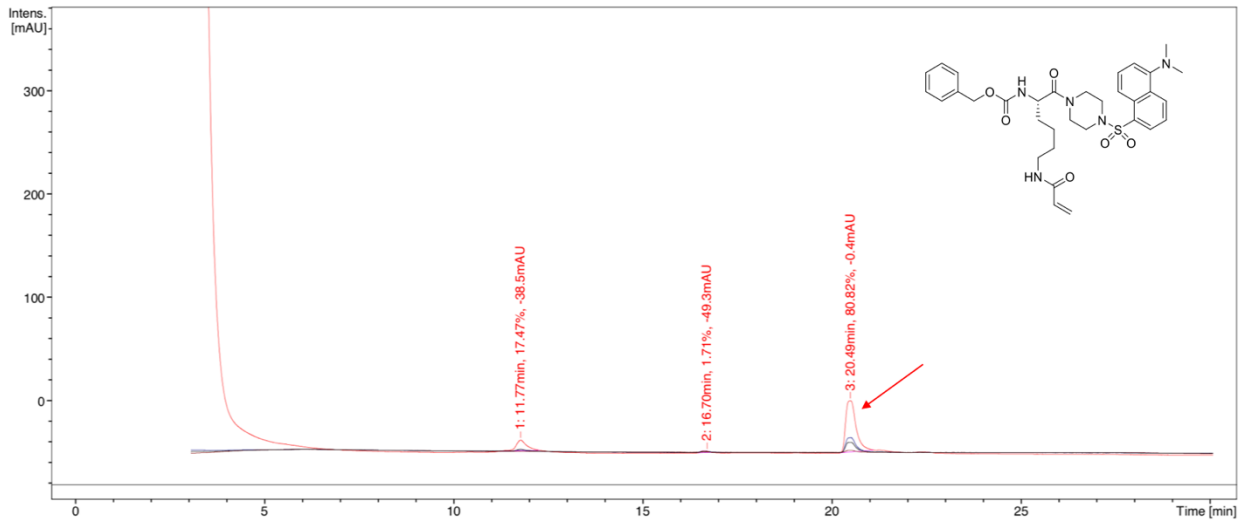

Figure B.4 Chromatogram for the theoretical equilibrium solution of VA4. Compound VA4 was run through PAMPA at a concentration of 100 µM. The theoretical equilibrium solution (43 µM) was run through the HPLC and the area of the corresponding peak was calculated to be 4 707.0 mAU*s. All samples were run in triplicate, but only one replicate was shown here. Peak area at 220 nm (red trace) was used for calculations.

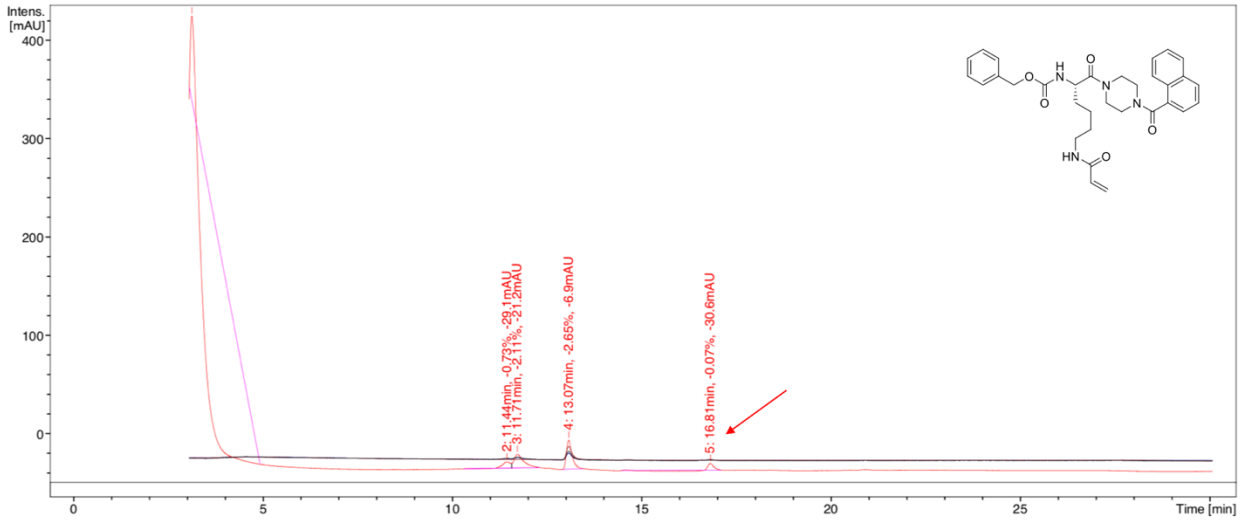

Figure B.5. Chromatogram for the acceptor solution of AA9. Compound AA9 was run through PAMPA at a concentration of 400 µM. The resulting acceptor solution was run through the HPLC and the area of the corresponding peak was calculated to be 333.2 mAU*s. All samples were run in triplicate, but only one replicate was shown. Peak area at 220 nm (red trace) was used for calculations.

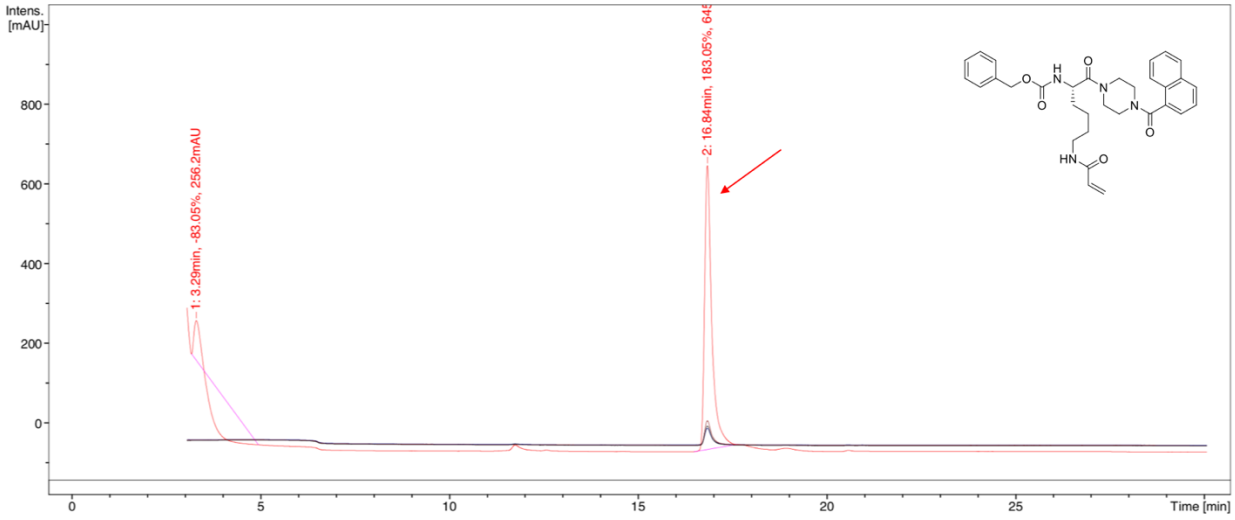

Figure B.6. Chromatogram for the theoretical equilibrium solution of AA9. Compound AA9 was run through PAMPA at a concentration of 172 µM. The theoretical equilibrium solution was run through the HPLC and the area of the corresponding peak was calculated to be 47 246.6 mAU*s. All samples were run in triplicate, but only one replicate was shown here. Peak area at 220 nm (red trace) was used for calculations.

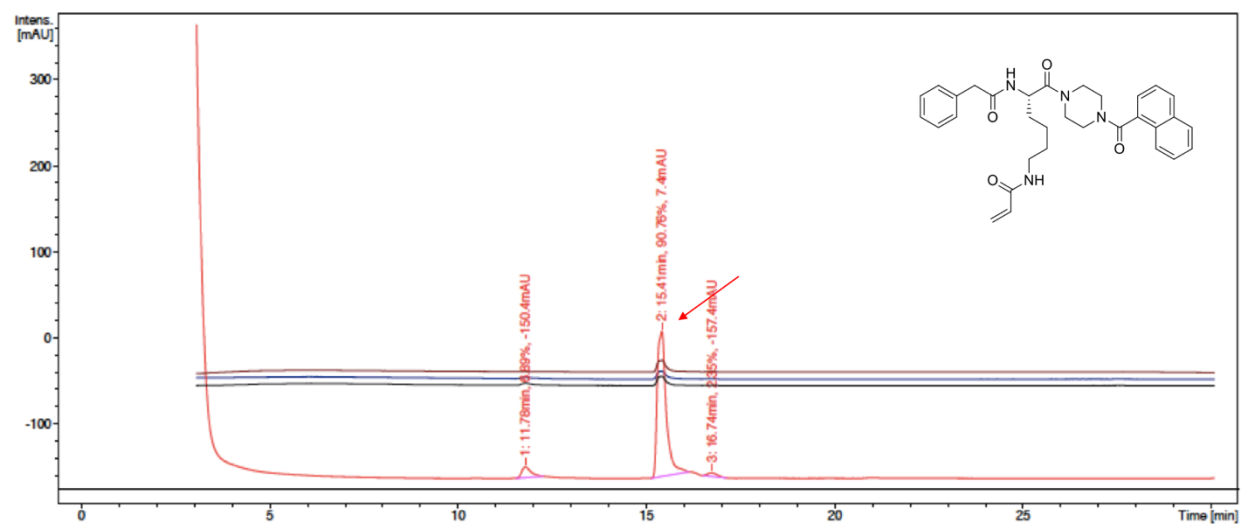

Figure B.7 Compound NM-III-46 at theoretical equilibrium (64 µM). Assay concentration was 150 µM. Nothing was detected in the acceptor compartment. Peak area at 220 nm (red trace) was used for calculations.

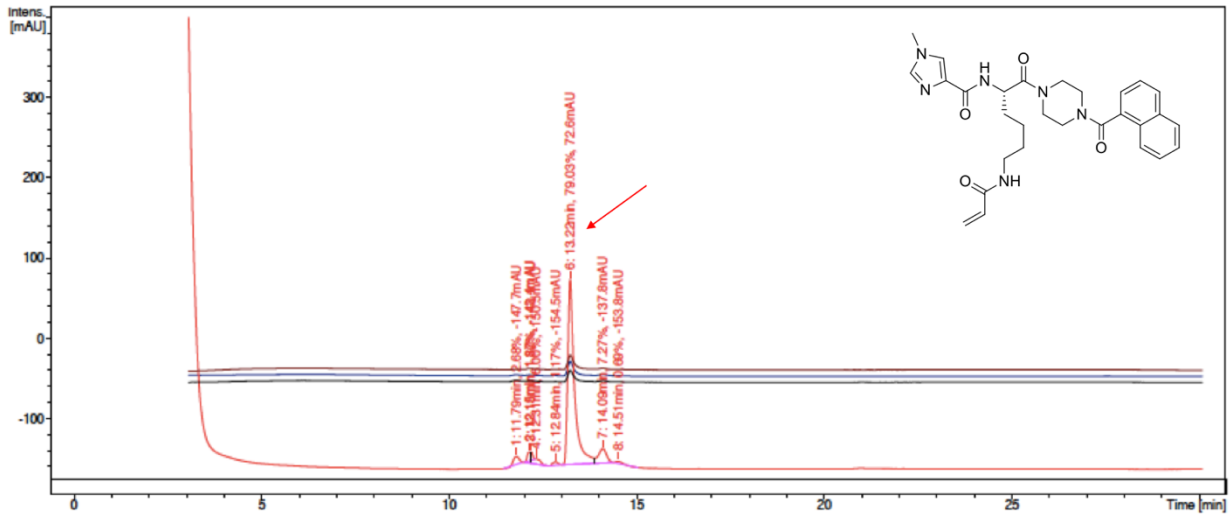

Figure B.8. Compound NM-III-72 at theoretical equilibrium (64 µM). Assay concentration was 150 µM. Assay concentration was 150 µM. Nothing was detected in the acceptor compartment. Peak area at 220 nm (red trace) was used for calculations.

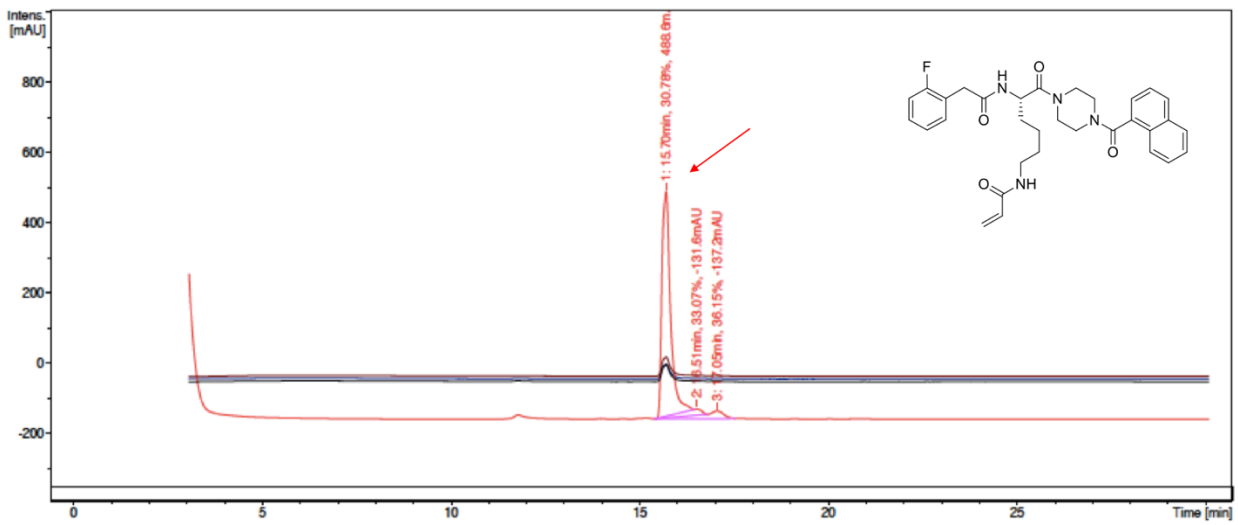

Figure B.9. Compound NM-V-12 at theoretical equilibrium (214 µM). Assay concentration was 500 µM. Assay concentration was 150 µM. Nothing was detected in the acceptor compartment. Peak area at 220 nm (red trace) was used for calculations.

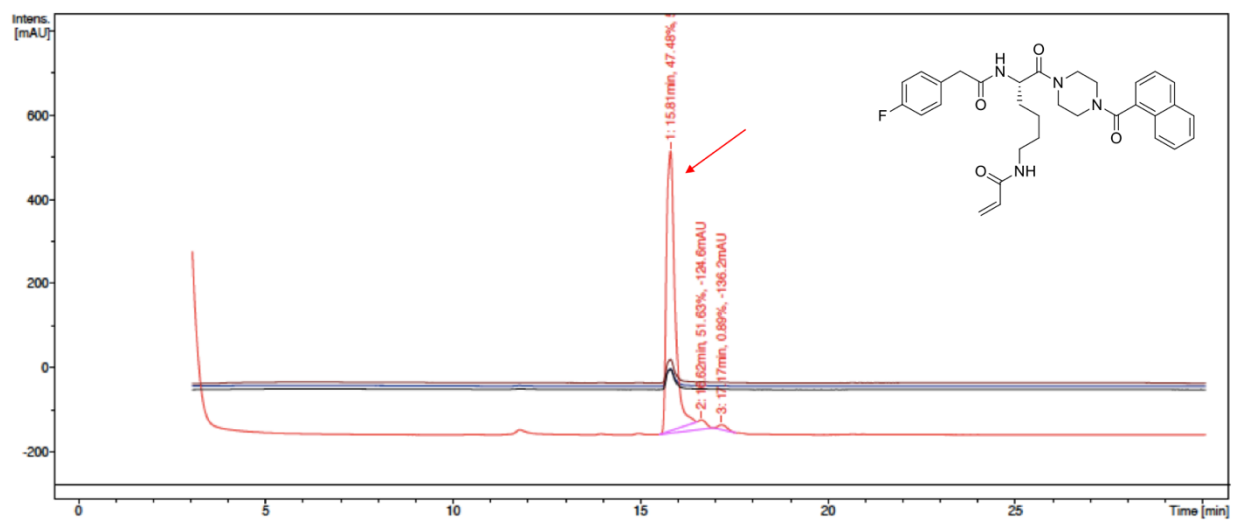

Figure B.10. Compound NM-V-14 at theoretical equilibrium (214 µM). Assay concentration was 500 µM. Assay concentration was 150 µM. Nothing was detected in the acceptor compartment. Peak area at 220 nm (red trace) was used for calculations.

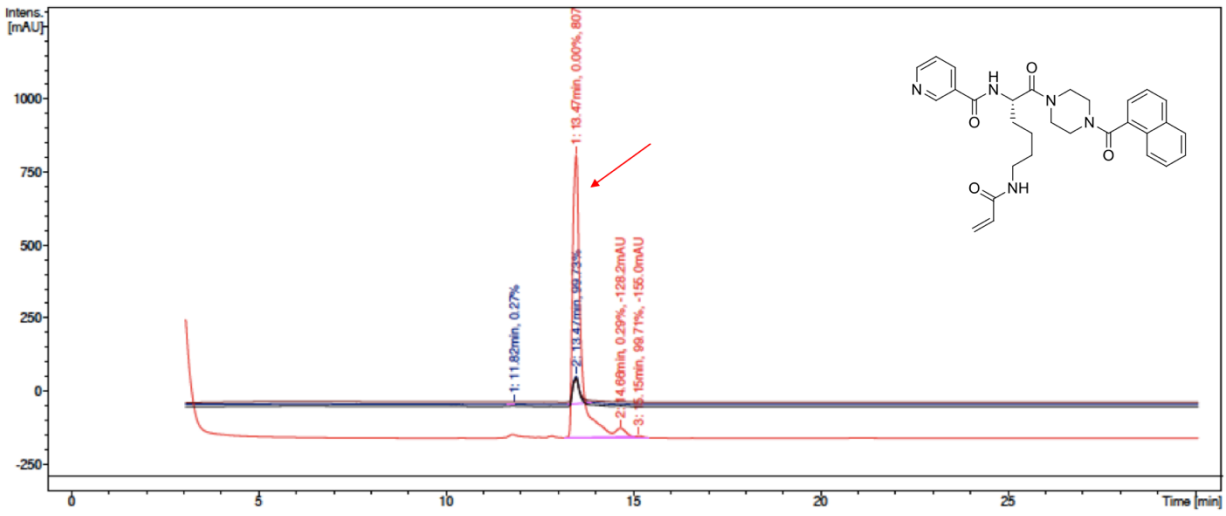

Figure B.11. Compound NM-V-36 at theoretical equilibrium (214 µM). Assay concentration was 500 µM. Assay concentration was 150 µM. Nothing was detected in the acceptor compartment. Peak area at 220 nm (red trace) was used for calculations.

APPENDIX C

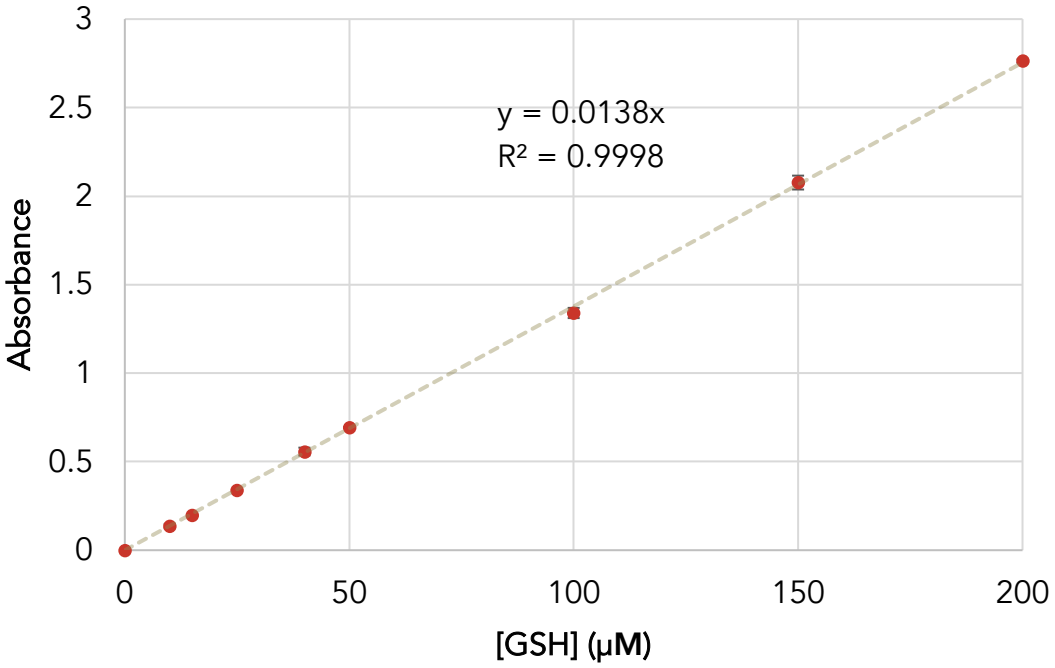

Figure C.12. Determination of an apparent extinction coefficient (ε*) for TNB. 1 000 µM of DTNB was reacted at 37°C with increasing concentrations of GSH ranging from 0 to 200 µM at physiologically relevant conditions, namely using 100 mM MOPS buffer at pH 7.4. Absorbances were measured at 412 nm, and the extinction coefficient was extracted from the slope of the linear regression of the curve. The numerical value of ε* was calculated to be 13 800 ± 153 $M^{-1}cm^{-1}$.

VERIFYING COMPOUND STABILITY BY NMR

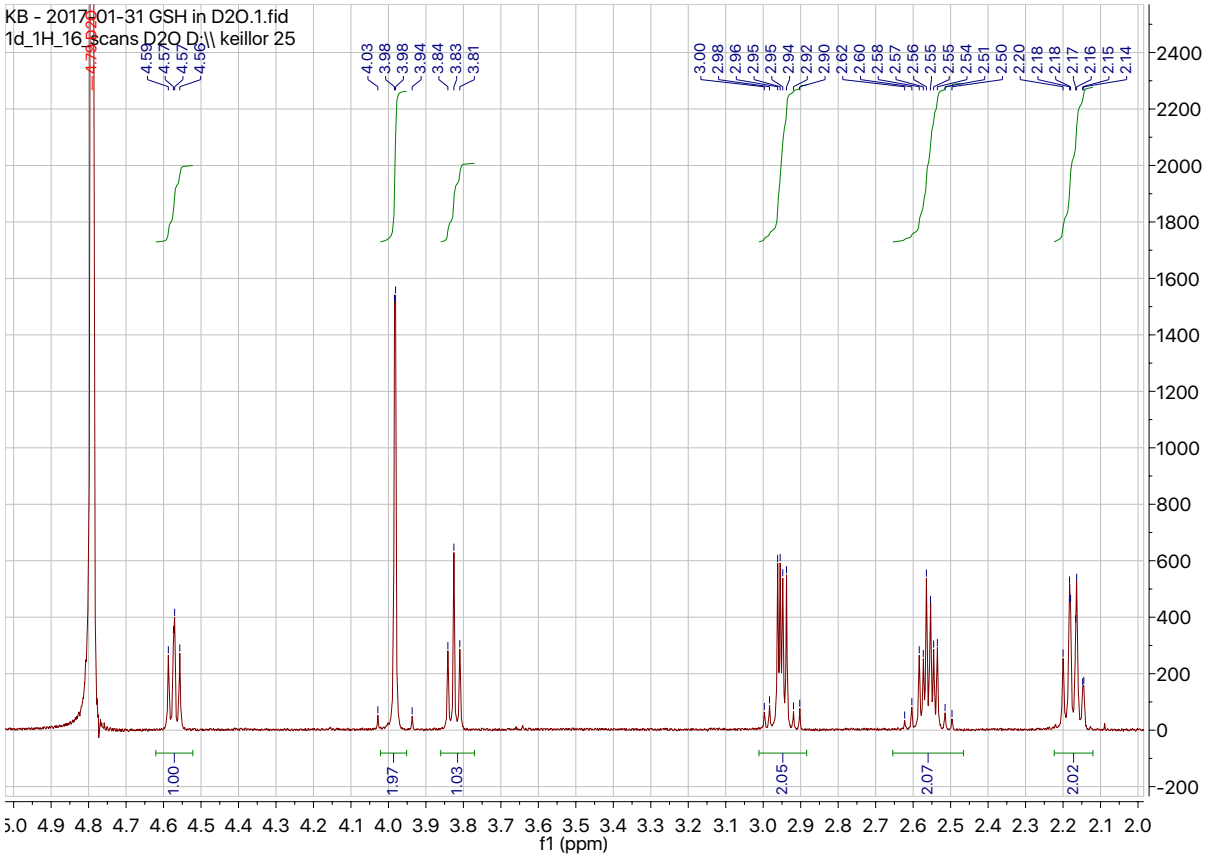

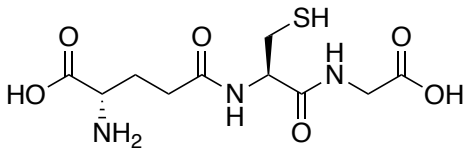

Figure C.13. ^{1}H-NMR GSH in D_2O (referenced to D_2O). t = 0. Aliphatic region.

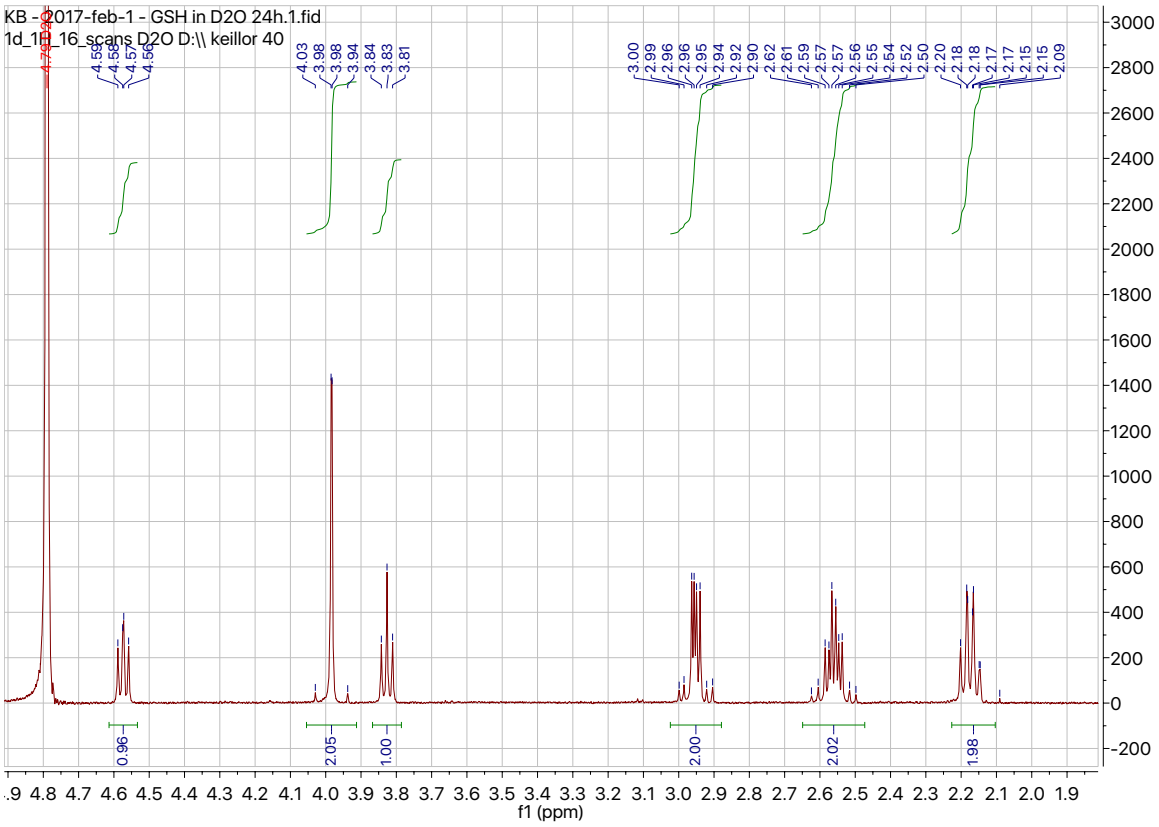

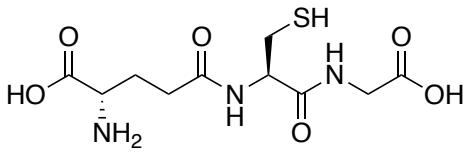

Figure C.14. ^{1}H-NMR GSH in D_2O (referenced to D_2O). t = 24 hours. Aliphatic region.

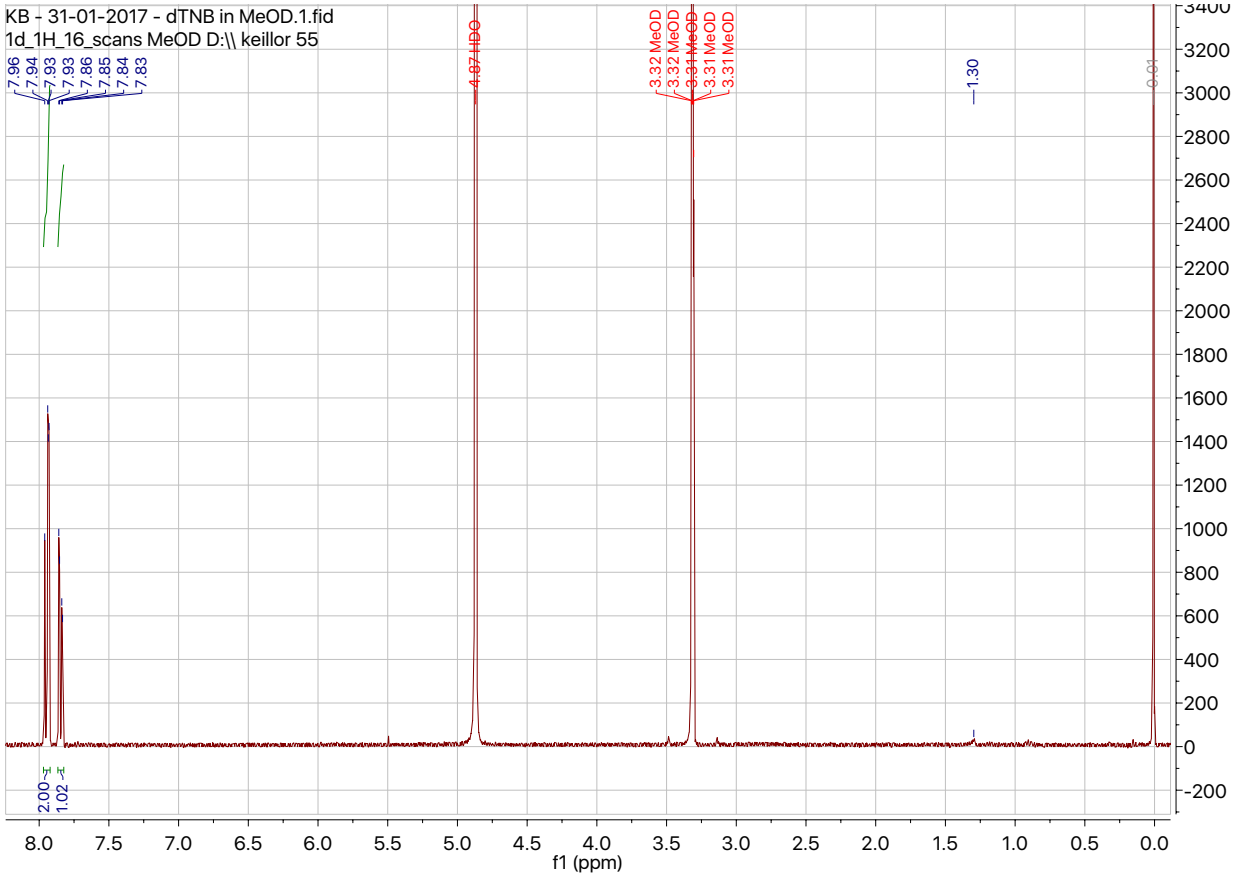

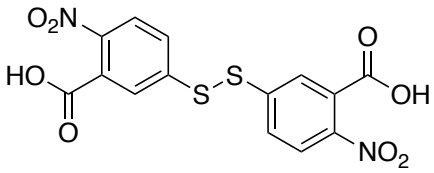

Figure C.15. [1]H-NMR of dTNB in MeOD. full spectrum. Referenced to MeOD. t = 0.

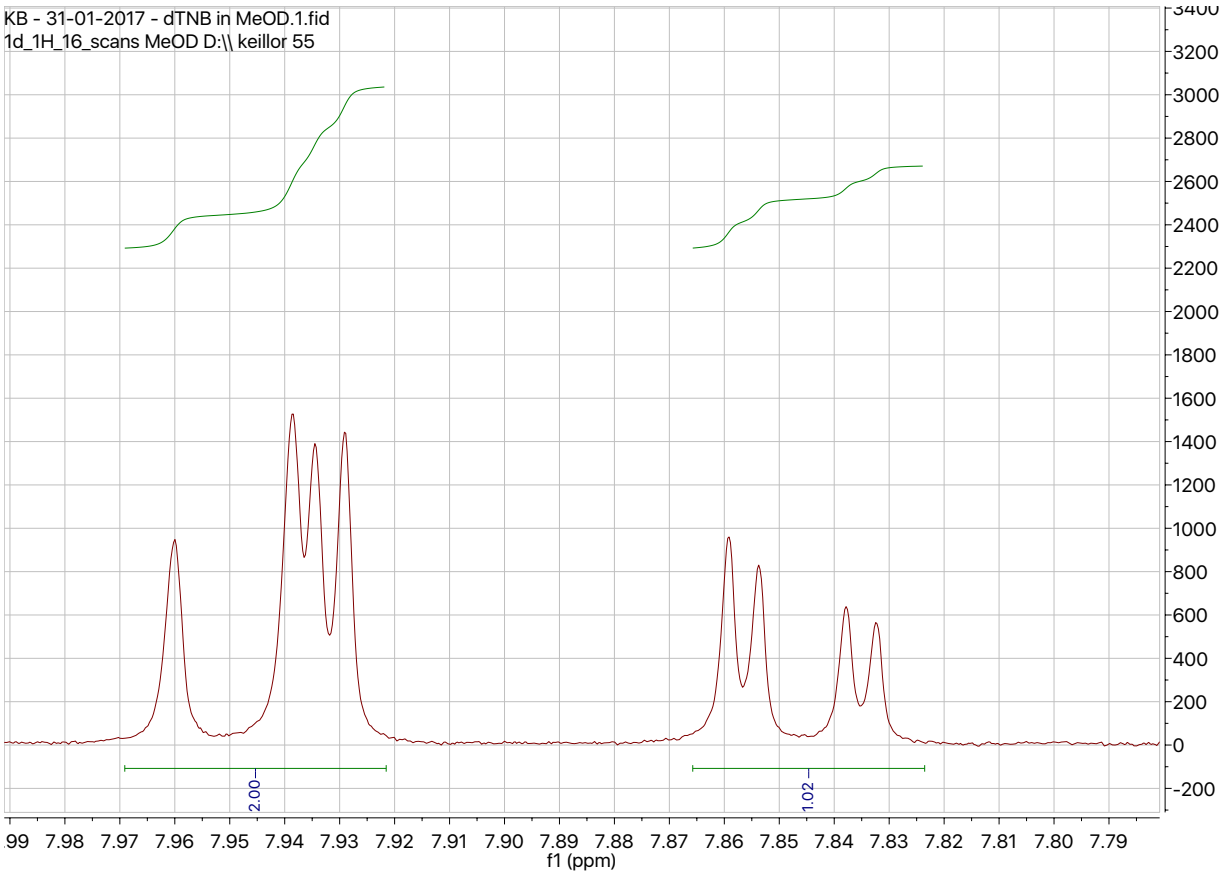

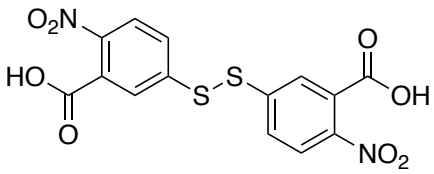

Figure C.16. ^{1}H-NMR of dTNB in MeOD. Full spectrum. Referenced to MeOD. t = 0 h.

Aromatic region. No peaks observed in the aliphatic region.

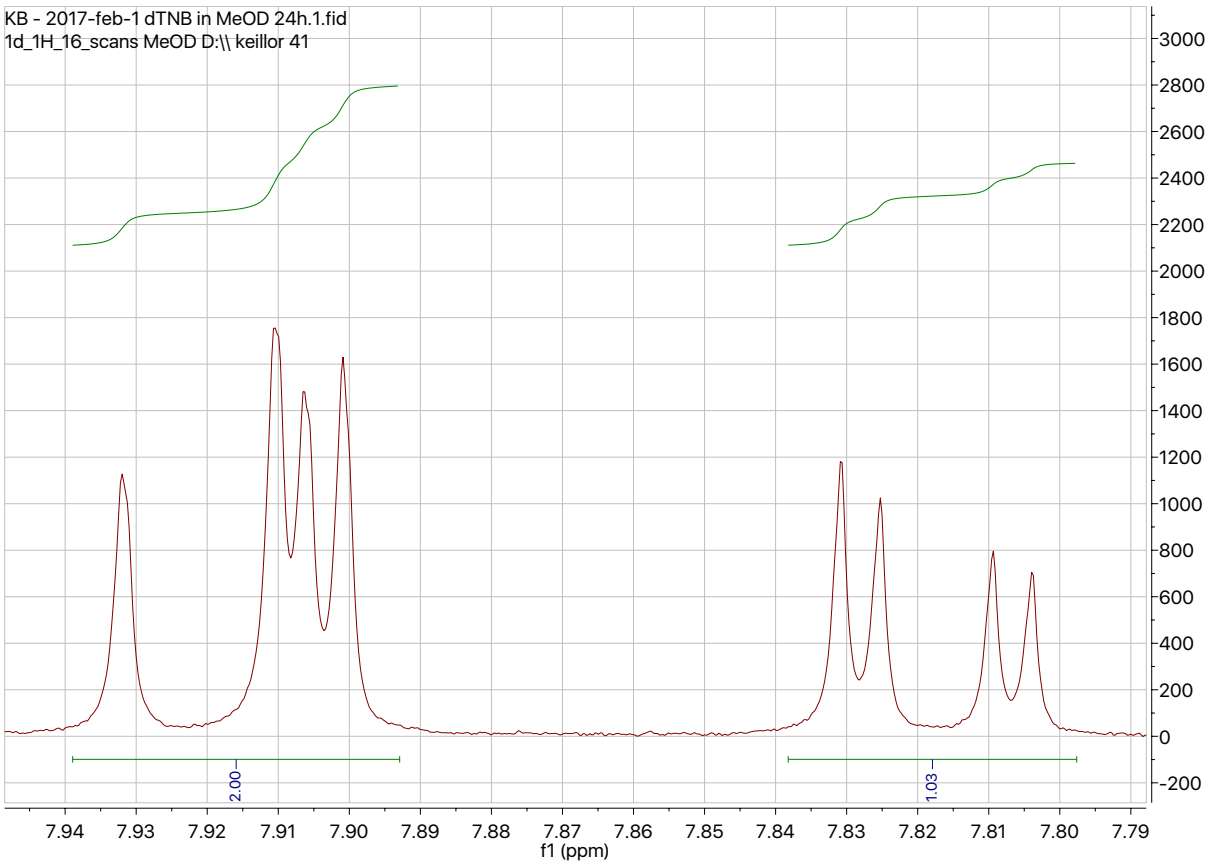

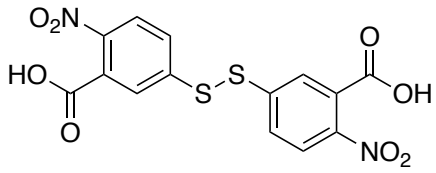

Figure C.17. ^{1}H-NMR of dTNB in MeOD. Full spectrum. Referenced to MeOD. t = 24 h.

Aromatic region. No peaks observed in the aliphatic region.

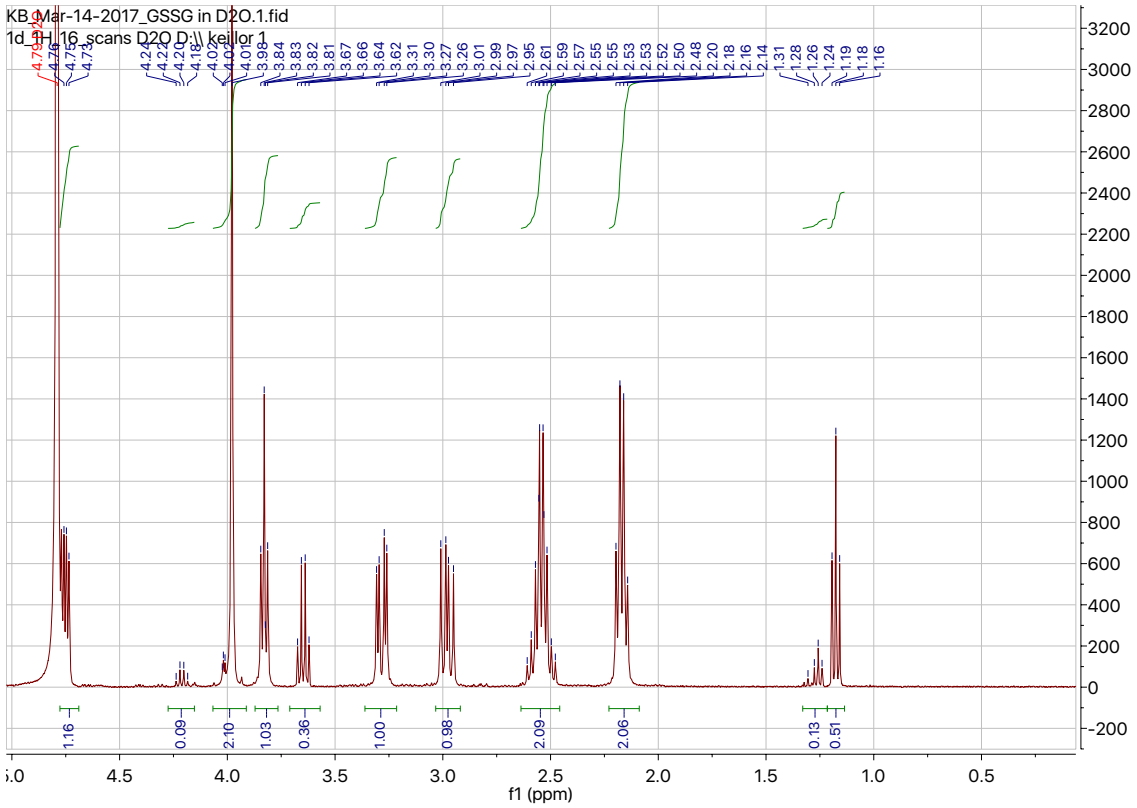

Figure C.18. ^{1}H-NMR of oxidized GSH (GSSG) in D_2O. Referenced to D_2O.

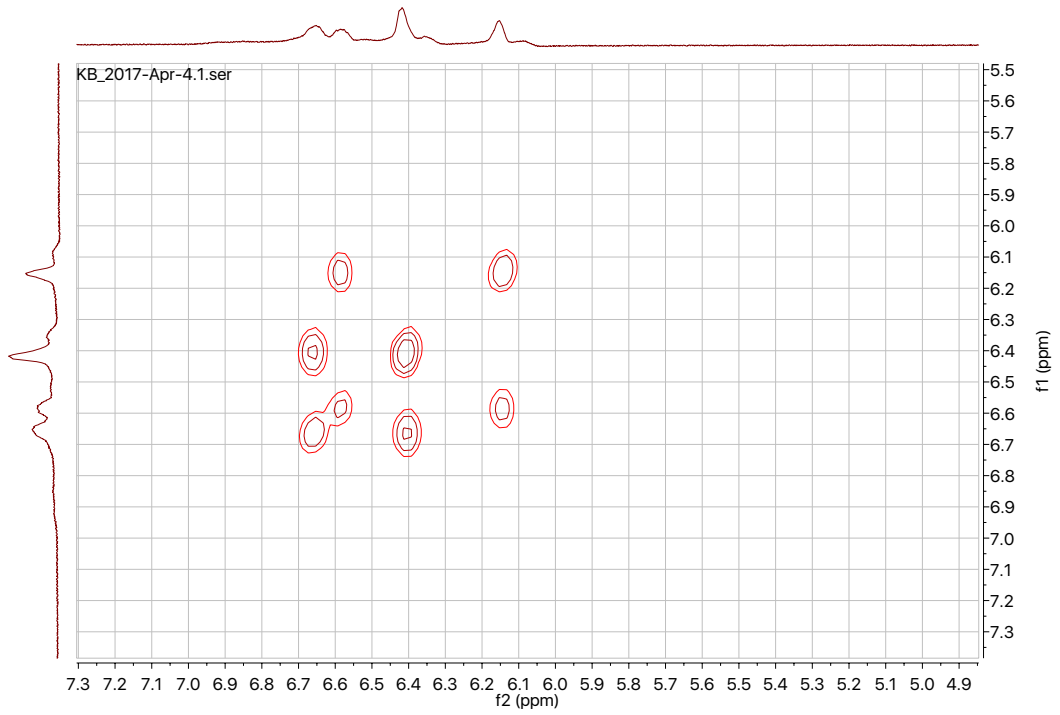

Figure C.19. COSY NMR of dTNB + GSH in MeOD/D_2O cosolvent (aromatic region).

Table C.4. COSY NMR correlation peaks for the reaction of DTNB with GSH

Shift (ppm)	COSY shows correlation to protons at δ (ppm)
0.78	1.12, 2.52
0.83	1.20
1.12	0.78
1.20	-
1.56	3.18
1.71	-
1.94	-
3.18	-
3.26	1.71, 1.94
6.14	6.58
6.42	6.66
6.58	-
6.66	-

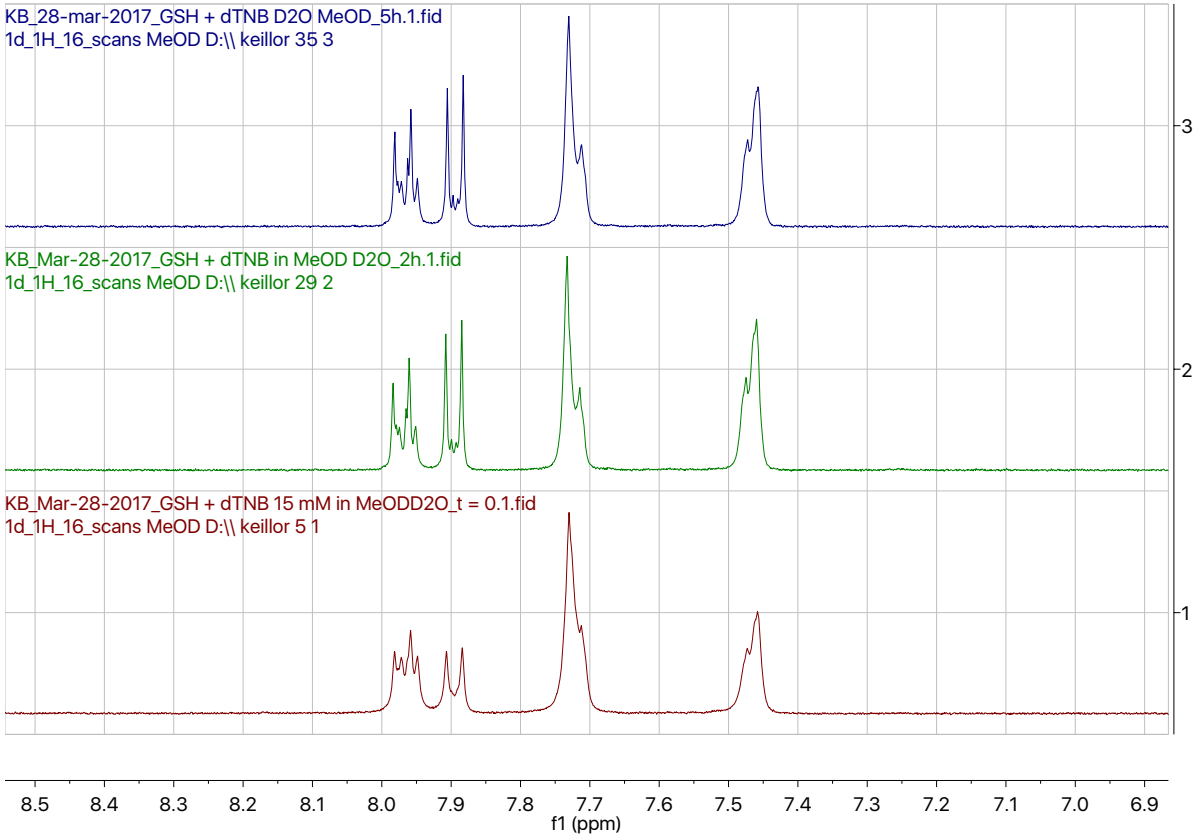

Figure C.20. ^{1}H-NMR spectra of GSH and DTNB in a cosolvent of D2O and MeOD (aromatic region). The bottom spectrum is t = 0, the middle spectrum is t = 2 hours, and the top spectrum is t =5 hours. Spectra were referenced to D2O.

[Chapter text begins here. Click “Insert” → “Object” → “Text from file”]

[Remember to click on “insert” → “Page Break” before inserting a new chapter. This will ensure your chapter starts on a new page. http://grad.ucalgary.ca/current/thesis/msword]

References

1. Lockemann, G. Friedrich Wilhelm Sertürner, the Discoverer of Morphine. *J. Chem. Educ.* 277–279 (1951).
2. von Liebig, J. Ueber die Zersetzung des Alkohols durch Chlor. *Ann. der Pharm.* **1**, 1–2 (1832).
3. Sneader, W. The discovery of aspirin: a reappraisal. *British Medical Journal* **321**, 1591–1594 (2002).
4. Anand, S. S., Philip, B. K. & Mehendale, H. M. Safety Pharmacology. *Encycl. Toxicol. Third Ed.* 198–202 (2014).
5. Bisson, W. H., Cheltsov, A. V., Bruey-Sedano, N., Lin, B., Chen, J. Goldberger, N. May, L.T., Christopoulos, A., Dalton, J. T., Sexton, P. M., Zhang, X.-K. & Abagyan, R. Discovery of antiandrogen activity of nonsteroidal scaffolds of marketed drugs. *Proc. Natl. Acad. Sci.* **104**, 11927–11932 (2007).
6. Kohanski, M. A., Dwyer, D. J. & Collins, J. J. How antibiotics kill bacteria: from targets to networks. *Nat. Rev. Microbiol.* **8**, 423–435 (2010).
7. Shin, J. M. & Sachs, G. Pharmacology of Proton Pump Inhibitors. *Curr. Gastroenterol. Rep.* **10**, 528–534 (2008).
8. Rowland, M. & Tozer, T. N. Clinical Pharmacokinetics and Pharmacodynamics. *Pharm. Sci.* **55** (2011).
9. Grasela, T. H. Pharmacokinetics in Clinical Practice. *J. Pharm. Sci.* **75**, 824–825 (2006).
10. Gomez-Orellana, I. Strategies to improve oral drug bioavailability. *Expert Opin. Drug Deliv.* **2**, 419–433 (2005).

11. Pleuvry, B. J. Factors affecting drug absorption and distribution. *Anaesth. Intensive Care Med.* **6**, 135–138 (2005).

12. Maleki Dizaj, S., Vazifehals, Z., Salatin, A., Adibkia, K. & Javadzadeh, Y. Nanosizing of drugs: Effects on dissolution rate. *Res. Pharm. Sci.* **10**, 95.108 (2015).

13. Dowd, F. J. Pharmacokinetics: The Absorption, Distribution, and Fate of Drugs. Elsevier. 15–43

14. Martinez, M. N. & Amidon, G. L. A Mechanistic Approach to Understanding the Factors Affecting Drug Absorption: A Review of Fundamentals. *J. Clin. Pharmacol.* **42**, 620–643 (2002).

15. Rautio, J., Meanwell, N. A., Di, L. & Hageman, M. J. The expanding role of prodrugs in contemporary drug design and development. *Nat. Rev. Drug Discov.* **17**, 559–587 (2018).

16. Kumar, G. N. & Surapaneni, S. Role of drug metabolism in drug discovery and development. *Med. Res. Rev.* **21**, 397–411 (2001).

17. Masereeuw, R. & Russel, F. G. M. Mechanisms and clinical implications of renal drug excretion. *Drug Metab. Rev.* **33**, 299–351 (2001).

18. Clarke, D. D., Mycek, M. J., Neidle, A. & Waelsch, H. The Incorporation of Amines into Protein. *Arch. Biochem. Biophys.* **79**, 338–354 (1959).

19. Savoca, M. P., Tonoli, E., Atobatele, A. G. & Verderio, E. A. M. Biocatalysis by transglutaminases: A review of biotechnological applications. *Micromachines* **9**, 9–11 (2018).

20. Eckert, R. L., Kaartinen, M.T., Nurminskaya, M., Belkin, A. M., Colak, G., Johnson, G. V.W. & Mehta, K. Transglutaminase Regulation of Cell Function. *Physiol. Rev.* **94**, 383–417 (2014).

21. Eckert, R. L., Sturniolo, M. T., Broome, A. M., Ruse, M. & Rorke, E. A. Transglutaminase function in epidermis. *J. Invest. Dermatol.* **124**, 481–492 (2005).

22. Pinkas, D. M., Strop, P., Brunger, A. T. & Khosla, C. Transglutaminase 2 undergoes a large conformational change upon activation. *PLoS Biol.* **5**, 2788–2796 (2007).

23. Nurminskaya, M. V. & Belkin, A. M. Cellular Functions of Tissue Transglutaminase. *Int Rev. Cell. Mol. Biol.* **5**, 379–390 (2012).

24. John, S., Thiebach, L., Frie, C., Mokkapati, S., Bechtel, M., Nischt, R., Rosser-Davies, S., Paulsson, M. & Smyth, N. Epidermal transglutaminase (TGase 3) is required for proper hair development, but not the formation of the epidermal barrier. *PLoS One* **7**, e34252 (2012).

25. Sardy, M. Epidermal Transglutaminase (TGase 3) Is the Autoantigen of Dermatitis Herpetiformis. *J. Exp. Med.* **195**, 747–757 (2002).

26. Jiang, W. G., Ye, L., Sanders, A. J., Ruge, F., Kynaston, H. G., Ablin, R. J. & Mason, M. D. Prostate transglutaminase (TGase-4, TGaseP) enhances the adhesion of prostate cancer cells to extracellular matrix, the potential role of TGase-core domain. *J. Transl. Med.* **11**, 1–12 (2013).

27. Ablin, R. J., Owen, S. & Jiang, W. G. Prostate Transglutaminase (TGase-4) Induces Epithelial– to-Mesenchymal Transition in Prostate Cancer Cells. *Anticancer Res.* **37**, 481–488 (2017).

28. Cassidy, A. J., van Steensel, M. A. M., Steijlen, P. M., van Geel, M., van der Velden, J., Morley, S. M., Terrinoni, A., Melino, G., Candi, E. & McLean, W. H. A Homozygous Missense Mutation in TGM5 Abolishes Epidermal Transglutaminase 5 Activity and Causes Acral Peeling Skin Syndrome. *Am. J. Hum. Genet.* **77**, 909–917 (2005).

29. Thomas, H., Beck, K., Adamczyk, M., Aeschlimann, P., Langley, M. Oita, R. C., Thiebach, L., Hils, M. & Aeschlimann, D. Transglutaminase 6: A protein associated with central nervous system development and motor function. *Amino Acids* **44**, 161–177 (2013).

30. Guo, Y. C., Lin, J. J., Liao, Y. C., Tsai, P. C., Lee, Y. C. & Soong, B. W. Spinocerebellar ataxia 35: Novel mutations in TGM6 with clinical and genetic characterization. *Neurology* **83**, 1554–1561 (2014).

31. Pan, L. L., Huang, Y. M., Wang, M., Zhuang, X. E., Luo, D. F., Guo, S. C. Zhang, Z. S., Huang, Q., Lin, S. L. & Wang, S. Y. Positional cloning and next-generation sequencing identified a TGM6 mutation in a large Chinese pedigree with acute myeloid leukaemia. *Eur. J. Hum. Genet.* **23**, 218–223 (2015).

32. Aeschlimann, D., Koeller, M. K., Allen-Hoffmann, B. L. & Mosher, D. F. Isolation of a cDNA Encoding a Novel Member of the Transglutaminase Gene Family from Human Keratinocytes. *J. Biol. Chem.* **273**, 3452–3460 (2002).

33. Kuramoto, K., Yamasaki, R., Shimizu, Y., Tatsukawa, H. & Hitomi, K. Phage-displayed peptide library screening for preferred human substrate peptide sequences for transglutaminase 7. *Arch. Biochem. Biophys.* **537**, 138–143 (2013).

34. Muszbek, L., Bereczky, Z., Bagoly, Z., Komáromi, I. & Katona, É. Factor XIII: A Coagulation Factor With Multiple Plasmatic and Cellular Functions. *Physiol. Rev.* **91**, 931–972 (2011).

35. Korsgren, C., Lawler, J., Lambert, S., Speicher, D. & Cohen, C. M. Complete amino acid sequence and homologies of human erythrocyte membrane protein band 4.2. *Proc. Natl. Acad. Sci. U. S. A.* **87**, 613–7 (1990).

36. Begg, G. E., Carrington, L., Stokes, P. H., Matthews, J. M., Wouters, M. A., Husain, A., Lorand, L., Iismaa, S. E. & Graham, R. M. Mechanism of allosteric regulation of transglutaminase 2 by GTP. *Proc. Natl. Acad. Sci.* **103**, 19683–19688 (2006).

37. Tatsukawa, H., Furutani, Y., Hitomi, K. & Kojima, S. Transglutaminase 2 has opposing roles in the regulation of cellular functions as well as cell growth and death. *Cell Death Dis.* **7**, 1–12 (2016).

38. Belkin, A. M. Extracellular TG2: emerging functions and regulation. *FEBS* **278**, 4704–4716 (2011).

39. Klöock, C. & Khosla, C. Regulation of the activities of the mammalian transglutaminase family of enzymes. *Protein Sci.* **21**, 1781–1791 (2012).

40. Pavlyukov, M. S., Antipova, N. V, Balashova, M. V & Shakhparonov, M. I. Biochemical and Biophysical Research Communications Detection of Transglutaminase 2 conformational changes in living cell. *Biochem. Biophys. Res. Commun.* **421**, 773–779 (2012).

41. Caron, N. S., Munsie, L. N., Keillor, J. W. & Truant, R. Using FLIM-FRET to Measure Conformational Changes of Transglutaminase Type 2 in Live Cells. *PLoS One* **7**, (2012).

42. Iversen, R. & Sollid, L. M. Transglutaminases: Multiple functional modifiers and targets for new drug discovery. *Transglutaminases Mult. Funct. Modif. Targets New Drug Discov.* **2**, 1–391 (2016).

43. Ruan, Q. & Johnson, G. V. W. Transglutaminase 2 in neurodegenerative disorders. *Front. Biosci.* **12**, 891–904 (2007).

44. Salter, N. W., Ande, S. R., Nguyen, H. K., Grégoire Nyomba, B. L. & Mishra, S. Functional characterization of naturally occurring transglutaminase 2 mutants implicated in early-onset type 2 diabetes. *J. Mol. Endocrinol.* **48**, 203–216 (2012).

45. Olsen, K. C., Sapinoro, R. E., Kottmann, R. M., Kulkarni, A. A., Iismaa, S. E., Johnson, G. V. W., Thatcher, T. H., Phipps, R. P. & Sime, P. J. Transglutaminase 2 and its role in pulmonary fibrosis. *Am. J. Respir. Crit. Care Med.* **184**, 699–707 (2011).

46. Shweke, N., Boulos, N., Jouanneau, C., Vandermeersch, S., Melino, G., Dussaule, J. C., Chatziantoniou, C., Ronco, P. & Boffa, J. J. Tissue transglutaminase contributes to interstitial renal fibrosis by favoring accumulation of fibrillar collagen through TGF-β activation and cell infiltration. *Am. J. Pathol.* **173**, 631–642 (2008).

47. Huang, L., Xu, A. M. & Liu, W. Transglutaminase 2 in cancer. *Am. J. Cancer Res.* **5**, 2756–2776 (2015).

48. Eckert, R. L., Fisher, M. L., Grun, D., Adhikary, G., Xu, W. & Kerr, C.. Transglutaminase Is a Tumor Cell and Cancer Stem Cell Survival Factor. *Mol. Carcinog.* **54**, 947–958 (2015).

49. Szondy, Z., Korponay-Szabó, I., Király, R., Sarang, Z. & Tsay, G. J. Transglutaminase 2 in human diseases. *BioMedicine* **7**, 15 (2017).

50. Keillor, J. W., Apperley, K. Y. P. & Akbar, A. Inhibitors of tissue transglutaminase. *Trends Pharmacol. Sci.* **36**, 32–40 (2015).

51. Choi, K., Siegel, M., Piper, J. L., Yuan, L., Cho, E., Strnad, P., Omary, B., Rich, K. M. & Khosla, C. Chemistry and biology of dihydroisoxazole derivatives: Selective inhibitors of human transglutaminase 2. *Chem. Biol.* **12**, 469–475 (2005).

52. Klöck, C., Herrera, Z., Albertelli, M. & Khosla, C. Discovery of potent and specific dihydroisoxazole inhibitors of human transglutaminase 2. *J. Med. Chem.* **57**, 9042–9064 (2014).

53. Dafik, L., Albertelli, M., Stamnaes, J., Sollid, L. M. & Khosla, C. Activation and inhibition of Transglutaminase 2 in mice. *PLoS One* **7**, 1–7 (2012).

54. Keillor, J. W., Chica, R. A., Chabot, N., Vinci, V., Pardin, C., Fortin, E., Gillet, S. M. F. G., Nakano, Y., Kaartinen, M. T., Pelletier, J. N. & Lubell, W. D. The bioorganic chemistry of transglutaminase — from mechanism to inhibition and engineering. *Can. J. Chem.* **86**, 271–276 (2008).

55. Akbar, A., McNeil, N. M. R., Albert, M. R., Ta, V., Adhikary, G., Bourgeois, K., Eckert, R. L. & Keillor, J. W. Structure-Activity Relationships of Potent, Targeted Covalent Inhibitors That Abolish Both the Transamidation and GTP Binding Activities of Human Tissue Transglutaminase. *J. Med. Chem.* **60**, 7910–7927 (2017).

56. Press Release: Dr . Falk Pharma and Zedira announce start of the phase 2a proof of concept study of ZED1227 for the treatment of celiac disease. (2018). Available at: https://zedira.com/News/Press-release-Dr-Falk-Pharma-and-Zedira-announce-start-of-the-phase-2a-proof-of-concept-study-of-ZED1227-for-the-treatment-of-celiac-disease_107?oswsid=4ca41db6f816b46603f6d9c11b374018.

57. Yang, N. J. & Hinner, M. J. Getting Across the Cell Membrane: An Overview for Small Molecules, Peptides, and Proteins. *Methods Mol Biol.* **1266**, 29–53 (2015).

58. Peck, T. E., Hill, S. A., Peck, T. E. & Hill, S. A. Drug passage across the cell membrane. *Pharmacol. Anaesth. Intensive Care* 1–8 (2014).

59. Piafsky, K. M. & Borga, O. Plasma protein binding of basic drugs. *Clin. Pharmacol. Ther.* **22**, 545–549 (2016).

60. Choi, C.-H. ABC transporters as multidrug resistance mechanisms and the development of chemosensitizers for their reversal. *Cancer Cell Int.* **5**, 1–13 (2005).

61. Zhang, L., Brett, C. M. & Giacomini, K. M. Role of Organic Cation Transporters in Drug Absorption and Elimination. *Annu. Rev. Pharmacol. Toxicol.* **38**, 431–460 (2002).

62. Lipinski, C. A. Drug-like properties and the causes of poor solubility and poor permeability. *J. Pharmacol. Toxicol. Methods* **44**, 235–249 (2000).

63. Lipinski, C. A., Lombardo, F., Dominy, B. W. & Feeney, P. J. Experimental and Computational Approaches to Estimate Solubility and Permeability in Drug Discovery and Development Settings. *Adv. Drug Deliv. Rev.* **46**, 3–26 (2001).

64. Veber, D. F., Johnson, H., Cheng, H.-Y., Smith, B. R., Ward, K. W. & Kopple, K. D. Molecular Properties That Influence the Oral Bioavailability of Drug Candidates. *J. Med. Chem.* **45**, 2615–2623 (2002).

65. Navia, M. A. & Chaturvedi, P. R. Design Principles for Orally Bioavailable Drugs. *Drug Discovery Today* **1**, 179–189 (1996).

66. Clark, D. E. Rapid Calculation of Polar Molecular Surface Area and Its Application to the Prediction of Transport Phenomena. 1. Prediction of Intestinal Absorption. *J. Pharm. Sci.* **88**, 807–814 (1999).

67. Artursson, P., Palm, K. & Luthman, K. Caco-2 monolayers in experimental and theoretical drug transport predictions of drug transport. *Adv. Drug Deliv. Rev.* **46**, 27–43 (2001).

68. Gan, L. S. L. & Thakker, D. R. Applications of the Caco-2 model in the design and development of orally active drugs: elucidation of biochemical and physical barriers posed by the intestinal epithelium. *Adv. Drug Deliv. Rev.* **23**, 77–98 (1997).

69. Di, L. & Kerns, E. H. Chapter 26: Permeability Methods. *Drug-Like Prop.* 325–337 (2016).

70. Kansy, M., Senner, F. & Gubernator, K. Physicochemical High Throughput Screening: Parallel Artificial Membrane Permeation Assay in the Description of Passive Absorption Processes. *J. Med. Chem.* **41**, 1008–1010 (1998).

71. Wohnsland, F. & Faller, B. High-Throughput Permeability pH Profile and High-Through put Alkane/Water log P with Artificial Membranes. *J. Med. Chem.* **44**, 923–930 (2001).

72. Bujard, A., Petit, C., Carrupt, P. A., Rudaz, S. & Schappler, J. HDM-PAMPA to predict gastrointestinal absorption, binding percentage, equilibrium and kinetics constants with human serum albumin and using 2 end-point measurements. *Eur. J. Pharm. Sci.* **97**, 143–150 (2017).

73. Williams, A. C. & Barry, B. W. Penetration enhancers. *Adv. Drug Deliv. Rev.* **64**, 128–137 (2012).

74. Bagheri, H., Lhiaubet, V., Montastruc, J. L. & Chouini-Lalanne, N. Photosensitivity to ketoprofen: Mechanisms and pharmacoepidemiological data. *Drug Saf.* **22**, 339–349 (2000).

75. Costanzo, L. L., Guidi, G. De, Condorelli, G., Cambria, A. & Fama, M. Molecular mechanism of drug photosensitization II. Photoemolysis sensitized by ketoprofen. *Photochem. Photobiol.* **50**, 359–365 (1989).

76. Monti, S., Sortino, S., De Guidi, G. & Marconi, G. Photochemistry of 2-(3-benzoylphenyl)propionic acid (ketoprofen): Part 1. A picosecond and nanosecond time resolved study in aqueous solution. *J. Chem. Soc. - Faraday Trans.* **93**, 2269–2275 (1997).

77. Rosa, G. M., Gigli, L., Tagliasacchi, M. I., Di Iorio, C., Carbone, F., Nencioni, A., Montecucco, F. & Brunelli, C. Update on cardiotoxicity of anti-cancer treatments. *Eur. J. Clin. Invest.* **46**, 264–284 (2016).

78. Ashburn, T. T. & Thor, K. B. Drug repositioning: Identifying and developing new uses for existing drugs. *Nat. Rev. Drug Discov.* **3**, 673–683 (2004).

79. Poole, L. B. The Basics of Thiols anf Cysteines in Redox Biology and Chemistry. *Free Radic. Biol. Med.* **118**, 6072–6078 (2015).

80. Reichen, J. Glutathione metabolism and its role in hepatotoxicity. **52**, 287–305 (1992).

81. Lumb, R. A. & Bulleid, N. J. Is protein disulfide isomerase a redox-dependent molecular chaperone? *EMBO J.* **21**, 6763–6770 (2002).

82. Curry, S., Mandelkow, H., Brick, P. & Franks, N. Crystal structure of human serum albumin complexed with fatty acid reveals an asymmetric distribution of binding sites. *Nat. Struct. Biol.* **5**, 827–835 (1998).

83. Hwang, C., Sinskey, A. J. & Lodish, H. F. Oxidized Redox State of Glutathione in the Endoplasmic Reticulum. *Science.* **257**, 1469–1502 (1992).

84. Epps, D. E. & Taylor, B. M. A Competitive Fluorescence Assay to Measure the Reactivity of Compouds. *Anal. Biochem.* **295**, 101–106 (2001).

85. McCallum, M. M., Nandhikonda, P., Temmer, J. J., Eyermann, C., Simeonov, A., Jadhav, A., Yasgar, A., Maloney, D. & Arnold, A.. High-throughput identification of promiscuous inhibitors from screening libraries with the use of a thiol-containing fluorescent probe. *J. Biomol. Screen.* **18**, 705–713 (2013).

86. Sameshima, T., Miyahisa, I., Yamasaki, S., Gotou, M., Kobayashi, T. & Sakamoto, J. High-Throughput Quantitative Intrinsic Thiol Reactivity Evaluation Using a Fluorescence-Based Competitive Endpoint Assay. *SLAS Discov.* **22**, 1168–1174 (2017).

87. Lee, K. S., Kim, T. K., Lee, J. H., Kim, H. J. & Hong, J. I. Fluorescence turn-on probe for homocysteine and cysteine in water. *Chem. Commun.* 6173–6175 (2008).

88. Huo, F.-J., Sun, Y.-Q., Su, J., Chao, J.-B., Zhi, H.-J. & Yin, C.-X.. Colorimetric Detection of Thiols Using a Chromene Molecule. *Org. Lett.* **11**, 4918–4921 (2009).

89. Winther, J. R. & Thorpe, C. Quantification of Thiols and Disulfides. *Biochim. Biophys. Acta.* **29**, 997–1003 (2014).

90. Naven, R. T., Kantesaria, S., Nadanaciva, S., Schroeter, T. & Leach, K. L. High throughput glutathione and Nrf2 assays to assess chemical and biological reactivity of cysteine-reactive compounds. *Toxicol. Res. (Camb).* **2**, 235–244 (2013).

91. Cee, V. J., Volak, L. P., Chen, Y., Bartberger, M. D., Tegley C., Arvedson, T., McCarter, J., Tasker, A. S. & Fotsch, C. Systematic study of the glutathione (GSH) reactivity of N-arylacrylamides: 1. Effects of aryl substitution. *J. Med. Chem.* **58**, 9171–9178 (2015).

92. Saal, C. & Petereit, A. C. Optimizing solubility: Kinetic versus thermodynamic solubility temptations and risks. *Eur. J. Pharm. Sci.* **47**, 589–595 (2012).

93. Di, L. & Kerns, E. H. Plasma Stability Methods. *Drug-Like Prop.* 393–400 (2016).

94. Di, L., Kerns, E. H., Hong, Y. & Chen, H. Development and application of high throughput plasma stability assay for drug discovery. *Int. J. Pharm.* **297**, 110–119 (2005).

95. Obach, R. S. Prediction of Human Clearance of Twenty-Nine Drugs From Hepatic Microsomal Intrinsic Clearance Data: an Examination of in Vitro Half-Life Approach and Nonspecific Binding To Microsomes. *Drug Metab. Dispos.* **27**, 1350–1359 (1999).